UNIVERSIDAD DE JAÉN

ESCUELA POLITÉCNICA SUPERIOR DE JAÉN
DEPARTAMENTO DE INGENIERÍA ELECTRÓNICA Y AUTOMÁTICA

TESIS DOCTORAL

ANÁLISIS DE LA INFLUENCIA ESPECTRAL EN DISPOSITIVOS DE ALTA CONCENTRACIÓN FOTOVOLTAICA: DESARROLLO DE TÉCNICAS PARA SU EVALUACIÓN BAJO DIFERENTES CONDICIONES ATMOSFÉRICAS Y TEMPORALES

PRESENTADA POR:
ALBERTO SORIA MOYA

DIRIGIDA POR:
DRA. D.ª FLORENCIA ALMONACID CRUZ
DR. D. EDUARDO FERNÁNDEZ FERNÁNDEZ

JAÉN, 14 DE JUNIO DE 2017

ISBN 978-84-9159-121-4

UNIVERSIDAD DE JAÉN

TESIS DOCTORAL

ANÁLISIS DE LA INFLUENCIA ESPECTRAL EN DISPOSITIVOS DE ALTA CONCENTRACIÓN FOTOVOLTAICA: DESARROLLO DE TÉCNICAS PARA SU EVALUACIÓN BAJO DIFERENTES CONDICIONES ATMOSFÉRICAS Y TEMPORALES

AUTOR

Alberto Soria Moya

DIRECTORES

Dra. Dª. Florencia Almonacid Cruz

Dr. D. Eduardo Fernández Fernández

CENTRO DE ESTUDIOS AVANZADOS EN ENERGÍA Y MEDIO AMBIENTE

JAÉN, JUNIO 2017

UNIVERSIDAD DE JAÉN

TESIS DOCTORAL

ANÁLISIS DE LA INFLUENCIA ESPECTRAL EN DISPOSITIVOS DE ALTA CONCENTRACIÓN FOTOVOLTAICA: DESARROLLO DE TÉCNICAS PARA SU EVALUACIÓN BAJO DIFERENTES CONDICIONES ATMOSFÉRICAS Y TEMPORALES

TRIBUNAL EVALUADOR

Presidente: Dr. Antonio García Loureiro (Universidad de Santiago de Compostela)

Secretario: Dr. Pedro Jesús Pérez Higueras (Universidad de Jaén)

Vocal: Dr. Daniel Chemisana Villegas (Universidad de Lleida)

Suplente: Dr. Gustavo Nofuentes Garrido (Universidad de Jaén)

Suplente: Dra. Natalia Seoane Iglesias (Universidad de Santiago de Compostela)

UNIVERSIDAD DE JAÉN

CENTRO DE ESTUDIOS AVANZADOS EN ENERGÍA Y MEDIO AMBIENTE

TESIS DOCTORAL

La memoria titulada: "**Análisis de la influencia espectral en dispositivos de alta concentración fotovoltaica: desarrollo de técnicas para su evaluación bajo diferentes condiciones atmosféricas y temporales**" ha sido desarrollada dentro del Centro de Estudios Avanzados en Energía y Medio Ambiente (CEAEMA) de la Universidad de Jaén y presentada por el aspirante a doctor en ciencias físicas D. Alberto Soria Moya, bajo la dirección de la Dra. Dª. Florencia Almonacid y el Dr. D. Eduardo F. Fernández.

Jaén, junio 2017

El doctorando

Fdo. Alberto Soria Moya

Los directores de la tesis

Fdo. Dra. Dª. Florencia Almonacid Cruz Fdo. Dr. D. Eduardo Fernández Fernández

A mi abuelo Sebastián.

In memoriam.

"Scheue dich nicht zu fragen, Genosse!
Laß dir nichts einreden
Sieh selber nach!
Was du nicht selber weißt
Weißt du nicht.
Prüfe die Rechnung
Du mußt sie bezahlen.
Lege den Finger auf jeden Posten
Frage: Wie kommt er hierher?
Du mußt die Führung übernehmen."

Beltord Bretch

AGRADECIMIENTOS

He tenido la fortuna de contar con los mejores directores de tesis posibles: Florencia Almonacid y Eduardo Fernández confiaron en mí en la realización de este proyecto; su paciencia, generosidad, conocimientos y buen hacer dirigiéndome han hecho posible que esta memoria viera la luz. Vaya mi más sincero agradecimiento a los dos.

Agradezco a Christof Wittwer haberme dado la oportunidad de ingresar en el grupo de investigación *Control Devices BSR* del Fraunhofer ISE, donde realicé mis primeros trabajos en fotovoltaica con la ayuda, entre otros, de Jochan Link, Mark Schumann, Bernhard Wille-Haussmann, que me introdujo en R, y, principalmente, de Jara Fernández, Teresa Orellana y Juan Pablo Ferrer.

A Raimundo González le estoy enormemente agradecido por enseñarme la importancia de trabajar con rigurosidad y escribir con exactitud. Además, me abrió las puertas de Censolar, donde aprendo algo valioso cada día, gracias a todo su equipo, y especialmente, a Francisco Chica, Jesús Poveda y Enrique Carmona.

A Pilar León le agradezco su inestimable ayuda con el idioma de Chesterton.

No quiero olvidarme aquí de Antonio, Rafa, Agustín, Lola, Perico y Jesús, buenos amigos que me ayudaron sin objeciones. Ni de Concha y Néstor, que me cuidan y me regalan sabios consejos.

A mi compañera y amiga Laura, que me brinda soluciones cuando no las hay, le debo muchas cosas, entre ellas sacarme con frecuencia de mi inherente estado de despediste.

Por supuesto, llegar hasta aquí no hubiera sido posible sin el respaldo incansable e incondicional de mis padres y el apoyo leal de mis hermanos y amigos. A todos vosotros: gracias.

RESUMEN

La humanidad se enfrenta actualmente a dos problemas de enorme importancia. El primero de ellos es la aparición, en las próximas décadas, del pico de extracción de la mayoría de combustibles fósiles (especialmente el del petróleo); el segundo es el calentamiento global causado por las emisiones antropogénicas de gases de efecto invernadero (GEI). La solución conjunta a los dos anteriores problemas pasa, ineludiblemente, por generar el 100% de la energía consumida a partir de fuentes de energía renovables. Existen varios estudios que avalan esta posibilidad. Para ello, sería necesario que en el futuro *mix* de generación energética la tecnología fotovoltaica convencional (PV) y la de alta concentración fotovoltaica (HCPV) jugaran un papel fundamental. Ante este escenario, durante los últimos 30 años se ha realizado un importante esfuerzo en investigación enfocado en el desarrollo de ambas tecnologías. No obstante, aunque la tecnología PV sí ha alcanzado un alto grado de madurez científico-tecnológica y está sólidamente implantada en el mercado energético, en comparación, y a pesar de los grandes avances de los últimos tiempos, la HCPV todavía no ha conseguido alcanzar un nivel similar.

Es necesario, por lo tanto, seguir investigando en el campo de la alta concentración fotovoltaica, con el objetivo de conseguir generar la confianza suficiente en los potenciales inversores y promotores, de forma que los sistemas HCPV se erijan como una alternativa real y complementaria a los sistemas fotovoltaicos convencionales.

Uno de los aspectos necesarios para el adecuado desarrollo de esta tecnología es el estudio de su comportamiento en condiciones reales de funcionamiento. En concreto, el estudio de la respuesta de los dispositivos HCPV ante las variaciones espectrales de la radiación solar incidente es crucial, ya que esta tecnología se ve más afectada por estos cambios que la PV convencional. Esto es principalmente debido al uso de células multiunión (MJ, por sus siglas en inglés) —las cuales, como es sabido, presentan una mayor sensibilidad a variaciones de la distribución espectral de la radiación solar— y de dispositivos ópticos que modifican el espectro antes de incidir en la célula.

Con el desarrollo de la presente tesis se pretende arrojar luz sobre esta cuestión clave, realizando un estudio profundo del impacto que producen las variaciones espectrales en los sistemas HCPV. Para ello, se ha efectuado en primer un lugar un análisis sobre la necesidad de incluir factores de corrección espectrales en los modelos de predicción de la potencia máxima. Además, se ha llevado a cabo un estudio sobre los diferentes índices y métodos existentes de estimación del impacto espectral y se ha realizado una validación de las predicciones basadas en los mismos. Asimismo, se ha estudiado la relación que existe entre la variación de los principales parámetros atmosféricos que influyen en la distribución espectral de la radiación solar incidente y el comportamiento espectral de los sistemas HCPV, cuantificando la influencia espectral de cada parámetro de manera individualizada, de forma teórica y bajo condiciones reales de operación, durante al

menos un año, para diversas tecnologías de alta concentración fotovoltaica y diferentes perfiles climatológicos.

Una vez conocido el impacto espectral que tiene la variación de los parámetros más influyentes, se ha estudiado el peso real del mismo en la respuesta de los sistemas HCPV bajo condiciones reales de operación. Además, habida cuenta de que la masa de aire (AM) ha demostrado ser el parámetro atmosférico más influyente en las variaciones espectrales de la radiación solar incidente y que la misma viene determinada exclusivamente por la posición aparente del Sol, se han analizado las pérdidas y ganancias espectrales en función de la latitud y el peso de estas en el impacto espectral total de los sistemas HCPV.

Por último, se ha llevado a cabo una estimación comparativa del impacto espectral en la generación energética entre la tecnología HCPV y la PV, bajo diferentes condiciones climáticas, a escala tanto mensual como anual.

Los resultados obtenidos en los anteriores análisis permitieron concluir que los parámetros atmosféricos de mayor impacto espectral en el comportamiento de un módulo HCPV son la masa de aire y la profundidad óptica de aerosoles ($\tau_{0.55}$). Asimismo, se ha probado que el denominado *spectral factor* (SF) es un buen índice para evaluar la influencia espectral en la potencia máxima de generación de un dispositivo HCPV. En cuanto a la relación entre las pérdidas espectrales y la latitud, se han encontrado unas pérdidas espectrales entre el 4% y el 5%, independiente de la latitud, para latitudes menores de 30º. Para latitudes mayores, las pérdidas crecen fuertemente a medida que ésta aumenta, hasta latitudes alrededor de 75º, para la cual se obtuvieron pérdidas de entre el 12% y el 15%. Para latitudes mayores de 75º se han obtenido unas pérdidas espectrales prácticamente constantes.

La valoración comparativa del impacto espectral de la generación energética mensual y anual entre las tecnologías HCPV y PV en diferentes localizaciones, con condiciones climáticas dispares, arrojó que los actuales sistemas HCPV presentan unas pérdidas energéticas anuales de aproximadamente el 5% más que las asociadas a los dispositivos de tecnología PV. Esto indica que la sensibilidad espectral de los módulos HCPV no es una limitación crucial para la expansión del mercado de esta tecnología y más aun teniendo en cuenta que sus eficiencias de conversión son mucho más altas que las de la tecnología fotovoltaica convencional.

ABSTRACT

Humanity is currently facing two major problems. First of all, the peak of fossil fuel extraction, especially peak oil, will be reached in the coming decades. Secondly, global warming is increasing due to anthropogenic emissions of greenhouse gases (GHGs). Both problems could be jointly tackled by achieving 100% renewable power. Several studies support this approach provided that conventional photovoltaic (PV) and high concentration photovoltaic (HCPV) technologies played a fundamental role in the future energy mix.

Unfortunately, even though both of them have been widely researched for over 30 years, HCPV technology is not as mature as PV technology when operating outdoors. Therefore, further research is still needed to achieve a better understanding of HCPV in order to increase investor confidence and, consequently, promote the market expansion of HCPV systems as a real and complementary alternative to conventional PV systems.

One of the main challenges associated with the development of this technology is the study of its behaviour under real operating conditions. In particular, the study of HCPV devices' response to the spectral variations of incident solar radiation is crucial, because this technology is more sensitive to these changes than conventional PV. This is due to the use of multijunction (MJ) solar cells –based on the internal series connection of several subcells with different energy gaps– together with optical devices that modify the spectral distribution before striking solar cells.

The aim of this doctoral thesis is to shed light on this key issue by studying the influence of spectral variations on the performance of HCPV systems. Firstly, it was analysed whether a spectral correction factor should be included in the models of estimation of an HCPV module maximum power. The different existing indexes and methods of estimation of the spectral impact were also studied, and the predictions based on them were validated. Likewise, a study was performed on the relationship between the spectral behaviour of the HCPV systems and the variation of the main atmospheric parameters that influence the spectral distribution of the incident solar radiation. This was done by quantifying, during a year, the spectral influence of each parameter on different HCPV systems and climatological profiles, both theoretically and under real operating conditions.

Once the spectral impact of the most influential parameters' variation was known, its actual weight on the response of HCPV systems was studied under real operating conditions. Furthermore, since air mass (AM) has proved to be the most influential atmospheric parameter in the spectral variations of incident solar radiation, which is mainly determined by the solar zenith angle, the spectral impact on the yearly energy yield of HCPV modules was analysed according to latitude. Finally, the spectral impact on the energy yield of HCPV was compared to that of PV technology under different climatic conditions both monthly and annually.

The results of the above-mentioned analysis showed that the parameters with the largest influence on the performance of a HCPV module are AM and aerosol optical depth ($\tau_{0.55}$).

Moreover the spectral factor (SF) proved to be a good index for evaluating the spectral influence on the maximum power of an HCPV module. On the other hand, the study of the spectral impact with regards to latitude showed that the spectral losses could be considered latitude-independent until approximately 30º, with a value at around -4% and -5%. For higher latitudes, the spectral losses strongly increase until around 75º, where they reach a value between -12% and -14%. For latitudes higher than 75º, the spectral losses kept almost constant.

The results of the comparative study between HCPV and PV technologies showed that the annual spectral losses of current HCPV systems are 5% higher than those of PV systems. This indicates that spectral changes are not a crucial limitation for the market expansion of HCPV systems, especially considering that their conversion efficiencies are is significantly higher than those of PV technology.

TABLA DE CONTENIDOS

ESTRUCTURA DE LA MEMORIA

La memoria de esta tesis doctoral se divide en dos partes. En la primera de ellas, se realiza una breve introducción sobre el objeto investigador de la tesis, se justifica su desarrollo, se especifican los objetivos que fueron planteados y se resumen los resultados obtenidos. Por último, se expresan las principales conclusiones alcanzadas y se identifican algunas líneas de investigación futuras.

La segunda parte de este documento es un compendio de cuatro artículos publicados en revistas científicas de calidad reconocida, los cuales han sido realizados en el ámbito de la presente tesis doctoral, en consonancia con lo que marca el reglamento correspondiente de la Universidad de Jaén. Además, se citan tres aportaciones relevantes efectuadas en congresos especializados surgidos en el proceso investigador del doctorado.

PARTE I: MEMORIA

Donde se realiza una muy breve introducción de la situación energética mundial y se exponen dos importantes problemas a los que se enfrenta actualmente la humanidad. Estos problemas hacen obligatorio avanzar en la investigación, desarrollo e implementación de fuentes de energía de origen renovable. Entre estas fuentes se encuentra la energía solar fotovoltaica y en particular la energía solar de alta concentración fotovoltaica (HCPV), objeto de estudio de este trabajo investigador. En el documento, se introducen los conceptos más básicos de la tecnología de alta concentración fotovoltaica, se identifican algunos aspectos de la misma que necesitan ser estudiados en profundidad y se justifica la necesidad de realizar un mayor esfuerzo de investigación sobre ellos. Además, se especifican los objetivos planteados para la realización de la presente tesis doctoral y se resumen los resultados obtenidos en el desarrollo de los análisis efectuados. Por último, se expresan las principales conclusiones alcanzadas y se identifican algunas líneas de investigación futuras.

INTRODUCCIÓN

En el año 1973, el consumo anual de energía primaria mundial fue de aproximadamente 6100 millones toneladas equivalentes de petróleo (tep), mientras que en el 2013 alcanzó la cifra de 13541 millones tep. Es decir, un aumento del 121% en 40 años. Más del 81% de esta energía proviene de combustibles fósiles y más del 86% de fuentes no renovables[1] [1]. El consumo final de energía se estima en unos 9425 millones[2] de tep, del cual, en el año 2014, el 38.4% fue efectuado en los países considerados más ricos [2], es decir, los asociados en la Organización para la Cooperación y el Desarrollo Económicos (OCDE), cuya población total supone menos del 18% de la población mundial. Con todo, la fracción del consumo de los países de la OCDE respecto del total no ha dejado de reducirse. Así, en 1973 este porcentaje era mucho mayor, en concreto del 61.3%. Este comportamiento es debido, principalmente, al aumento del consumo de los países denominados emergentes. Entre ellos, el más destacable es China, que ha pasado de consumir menos de un 8% de la demanda mundial en 1973 a más del 21% en 2014 [2].

De toda la energía finalmente consumida, tan solo alrededor de un 22% es utilizada en forma de electricidad, de la cual un 40.8% proviene del carbón, un 21.6% del gas natural y un 4.3 % del petróleo [2]. Por su parte, la energía fotovoltaica aportó aproximadamente el 1% de la electricidad consumida en 2014, aunque en algunos países como Italia —un 8%—, Grecia —más del 7.5%— o Alemania —casi el 7%— esta aportación fue considerablemente mayor [3].

Lo anteriormente expuesto evidencia la gran dependencia que tiene el mundo actual y, en especial, los países más ricos de los combustibles fósiles, cuya demanda anual mundial crece prácticamente de forma interrumpida [2], lo que contrasta con el aplanamiento de la extracción de petróleo crudo existente desde 2006 y con la estimación de que en adelante la misma será difícilmente incrementada [4]. Esto concuerda con el hecho de que la extracción del petróleo tiene, desde el 2005, un comportamiento inelástico, es decir, no se producen incrementos de la extracción cuando su demanda y precio aumentan; circunstancia que no ha podido ser compensada por el resto de combustibles fósiles [5]. Asimismo, algunos autores sostienen que el pico de extracción del carbón sucederá antes de lo esperado [6]; en concreto, existen estudios que estiman que el punto crítico de máxima extracción ocurrirá alrededor de 2020 [7]; mientras otros afirman que podría darse incluso antes [8, 9, 10]. En cuanto al gas natural, el estancamiento en su extracción se estima se producirá en la próxima década [7] o en la siguiente [10]. En definitiva: es probable que la extracción conjunta de todos los combustibles fósiles alcance su cenit en menos de 25 años [7, 8, 11]. Por otro lado, en una publicación del año 2014, el Grupo Intergubernamental de Expertos sobre el Cambio Climático (IPCC, por sus siglas en

[1]El desglose de esos combustibles respecto al total de la energía primaria consumida es el siguiente: 31.1 % petróleo, 28.9% carbón, 21.4% gas natural y 4.8% nuclear.

[2]Siguiendo el razonamiento de algunos autores [77], esto es equivalente a las necesidades energéticas alimenticias de más de 56000 millones de personas en plenitud.

inglés) afirmó, con una certeza del 95%, que las actividades humanas son la causa, por medio de la emisión de gases de efecto invernadero (GEI), del creciente calentamiento global, el cual es el origen del gran cambio observado en el comportamiento del sistema climático en todos continentes y océanos desde 1950 [12]. En el mismo informe también se pone de manifiesto los graves riesgos, generalizados e irreversibles, que estos cambios suponen en las personas y ecosistemas. Por todo ello, el IPCC aboga, entre otras políticas, por la reducción drástica de las emisiones de los GEI durante las próximas décadas hasta conseguir un nivel de emisión nulo para finales de este siglo. En este sentido, durante la cumbre de París de 2015 se alcanzó un acuerdo histórico mediante el cual 195 países se comprometieron a llevar a cabo políticas de reducción de las emisiones de gases de efecto invernadero con el objetivo de que la temperatura del planeta se mantenga por debajo de los 2 ºC de diferencia con respecto a la temperatura que existía en la época preindustrial [13].

Ante este escenario de creciente demanda energética global, cambio climático y aplanamiento de la extracción de los combustibles fósiles, la Unión Europea incluyó como objetivo en su estrategia de crecimiento 2020 generar al menos el 20% de las necesidades energéticas existentes a partir de fuentes renovables [14]. Más allá de esto, las energías renovables están llamadas a cubrir la demanda total de energía en un futuro no muy lejano [11, 15]. En ese sentido, existen varios estudios que avalan esta posibilidad [16, 17, 18, 19, 20, 21]. La energía fotovoltaica convencional (PV, por sus siglas en inglés), tendría un papel determinante en el posible futuro *mix* de fuentes de energías renovables. Así, algunos autores estiman que la potencia nominal fotovoltaica total instalada debería alcanzar, al menos, los 7 TW [18]. No obstante, a pesar del gran avance experimentado por esta tecnología en los últimos años [3, 22, 23], para alcanzar cifras tan altas es todavía necesario, entre otros requerimientos, desarrollar soluciones alternativas a algunos problemas como el que acarrea la escasez de ciertos materiales [17, 24].

Además, es también indispensable reducir los costes de producción de los módulos fotovoltaicos [16, 25]. En este último aspecto, la tecnología de concentración fotovoltaica (CPV, por sus siglas en inglés) es considerada una vía prometedora para el abaratamiento de la implantación de sistemas basados en el efecto fotovoltaico [26]. Desafortunadamente, la concentración fotovoltaica es todavía una tecnología emergente, como se puede deducir del hecho de que durante el año 2015 la potencia de todos los sistemas fotovoltaicos instalados fue de unos 57 GW; mientras que la potencia instalada de los sistemas CPV fue de menos de 20 MW [23]. En todo caso, existen estudios que prevén una rápida expansión en la implantación de la tecnología de concentración fotovoltaica durante los próximos años [26]. De igual forma, se estima que para el años 2020 los sistemas CPV podrían alcanzar una potencia instalada de 1 GWp [27] y que su LCOE[3] se verá reducido hasta situarse en un valor inferior a 10 c€/kWh en lugares con alto recurso solar [28].

[3] *Levelized Cost Of Electricity*, es decir, el coste de la energía eléctrica que genera una fuente concreta considerando toda su vida útil, la inversión inicial, la tasa de descuento y los costes de operación y mantenimiento.

La tecnología de CPV se basa en la concentración de la radiación solar, focalizando la misma, por medio de dispositivos ópticos, en células fotovoltaicas. La principal razón de operar de esta forma es el hecho de que la fabricación de los dispositivos ópticos es sensiblemente más barata que la de la mayoría de las células fotovoltaicas [29], esto es debido, entre otras causas, a que los dispositivos ópticos utilizan materiales relativamente convencionales (como lentes y espejos) mientras que las células están formadas por materiales semiconductores, los cuales son más caros y necesitan un tratamiento relativamente complejo para que puedan reproducir el efecto fotovoltaico. El enfoque que se utiliza en el desarrollo de los dispositivos de CPV es el de maximizar la superficie óptica y minimizar la semiconductora.

Los sistemas CPV pueden ser clasificados según su factor de concentración (CF, por sus siglas en inglés), es decir, según la cantidad de irradiancia que recibe la célula respecto a la que recibiría si no estuviera asociada a ningún dispositivo óptico. Para ello, es usual tomar como referencia una irradiancia de 1000 W/m^2, cantidad que suele denominarse sol. De ese modo, los sistemas CPV pueden ser divididos en cuatro grupos [30, 31]:

- Sistemas de baja concentración (LCPV, por sus siglas en inglés): con un CF comprendido entre 1 y 10 soles.
- Sistemas de media concentración (MCPV, por sus siglas en inglés): con un CF comprendido entre 10 y 100 soles.
- Sistemas de alta concentración fotovoltaica (HCPV, por sus siglas en inglés): con un CF comprendido entre 100 y 2000 soles.
- Sistemas de ultra alta concentración fotovoltaica (UHCPV, por siglas en inglés): con un CF comprendido entre 2000 y 10000 soles. Hay que destacar que esta tecnología está todavía en un estado muy temprano de investigación, por lo que no existen módulos comerciales de UHCPV.

Es importante señalar que algunos autores eliminan de la anterior clasificación a los sistemas MCPV, debido al alto LCOE que presentan, e incluyen en los sistemas LCPV a aquellos con hasta 100 soles de factor de concentración [32].

De los anteriores grupos, el que mayor implantación tiene es el de HCPV; así, hasta principios del 2016 más, del 90% de los sistemas CPV instalados eran de alta concentración, montados sobre seguidores solares a dos ejes [32]. A partir de la experiencia en el desarrollo de esas instalaciones, se ha concluido que los sistemas HCPV tienen un gran y mayor potencial de crecimiento y desarrollo que la tecnología LCPV, MCPV y PV convencional en lugares con alto recurso solar [33, 34]. Debido a esto, la presente tesis doctoral centra su estudio en estos dispositivos, por lo que no se abordará el funcionamiento del resto de sistemas CPV.

Un dispositivo HCPV se compone fundamentalmente de células fotovoltaicas, elementos ópticos de concentración, componentes periféricos y un seguidor solar.

Las células fotovoltaicas utilizadas mayoritariamente en los sistemas HCPV son las denominadas de multiunión (*Multijunction*, MJ), las cuales se basan en el apilamiento de dos o más células (también llamadas subcélulas) de diferente rango espectral —es decir, con distinto ancho de banda de energía (*band gap energy*)—, en un mismo dispositivo fotovoltaico. De esa manera, los fotones que sean transparentes para la primera subcélula alcanzarán a la segunda y así sucesivamente [26]. La subcélula situada en la parte superior del conjunto se caracteriza por tener un ancho de banda de energía mayor que las del resto, las cuales deben ser apiladas en orden decreciente de ancho de banda. De esa forma, aumenta el rango espectral y la eficiencia de la célula MJ [35]. El objetivo que se pretende con el uso de estas células es mejorar la eficiencia de conversión eléctrica ampliando el rango de la respuesta espectral del conjunto a todo el espectro de la radiación solar [26]. La eficiencia teórica de las células MJ aumenta a medida que se incrementa el número de uniones de la misma. No obstante, este aumento presenta una ganancia decreciente [30], lo que implica que a partir de cinco o seis uniones el incremento de la eficiencia sea despreciable [26].

Las células multiunión con dos subcélulas son comúnmente denominadas células tándem. Ejemplos de células tándem son las a-Si:H/CIS o las a-Si:H/nc-Si:H (también llamadas micromorfas). Una evolución de estas últimas son las células triple a-Si:H/a-Si:H/nc-Si:H o las a-Si:H/nc-Si:H/nc-Si:H. Estas células son normalmente utilizadas para formar módulos fotovoltaicos sin concentración.

Las células de tres elementos, diseñadas específicamente para ser empleadas en dispositivos HCPV, suelen estar constituidas por materiales III-V de la tabla periódica. La selección de estos materiales se basa fundamentalmente en dos criterios: En primer lugar, en que las respuestas espectrales (y por tanto el ancho de banda) de las subcélula sean complementarias entre sí, de manera que abarquen el máximo posible del espectro solar. En segundo lugar, que el parámetro de red[4] (*lattice constant*) de los diferentes materiales utilizados sea lo más parecido posible, ya que esto reduce defectos térmicos, mecánicos y eléctricos, con lo que se minimiza las pérdidas energéticas [26].

Debido a que las subcélulas se asocian normalmente en serie [37], la intensidad que atraviesa las mismas está limitada por aquella que genera menor intensidad, lo cual podría acarrear una pérdida considerable en la producción energética. Por ello, el escenario ideal es que todas las células generen la misma intensidad bajo las condiciones atmosféricas más relevantes [26]. Desgraciadamente, esto no es siempre posible y pueden darse multitud de circunstancias que hagan que, de forma más o menos importante, exista una subcélula limitante.

Una típica célula MJ de tres uniones es la formada por los materiales GaInP/GaInAs/Ge [26], la cual satisface adecuadamente los tres factores anteriores.

[4] El parámetro de red viene dado por la distancia en cada dimensión existente de la unidad (célula) de un material cristalino respecto a su estructura.

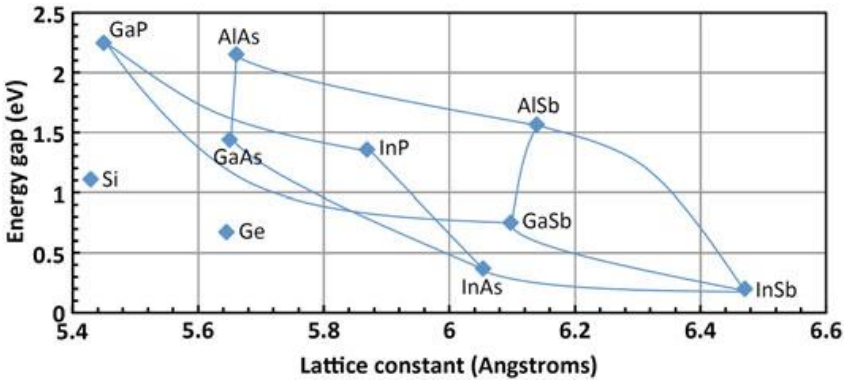

Figura 1: Representación del parámetro de red frente al ancho de banda de energía de diferentes materiales semiconductores [36].

La conexión de las diferentes uniones se suele realizar a partir de diodos túnel, los cuales se caracterizan por una resistencia y un grosor muy reducidos, de manera que las pérdidas asociadas a los mismos son relativamente pequeñas [38]. En la figura 2 se puede observar la típica estructura de una célula MJ formada por los materiales anteriormente indicados, donde la célula superior (*top cell*) es formada por GaInP (1.88 eV de *band gap*), la célula media (*middle cell*) está basada en GaInAs (1.41 eV de *band gap*) y la célula inferior (*bottom cell*) es de Ge (0.67 eV de *band gap*).

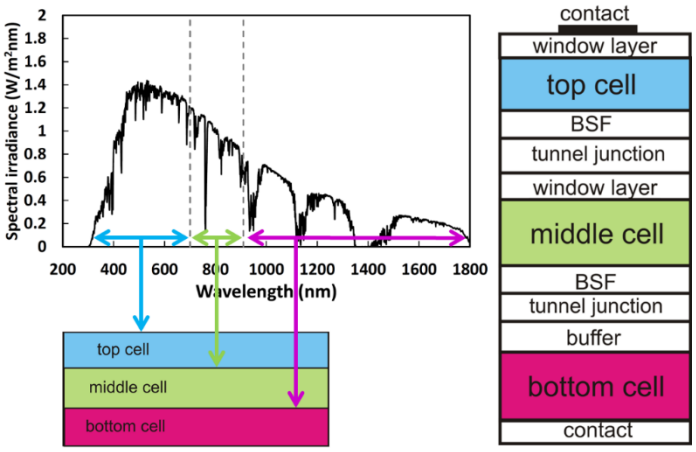

Figura 2. En el esquema de la derecha se puede observar la estructura de una célula MJ de tres uniones compuesta por GaInP/GaInAs/Ge. En la gráfica de la izquierda se pueden observar las diferentes fracciones del espectro solar en condiciones estándar (AM1.5D, ASTM G-173-03) que absorbe mayoritariamente cada una de las subcélulas [26].

El inconveniente que tienen las células MJ de materiales III-V es su alto coste de fabricación por lo que es usual utilizarlos en dispositivos de concentración fotovoltaica [26, 39]. Así, al utilizar ciertos dispositivos ópticos se puede colectar la radiación solar de una amplia área y concentrarla en una pequeña zona en la cual se sitúa la célula MJ [26]. Esto tiene dos grandes ventajas: por un lado, se utiliza muy poco material semiconductor con lo que se abaratan los costes; por el otro, debido a cuestiones termodinámicas, se mejora la eficiencia de conversión de la célula, la cual ya es de por sí alta incluso sin utilizar dispositivos concentradores [26, 39].

Todo lo anterior ha facilitado que las células MJ hayan alcanzado eficiencias muy superiores a las correspondientes a los dispositivos fotovoltaicos convencionales y se

espera que las mismas sigan aumentando [30, 40, 41]. La contrapartida es que para que la radiación se concentre en la célula MJ la pareja célula-lente debe estar siempre orientada hacia el Sol, por lo que suele ser necesario algún tipo de mecanismo de seguimiento solar.

Aunque por ahora no se comercializan células multiunión con más de tres subcélulas, sí se han desarrollado prototipos, en laboratorio, con cuatro uniones [42]. De hecho, la célula fotovoltaica que ha registrado hasta la fecha una mayor eficiencia de conversión eléctrica (sobre el 46 % utilizando concentración) es la célula multiunión compuesta de cuatro subcélulas (figura 3) de los siguientes materiales (GaInP/GaAs//GaInAsP/GaInAs) [43].

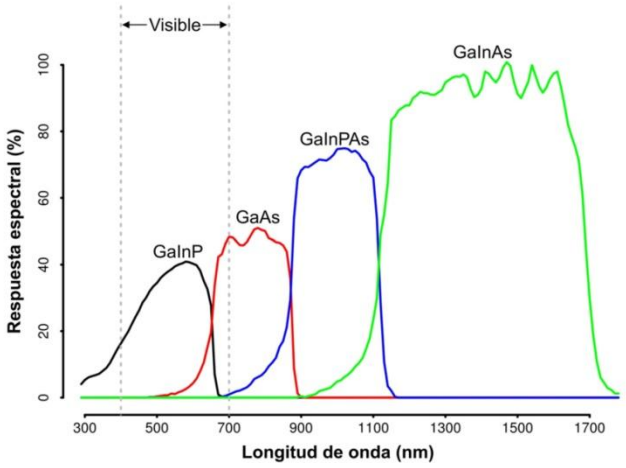

Figura 3. Respuesta espectral de una célula MJ de cuatro uniones y alta eficiencia [44].

En general, el dispositivo óptico de concentración normalmente utilizado consiste en un elemento primario y uno, opcional, secundario (*Secondary Optical Element*, SOE). El elemento primario suele ser una lente de Fresnel [45], que es un elemento óptico de gran apertura y pequeña distancia focal que se caracterizan por no presentar los grandes grosores de las lentes o lupas convencionales. Esto es posible debido a un diseño especial basado en anillos circulares de diferente grosor cada uno. La imagen que se forma a través de las lentes de Fresnel no es muy buena (o directamente es inexistente), debido a la dispersión producida por los anillos. Es por ello por lo que su uso está limitado a las aplicaciones, como la fotovoltaica de concentración, donde el objetivo sea concentrar energía o luz, sin necesidad de formar imágenes. Al tener mucho menor volumen que las lentes convencionales, el coste y peso del elemento óptico primario se reduce con el uso de lentes de Fresnel, por lo que se habilita la fabricación de lentes para sistemas CPV de más de 5 cm^2, lo cual resulta inviable con lentes convencionales [46].

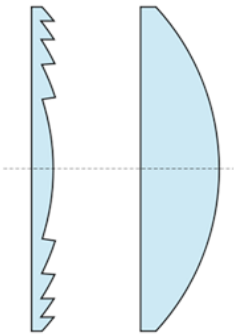

Figura 4. Esquema de una Lente convencional (derecha) y de Fresnel (izquierda) con la misma distancia focal.

En cuanto a los elementos ópticos secundarios, estos se denominan así porque reciben la luz del primario. Su función es la de homogeneizar la radiación solar concentrada sobre la superficie de la célula y mejorar, de esa forma, la aceptancia angular del sistema. A pesar de que la inclusión de un elemento óptico secundario, entre la lente primaria y la célula, podría generar una cantidad significativa de pérdidas ópticas, su uso es normalmente ventajoso ya que la mejora de la aceptancia angular y de la uniformidad de la luz incidente sobre la célula receptora, además de la posibilidad de aumentar el factor de concentración del dispositivo, suelen compensar dichas pérdidas. Es por ello, que la mayoría de los sistemas HCPV utilizan actualmente elementos ópticos secundarios [47].

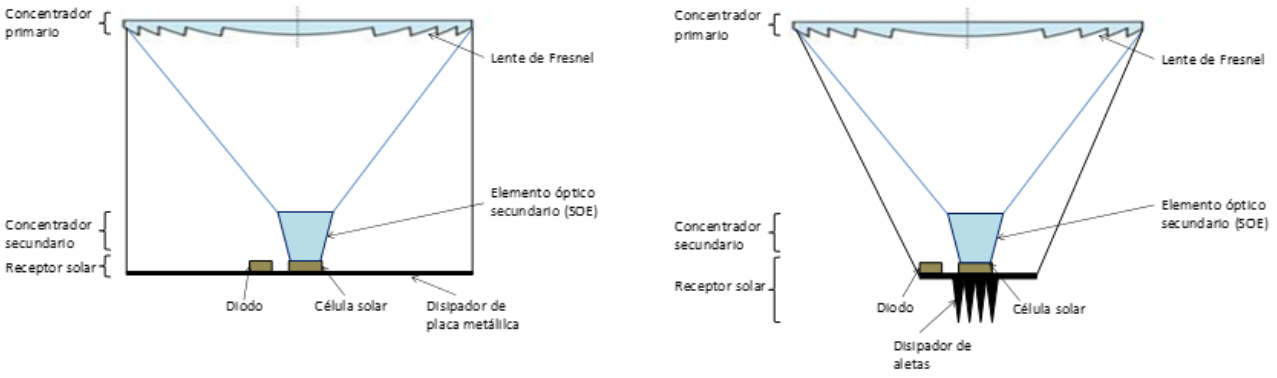

Figura 5. Esquemas de dos módulos HCPV de una sola célula.

Por otro lado, los dispositivos ópticos de los sistemas CPV solo son capaces de concentrar la radiación normal directa que reciben. Además, debido al alto factor de concentración de los dispositivos HCPV, los mismos deben estar equipados con un seguidor solar a dos ejes lo que habilita que el dispositivo óptico pueda situarse, en todo momento, perpendicularmente a los rayos solares, de manera que se aproveche siempre toda la irradiancia normal directa (DNI). Si no se operara así, la captación de radiación solar sería despreciable. Obviamente, esto implica que a diferencia de los sistemas fotovoltaicos convencionales y de los de baja concentración, los dispositivos HCPV no son capaces de aprovechar la radiación solar difusa. Esto, no obstante, es compensado por la captación máxima de la DNI.

El mecanismo de la mayoría de seguidores solares de dos ejes está basado en dos motores eléctricos y un dispositivo electrónico de ajuste automático, el cual puede efectuarse básicamente a partir de dos técnicas: la de lazo cerrado y la de lazo abierto. La técnica de lazo cerrado se caracteriza por la necesidad de contar con algún tipo de sensor que localice la posición del Sol, de forma que la trasmita al control de los motores. Lo más usual es que estos sensores se compongan de células fotovoltaicas, fotorresistencias (LDR) o sensores en chip [48]. Por el contrario, el lazo abierto consiste en incorporar al seguidor algún tipo de dispositivo electrónico programable (como un microchip o un ordenador) al cual se le introducen unos algoritmos capaces de calcular la posición del Sol a partir de las coordenadas del lugar y de la hora solar. Es por ello, que muchos seguidores incorporan un dispositivo GPS, de forma que no sea necesario introducir ningún dato manualmente. Debido a todo lo anterior, los seguidores de lazo abierto funcionan independientemente de la posición real del Sol; en consecuencia, estos seguidores son capaces de alinearse incluso en días nublados. En la práctica la mayoría de los seguidores utilizados en los sistemas HCPV complementan ambos métodos. Por último, cabe mencionar que los mecanismos de seguimiento han de ser diseñados, lógicamente, en función del peso, aceptancia angular y dimensiones del dispositivo HCPV que albergan [39, 49].

JUSTIFICACIÓN

La alta concentración fotovoltaica es una tecnología joven y en desarrollo que ha mostrado resultados prometedores y un gran potencial de crecimiento en los últimos años. En este tiempo, se han creado un gran número de empresas que desarrollan sistemas basados en esta tecnología y las instalaciones de alta concentración fotovoltaica han pasado de sumar algunos pocos kilovatios situados en laboratorios especializados, a formar grandes proyectos comerciales de varios megavatios [32]. Sin embargo, la potencia total instalada de sistemas CPV es muy pequeña —360 MW— en comparación con el total de la fotovoltaica —242 GW— [23, 32]. A pesar de esto, estudios recientes muestran que los sistemas de generación de electricidad basados en esta tecnología pueden penetrar con fuerza en el mercado energético en los próximos años [42, 50, 51, 52]. Hay que tener en cuenta que después de más de 30 años de investigación en el campo de la alta concentración fotovoltaica, esta fuente de energía renovable por fin está llegando a ser competitiva [29, 53]. En esa misma línea, un estudio reciente [54] ha concluido que, en la mayoría de los países estudiados, la tecnología de alta concentración fotovoltaica podría disminuir en los próximos años su LCOE por debajo del de los sistemas fotovoltaicos convencionales.

Con todo, es todavía necesario seguir realizando esfuerzos en investigación y desarrollo con el objeto de que se genere la confianza necesaria en los potenciales inversores y promotores para que las anteriores expectativas se hagan realidad.

Un aspecto de estudio identificado como fundamental es el análisis del comportamiento de los sistemas HCPV bajo condiciones reales de operación. Esto es debido a que el conocimiento al respecto, en comparación con el relacionado con los sistemas fotovoltaicos convencionales, es muy escaso [55, 56, 57].

Una diferencia fundamental entre los dispositivos HCPV y PV es la influencia que la distribución espectral de la radiación solar tiene en su respuesta eléctrica [58]. Esto se puede explicar teniendo en cuenta que la tecnología HCPV utiliza células MJ, caracterizadas por utilizar varias subcélulas con ancho de banda de energía diferente, asociadas en serie [55, 59]. Además, es de destacar que los módulos HCPV se equipan con dispositivos ópticos que introducen una fuerte dependencia angular y modifican la distribución espectral solar que incide en la superficie de las células [60, 61]. Todo esto hace que los dispositivos HCPV sean más sensibles a la distribución del espectro solar que los fotovoltaicos convencionales. Sin embargo, existe todavía un desconocimiento cuantitativo sobre la influencia del espectro en estos sistemas para distintas escalas temporales en emplazamientos con condiciones atmosféricas dispares. Asimismo, la diferencia en el comportamiento espectral entre esta tecnología y la PV convencional requiere un mayor conocimiento. Es por tanto necesario estudiar y analizar el impacto que producen las variaciones espectrales en el rendimiento de los sistemas HCPV con un mayor nivel de detalle. Es importante señalar que esta tecnología, al igual que la

fotovoltaica convencional, también se ve afectada por la radiación solar incidente y la temperatura.

El análisis del funcionamiento de la tecnología de alta concentración fotovoltaica en condiciones de funcionamiento a Sol real y, sobre todo, el estudio de la influencia de la distribución espectral de la radiación solar en los dispositivos HCPV es clave en el desarrollo de modelos teóricos que permitan predecir adecuadamente el comportamiento de este tipo de sistemas. De esta forma, investigadores e ingenieros podrían hacer estimaciones precisas del comportamiento de los mismos en localidades con diferentes condiciones climáticas. Además, esto abriría la puerta a la optimización de los sistemas HCPV para maximizar la producción energética en función de las características espectrales de cada emplazamiento.

En la actualidad existen modelos que permiten estimar la potencia máxima de un módulo HCPV y que consideran la distribución espectral incidente de forma detallada [62, 63, 64]. Estos modelos permitirían, en principio, estudios espectrales similares a los planteados en esta tesis. Sin embargo, estos modelos presentan un alto grado de complejidad y requieren la utilización de dispositivos específicos o el conocimiento de las propiedades físicas de los materiales que lo forman. Esto hace que su aplicación sea inviable en la mayoría de los casos [65]. Debido a esto, también se puede concluir que uno de los problemas que presenta la tecnología de alta concentración fotovoltaica es el de carecer de métodos simples y exactos que permitan predecir el comportamiento espectral de este tipo de dispositivos bajo condiciones reales de operación. En consecuencia, los estudios sobre este aspecto presentan un gran interés y novedad.

OBJETIVOS

El objetivo final de esta tesis doctoral es **analizar y cuantificar el impacto de la distribución espectral de la radiación solar incidente en los dispositivos de alta concentración fotovoltaica para distintas zonas climáticas y escalas temporales**. Para alcanzar este objetivo principal se han planteado los siguientes objetivos intermedios:

1. **Analizar y comparar algunos de los modelos existentes para el cálculo de la potencia máxima de los dispositivos HCPV en condiciones reales de operación.** Los modelos actuales que permiten predecir la potencia generada por un módulo HCPV, bajo ciertas condiciones ambientales, presentan distintos niveles de complejidad y requieren medidas específicas de diversos instrumentos para su aplicación [65]. El primer objetivo intermedio que se plantea es el de analizar algunos de estos modelos y estudiar el comportamiento de los mismos frente a las variaciones espectrales. Los resultados que se obtengan con este análisis permitirán discernir, de forma experimental, si es necesario incluir una corrección debida a la influencia espectral en los modelos de predicción del comportamiento eléctrico de los sistemas HCPV.

2. **Estudiar y aplicar algunos de los índices y métodos de estimación del impacto espectral existentes para dispositivos fotovoltaicos y desarrollar uno aplicable a la tecnología HCPV.** Se pretende identificar y analizar que índices y métodos existen y validar las estimaciones basadas en los mismos a partir de la comparación de estos con medidas experimentales realizadas bajo condiciones reales de operación. Además, se intentará desarrollar una alternativa a estos índices y modelos aplicable a la tecnología HCPV.

3. **Analizar la influencia individual de los principales parámetros atmosféricos en el comportamiento espectral de los dispositivos HCPV.** La distribución espectral de la radiación solar está determinada por distintos parámetros atmosféricos. El estudio de series temporales de algunos de ellos posibilitan analizar el impacto espectral en los dispositivos HCPV. Este enfoque ha sido ya utilizado por varios autores [62, 66]. En concreto, los parámetros atmosféricos que se suelen considerar tienen una mayor influencia en la distribución espectral de la radiación solar son, en orden de importancia, la masa de aire (*air mass*, AM), la profundidad óptica de aerosoles *(aerosol optical depth*, AOD) y el agua precipitable (*precipitable water*, PW) [67]. Sería muy útil, por consiguiente, alcanzar un entendimiento profundo de la relación existente entre estos parámetros y la respuesta espectral de los sistemas HCPV. Para ello, el primer paso es cuantificar de forma individualizada la influencia de los mismos en la distribución espectral de la radiación, y por lo tanto, en el comportamiento espectral de los dispositivos HCPV.

4. **Analizar teóricamente el impacto espectral en los dispositivos HCPV bajo diferentes condiciones atmosféricas.** Una vez conocido el impacto espectral individual que producen los valores de los parámetros atmosféricos más influyentes, se hace necesario estudiar el peso real de los mismos bajo condiciones reales de operación. Esto es debido a que podría ocurrir, por ejemplo, que un cierto parámetro fuera muy influyente pero que su valor respecto a las condiciones estándar de medida (CEM) variase poco en la mayoría de climas; o al contrario: que un parámetro de poca influencia tuviera grandes variaciones en una determinada localización a lo largo del año, lo que podría acarrear un comportamiento de los sistemas HCPV distinto al esperado. Por consiguiente, es necesario evaluar el impacto espectral individual de los parámetros atmosféricos bajo condiciones reales de operación, durante al menos un año, para diversas tecnologías de alta concentración fotovoltaica y diferentes perfiles climatológicos.

5. **Analizar las pérdidas energéticas espectrales anuales en los dispositivos HCPV en función de la latitud.** Teniendo en cuenta que, en primera aproximación, la masa de aire está determinada exclusivamente por la posición aparente del Sol [68] y que la misma es, en principio, el parámetro atmosférico más influyente [67], parece interesante analizar las pérdidas y ganancias espectrales en función de la latitud y el peso de estas en el impacto espectral total de los sistemas HCPV bajo condiciones reales de operación.

6. De forma independiente a lo anterior y con el propósito de, primero, adquirir un conocimiento mayor sobre el rendimiento energético de la tecnología HCPV en condiciones reales de operación y, segundo, examinar las ventajas y desventajas de la misma respecto al resto de tecnologías fotovoltaicas, se ha planteado como objetivo adicional de esta tesis **estimar comparativamente el impacto espectral en la generación de los sistemas HCPV y PV, bajo diferentes condiciones climáticas, a escala tanto mensual como anual.**

PUBLICACIONES

A continuación se especifican las publicaciones donde han sido desarrollados los análisis y estudios necesarios para la consecución de los objetivos planteados.

El **primer objetivo** planteado —**analizar y comparar algunos de los modelos existentes para el cálculo de la potencia máxima de los dispositivos HCPV en condiciones reales de operación**— fue abordado en la publicación:

1. **Soria-Moya, A.**, Almonacid Cruz, F., Fernández, E. F., Rodrigo, P., Mallick, T. K. y Pérez-Higueras, P. (2015). *Performance Analysis of Models for Calculating the Maximum Power of High Concentrator Photovoltaic Modules. Photovoltaics, IEEE Journal of, 5*(3), 947-955.

En este artículo se seleccionaron cuatro modelos que permitían la estimación de la potencia de un módulo a partir, únicamente, de parámetros atmosféricos, fácilmente accesibles desde bases de datos o desde las medidas proporcionadas por una estación meteorológica. La idea era evitar aquellos modelos que necesitaban sofisticados y caros instrumentos de medida (como espectrorradiómetros), información detallada de los materiales que forman el módulo, que no suele estar disponible, un conocimiento avanzado de física de semiconductores u óptica, o complejos programas de ordenador especializados [65]. Los modelos elegidos fueron los siguientes:

- El estándar americano *ASTM E2527* [69].
- Un modelo basado en coeficientes lineales introducido por Fernández et al. [70].
- El modelo propuesto por *Sandia National Laboratories* [71].
- Un modelo basado en redes neuronales artificiales (RNA) introducido por Almonacid et al. [72].

Los resultados mostraron que los cuatro métodos tienen un comportamiento adecuado en la estimación de la potencia máxima de varios módulos HCPV de diferentes fabricantes. No obstante, el que peor resultados obtuvo —el estándar ASTM E2527— fue justamente el que no tenía en cuenta ninguna corrección espectral. El que mejor estimó la potencia de los módulos fue el basado en redes neuronales, lo que puede ser explicado teniendo en cuenta que el modelo incluye una corrección en función de la velocidad del viento y una corrección espectral adicional dependiente del agua precipitable, que los otros tres modelos no recogen,

Los resultados alcanzados en el desarrollo del **segundo objetivo —estudiar y aplicar algunos de los índices y métodos de estimación del impacto espectral existentes para dispositivos fotovoltaicos y desarrollar uno aplicable a la tecnología HCPV—** se desarrollaron en los dos siguientes artículos:

2. Fernández, E. F., Almonacid, F., Ruiz-Arias, J. A. y **Soria-Moya, A.** (2014). *Analysis of the spectral variations on the performance of high concentrator photovoltaic modules operating under different real climate conditions. Solar Energy Materials and Solar Cells,* 127, 179-187.

3. Fernández, E. F., Almonacid, F., **Soria-Moya, A**. y Terrados, J. (2015). *Experimental analysis of the spectral factor for quantifying the spectral influence on concentrator photovoltaic systems under real operating conditions. Energy*, 90, 1878-1886.

En la publicación número dos, se expone que el índice más útil para analizar el impacto espectral en el rendimiento de un dispositivo fotovoltaico es el *spectral factor* (SF), que está definida en el IEC (*International Electronic Commision*) 60904-7, para dispositivos fotovoltaicos basados en células de una sola unión [73, 74]. No obstante, el SF tal y como estaba formulado, no es válido para los dispositivos HCPV. Para paliar esta carencia, se propuso una reformulación de este índice que sí es aplicable a los sistemas de alta concentración fotovoltaicos.

En la publicación número tres, se efectuó un estudio comparativo entre las estimaciones teóricas realizadas a partir del SF reformulado y los resultados reales efectuados con medidas experimentales. Los resultados obtenidos mostraron que el SF estima ganancias espectrales algo mayores que las que realmente se producen en la potencia, lo que implica que el SF tiene mayor sensibilidad que la misma. A raíz de esto, se introdujo un nuevo índice, que se denominó SF_p, basado en la potencia. Los análisis realizados revelaron que el nuevo índice se ajusta mejor que el SF al comportamiento real espectral de un dispositivo HCPV en potencia. No obstante, es destacable el hecho de que ambos índices arrojaron una precisión elevada y muy parecida entre sí: la diferencia media de sus RMSE fue de aproximadamente el 0.5%. Este resultado, junto con el resto de los análisis realizados, llevó a la conclusión de que el SF puede ser considerado un buen índice, con un nivel de precisión aceptable, para la evaluación de la influencia espectral en la potencia y energía generada por un sistema HCPV bajo condiciones reales de operación.

El **tercer objetivo —analizar la influencia individualizada de los parámetros atmosféricos en el comportamiento espectral de los dispositivos HCPV—** fue abordado en la publicación:

2. Fernández, E. F., Almonacid, F., Ruiz-Arias, J. A. y **Soria-Moya, A.** (2014). *Analysis of the spectral variations on the performance of high concentrator photovoltaic modules operating under different real climate conditions. Solar Energy Materials and Solar Cells,* 127, 179-187.

En el artículo se analizó la influencia individualizada de los factores atmosféricos con más peso en la determinación de la distribución espectral de la radiación, que son los siguientes: la masa de aire, la profundidad óptica de aerosoles y el agua precipitable [60, 62].

Para ello, se simularon, con la ayuda del modelo *Simple Model of the Atmospheric Radiative Transfer of Sunshine* (SMARTS) [75], varias distribuciones espectrales, a partir de la variación de los parámetros atmosféricos más influyentes, y se calculó la respuesta de cuatro módulos HCPV de diferentes materiales.

Los resultados mostraron que, independientemente del módulo HCPV estudiado, los parámetros que mayor impacto tienen son, en orden de importancia, la masa de aire, la profundidad óptica de los aerosoles (que se estudió a 0.55 μm), el agua precipitable y el índice de Ångstrom. Es de destacar que la diferencia del impacto espectral debido a los dos primeros parámetros es considerablemente mayor que el causado por los dos últimos, los cuales influyen de forma muy leve.

El cuarto objetivo —analizar teóricamente el impacto espectral en los dispositivos HCPV bajo diferentes condiciones atmosféricas— se desarrolló en el siguiente artículo:

4. Fernández, E. F., **Soria-Moya, A.**, Almonacid, F y Aguilera, J. (2016). *Comparative assessment of the spectral impact on the energy yield of high concentrator and conventional photovoltaic technology, Solar Energy Materials and Solar Cells,* 147, 185-197.

Para la consecución de este objetivo, se evaluó el impacto espectral causado por la variación de los parámetros atmosféricos estudiados en el objetivo tercero, bajo condiciones reales de operación durante más de un año, para diversas tecnologías de alta concentración fotovoltaica.

Para realizar este análisis, se seleccionaron las siguientes cinco localidades, las cuales representan condiciones climáticas diversas en diferentes continentes y latitudes:

- Solar Village (Arabia Saudí): N 24º54’25’’, E 46º23’49’’
- Alta Floresta (Brasil): S 09º52’15’’, W 56º06’14’’
- Frenchman Flat (EUA): N 36º48’’32’’, W 115º56’06’’
- Granada (España): N 37º09’50’’, W 03º36’18’’
- Beijing (China): N 39º58’37’’, E 116º22’51’’

Para todas las localizaciones estudiadas se calcularon las pérdidas espectrales anuales en comparación con el espectro de referencia. El mejor comportamiento fue el correspondiente a Alta Foresta —donde se registran AM bajos y PW elevados—, con un impacto anual de entre -3.9% y -5.2%. Unos resultados parecidos se observaron en el estudio de Frenchman Flat, donde a pesar de que la AM es algo más elevada que en Alta Foresta, la profundidad óptica de aerosoles es mucho menor. Los resultados obtenidos

para Granada y Solar Village fueron muy similares entre sí, ya que el mayor valor de la profundidad óptica de aerosoles de Solar Village respecto a Granada se compensa con su AM levemente menor. En Beijing, el excepcionalmente alto valor de la profundidad óptica de aerosoles, produce un impacto espectral anual de entre -26.5% y -30.6%.

El quinto objetivo —analizar las pérdidas energéticas espectrales anuales en dispositivos HCPV en función de la latitud— se abordó en el siguiente artículo:

3. Fernández, E. F., Almonacid, F., **Soria-Moya, A**. y Terrados, J. (2015). *Experimental analysis of the spectral factor for quantifying the spectral influence on concentrator photovoltaic systems under real operating conditions. Energy*, 90, 1878-1886.

En dicha publicación se expone que las pérdidas espectrales anuales pueden ser consideradas independientes de la latitud hasta un valor de esta de 30^{o}. Las pérdidas obtenidas, para los dos módulos estudiados, fueron en ese rango de entre el 4% y el 5%. Para valores mayores de 30^{o}, las pérdidas espectrales se incrementan sensiblemente a medida que la latitud aumenta, hasta alcanzar unos valores de entre el 12% y el 15%. No obstante, a partir de los 75^{o}, las pérdidas espectrales se comportan de forma constante frente a la latitud.

El **sexto objetivo —la estimación comparativa del impacto espectral en la generación energética entre la tecnología HCPV y la PV, bajo diferentes condiciones climáticas, a escala tanto mensual como anual**— se dio por superado a raíz de la publicación del siguiente artículo, ya comentado:

4. Fernández, E. F., **Soria-Moya, A.**, Almonacid, F y Aguilera, J. (2016). *Comparative assessment of the spectral impact on the energy yield of high concentrator and conventional photovoltaic technology, Solar Energy Materials and Solar Cells,* 147, 185-197.

Para la realización de esta investigación se emplearon distintos materiales fotovoltaicos. El análisis realizado confirmó que, en general, los dispositivos HCPV son, bajo condiciones reales de operación, mucho más sensibles a las variaciones espectrales que los fotovoltaicos convencionales, tanto en la influencia individualizada de los diferentes parámetros como en su impacto energético, mensual y anual. Es de destacar que entre los materiales convencionales, el silicio amorfo fue el que presentó una mayor sensibilidad a las variaciones espectrales.

Los resultados arrojaron una diferencia anual media de las pérdidas energéticas entre los dispositivos HCPV y PV estudiados, en todas las localizaciones, de aproximadamente un 5%.

CONCLUSIONES y LINEAS FUTURAS

Con el desarrollo de esta tesis doctoral se pretendía realizar aportaciones relevantes que ayudaran a elevar el nivel de conocimiento existente sobre la tecnología de alta concentración fotovoltaica (HCPV) y, en concreto, sobre el impacto producido por las variaciones en la distribución espectral de la radiación solar bajo condiciones reales de operación en diferentes climas y escalas temporales. A continuación, se exponen las principales conclusiones alcanzadas:

- Los actuales modelos basados en parámetros atmosféricos fácilmente accesibles desde bases de datos son válidos para estimar la potencia y energía producida por un módulo HCPV al cabo de un año.

- La influencia de las variaciones espectrales en la respuesta eléctrica de los sistemas HCPV necesita ser tenida en cuenta.

- Los parámetros atmosféricos de mayor impacto espectral en el comportamiento de un dispositivo HCPV son, en este orden, la masa de aire (AM) y la profundidad óptica de aerosoles para λ = 0.55 μm ($\tau_{0.55}$); por el contrario, el exponente de Ångstrom (α) y el agua precipitable (PW) tienen una influencia pequeña. Esto significa que, en la mayoría de los casos, la respuesta a las variaciones espectrales de los sistemas HCPV bajo condiciones reales de operación pueden ser estimadas, con un margen de error aceptable, teniendo en cuenta solo la influencia de la AM y del $\tau_{0.55}$. Por el contrario, una corrección espectral utilizando únicamente la AM es solo válida para localizaciones caracterizadas por un nivel bajo de la profundidad óptica de aerosoles.

- El índice SF (*spectral factor*) que está adaptado a los dispositivos HCPV tiene una sensibilidad espectral mayor que la potencia. Con todo, los resultados evidencian que este índice podría ser considerado una herramienta útil para la evaluación, en primera aproximación, de la influencia espectral en la potencia máxima. En ese sentido, la estimación de la potencia de salida usando el SF como un factor de corrección mejora significativamente el resultado obtenido sin considerar ninguna otra corrección espectral. En particular, el error cuadrático medio (RMSE) decrece aproximadamente un 1.1% y el valor del coeficiente de determinación (R^2) se acerca más a la unidad. Tanto la influencia espectral en la potencia como el SF pueden ser relacionados de forma más precisa utilizando una ecuación lineal aproximada.

- El SF pude ser considerado un buen índice para estimar las pérdidas energéticas anuales, ya que la máxima desviación que se encontró fue del -2%.

- No se ha encontrado relación entre las pérdidas espectrales y la latitud para valores de la misma de menos de 30º. Para latitudes mayores, las pérdidas crecen

fuertemente a medida que ésta aumenta. A partir de los 75º las pérdidas espectrales vuelven a ser prácticamente constantes, con un valor entre el -12% y el -14%.

- Los módulos con células *metamorphic-mismatched* (MM) y lentes silicone-on-glass (SOG) registran menos pérdidas espectrales que los formados por células *lattice-matched* LM o lentes *poly-methylmethacrylate* (PMMA). Esto puede ser debido a que el ancho de energía de la subcélula superior de la MM es más estrecha que la de la LM, y a que la lente de SOG tiene una transmitancia más alta que la de PMMA en la región espectral que compete a dicha subcélula.

- Los dispositivos HCPV evidencian claramente una dependencia espectral sensiblemente más elevada que los PV. En concreto, las pérdidas espectrales, en la energía, encontradas para los dispositivos HCPV variaron entre el -0.6% y el -33.5%. Por otro lado, para los dispositivos PV se registraron ganancias espectrales desde el 8.6% hasta pérdidas del -5.6%.

- Los módulos de silicio amorfo (a-Si) y de teluro de cadmio (CdTe) presentan una dependencia espectral similar entre sí y sustancialmente mayor que la de los otros módulos de fotovoltaica convencional.

- Tanto los dispositivos HCPV como los PV tienen un comportamiento estacional en relación a las pérdidas espectrales.

- Los actuales sistemas HCPV presentan unas pérdidas energéticas anuales medias de aproximadamente el 5% más que los dispositivos de tecnología fotovoltaica convencional en sitios considerados representativos. Esto indica que la sensibilidad espectral de los módulos HCPV no es una limitación crucial para la expansión del mercado de la tecnología de alta concentración fotovoltaica. Sobre todo teniendo en cuenta que sus eficiencias de conversión son mucho más altas que las de la fotovoltaica convencional.

Independientemente de lo anterior, es importante destacar que existe poco conocimiento sobre la influencia de las variaciones de la distribución espectral de la radiación solar en la potencia de salida de un módulo fotovoltaico bajo los diferentes tipos y grados de nubosidad existentes. En ese sentido, es necesaria una herramienta que pueda estimar la distribución del espectro en días nublados a partir de un modelo de nubosidad simple, el cual también estaría por desarrollar.

La mayor parte de los sistemas fotovoltaicos convencionales se instalan en estructuras fijas, por lo que el ángulo de incidencia de los rayos solares respecto a su superficie activa varía. Algunos resultados parciales de la presente tesis doctoral, además de algunos autores [76], indican que es probable que el ángulo de incidencia determine en parte la influencia espectral, lo que significaría que módulos fotovoltaicos de las mismas características, pero instalados con inclinaciones diferentes, tendrían una respuesta

espectral también diferente. Por consiguiente, y aunque las pérdidas espectrales en la tecnología fotovoltaica convencional no son muy elevadas, podría ocurrir que los valores de inclinación de los sistemas fotovoltaicos fijos que siempre se han dado por óptimos no fueran tales.

Revestiría también de interés comparar el principal índice que ha sido empleado en esta tesis —el SF— con otros ampliamente utilizados por la comunidad científica dedicada al campo de la concentración fotovoltaica, como son el *Spectral matching Ratio* (SMR) o el parámetro espectral Z. Esto sería útil para comprender mejor el índice SF y su relación con otros procedimientos de caracterización espectral.

Por otro lado, a pesar de su baja aceptancia angular, los sistemas HCPV aprovechan parte de la denominada circumsolar proveniente de la región que rodea al Sol. La distribución angular y espectral de esta radiación varía principalmente según sea la concentración de aerosoles [77]. Durante el desarrollo de esta tesis siempre se ha supuesto un ángulo de aceptancia fijo para todos los módulos estudiados y una eficiencia angular óptima. Sería por lo tanto interesante estudiar la influencia que tienen los aerosoles en la radiación circumsolar, con el objeto de evaluar la influencia de la misma en la salida eléctrica de los módulos de alta concentración fotovoltaica.

REFERENCIAS

[1] International Energy Agency, «Key World Energy Statistics,» 2015.

[2] International Energy Agency, «Key World Energy Statistics,» 2016.

[3] International Energy Agency - PVPS, «Trends in photovoltaic applications. Executive summary,» 2015.

[4] Internation Energy Agency, «World Energy Outlock,» 2010.

[5] J. Murray y D. King, «Oil's tipping point has passed,» *Nature,* nº 481, pp. 433-435, 2012.

[6] R. Heinberg, Searching for a Miracle. 'Net Energy' Limits & the Fate of Industrial Society, Post Carbon Institute, 2009.

[7] L. Legget y D. Ball, «The implication for climate change and peak fossil fuel of the continuation of the current trend in wind and solar energy production,» *Energy Policy,* vol. 41, p. 610–617, 2012.

[8] S. Mohr, *Projection of World Fossil Fuel Production with Supply and Demand Interactions. Ph.D Thesis,* University of Newcastle. Australia, 2010.

[9] K. Aleklett, M. Höök, K. Jakobsson, M. Lardelli, S. Snowden y B. Söderbergh, «The Peak of the Oil Age – Analyzing the world oil production Reference Scenario in World Energy Outlook 2008,» *Energy Policy,* vol. 38, nº 3, pp. 1398-1414, 2012.

[10] G. Maggio y G. Cacciola, «When will oil, natural gas, and coal peak?,» *Fuel,* vol. 98, pp. 111-123, 2012.

[11] A. García-Olivares y J. Ballebrera-Poy, «Energy and mineral peaks, and a future steady state economy,» *Technological Forecasting & Social Change,* vol. 90B, pp. 587-598, 2015.

[12] R. Pachauri y L. Meyer, «Climate Change 2014: Synthesis Report. Contribution of Working Groups I, II and III to the Fifth Assessment Report of the Intergovernmental Panel on Climate Change,» Genova, 2014.

[13] UNFCCC, «Adoption of the Paris Agreement.,» de *FCCC/CP/2015/L.9/Rev.1*, Paris, 2015.

[14] European Commission, «Horizon 2020 - The EU Framework Programme for Research and Innovation,» [En línea]. Available: https://ec.europa.eu/programmes/horizon2020/en. [Último acceso: 18 Abril 2017].

[15] A. García-Olivares, «Substitutability of Electricity and Renewable Materials for Fossil Fuels in a Post-Carbon Economy,» *Energies,* vol. 8, nº 12, pp. 13308-13343, 2015.

[16] A. García-Olivares, J. Ballebrera-Poy, E. Garcia-Ladona y A. Turiel, «A global renewable mix with proven technologies and common materials,» *Energy Policy,* vol. 41, pp. 561-574, 2012.

[17] A. García-Olivares, «Substituting silver in solar photovoltaics is feasible and allows for decentralization in smart,» *Environmental Innovation and Societal Transitions,* vol. 17, pp. 15-21, 2015.

[18] G. Pleßmann, M. Erdmann, M. Hlusiak y C. Breyer, «Global energy storage demand for a 100% renewable electricity supply,» *Energy Procedia ,* vol. 46, pp. 22-31, 2014.

[19] M. Jacobson y M. Delucchi, «Providing all global energy with wind, water, and solar power, part I: technologies, energy resources, quantities and areas of infrastructure, and materials,» *Energy Policy,* vol. 39, nº 3, pp. 1154-1169, 2011.

[20] M. Delucchi y M. Jacobson, «Providing all global energy with wind, water, and solar power, part II: reliability, system,» *Energy Policy,* vol. 39, nº 3, pp. 1170-1190, 2011.

[21] B. Mathiesen, H. Lund, D. Connolly, H. Wenzel, P. Østergaard, B. Möller, S. Nielsen, I. Ridjan, P. Karnøe, K. Sperling y F. Hvelplund, «Smart Energy Systems for coherent 100% renewable energy and transport solutions,» *Applied Energy,* vol. 145, pp. 139-154, 2015.

[22] International Energy Agency, «Technology Roadmap. Solar Photovoltaic Energy,» París, 2014.

[23] Fraunhofer Institute for Solar Energy, «Photovoltaic Report,» Friburgo, 2016.

[24] A. Feltrin y A. Freundlich, «Material considerations for terawatt level deployment of photovoltaics,» *Renewable Energy,* vol. 33, nº 2, pp. 180-185, 2008.

[25] T. M. Razykov, C. Ferekides, D. Morel, E. Stefanakos, H. Ullal y H. Upadhyaya, «Solar photovoltaic electricity: Current status and future prospects,» *Solar Energy,* vol. 85, nº 8, pp. 1580-1608, 2011.

[26] P. Pérez-Higueras y E. Fernández, High Concentrator Photovoltaics. Fundamentals, Engineering and Power Plants, Springer, 2015.

[27] Globaldata, «Globaldata. Concentrated Photovoltaics (CPV) – Global Market Size, Competitive Landscape and Key Country Analysis to 2020. 2014;UK.,» 2014.

[28] D. Talavera, P. Pérez-Higueras, F. Almonacid y E. Fernández, «A worldwide assessment of economic feasibility of HCPV power plants: Profitability and competitiveness,» *Energy,* vol. 119, pp. 408-424, 2017.

[29] A. Luque, G. Sala y I. Luque-Heredia, «Photovoltaic concentration at the onset of its commercial deployment,» *Progress in Photovoltaics: Research and Applications,* vol. 14, nº 5, pp. 413-428, 2006.

[30] P. Pérez-Higueras, E. Muñoz, G. Almonacid y P. Vidal, «High Concentrator PhotoVoltaics efficiencies: Present status and forecast,» *Renewable and Sustainable Energy Reviews, 15 (4), pp. 1810-1815,* vol. 15, nº 4, pp. 1810-1815, 2011.

[31] K. Shanks, S. Senthilarasu y T. Mallick, «Optics for concentrating photovoltaics: Trends, limits and opportunities for materials and design,» *Renewable and Sustainable Energy Reviews,* vol. 60, pp. 394-407, 2016.

[32] Fraunhofer Institute for Solar Energy; National Renewable Energy Laboratory, «Current status of Concentrator Photovoltaic (CPV) Thecnology,» Friburgo; Golden, 2016.

[33] V. Fthenakis y H. Kim, «Life cycle assessment of high-concentration photovoltaic systems,» *Progress in Photovoltaics: Research and Applications,* vol. 21, nº 3, pp. 379-388, 2013.

[34] F. Gómez-Gil, X. Wang y A. Barnett, «Energy production of photovoltaic systems: Fixed, tracking, and concentrating,» *Renewable and Sustainable Energy Reviews,* vol. 16, nº 1, pp. 306-313, 2012.

[35] M. Meusel, R. Adelhelm, F. Dimroth, A. Bett y W. Warta, «Spectral mismatch correction and spectrometric characterization of monolithic III–V multi-junction solar cells,» *Progress in Photovoltaics:*

Research and Applications, vol. 10, nº 4, pp. 243-255, 2002.

[36] M. L. Cohen y T. K. Bergstresser, «Band structures and pseudopotential form factors for fourteen semiconductors of the diamond and zinc-blende structures,» *Physical Review,* vol. 141, nº 2, p. 789, 1966.

[37] W. Guter, J. Schöne, S. P. Philipps, M. Steiner, G. Siefer, A. Wekkeli y F. Dimroth, «Current-matched triple-junction solar cell reaching 41.1% conversion efficiency under concentrated sunlight,» *Applied Physics Letters,* vol. 94, nº 22, p. 223504, 2009.

[38] A. Walker, O. Theriault, M. M. Wilkins, J. F. Wheeldon y K. Hinzer, «Tunnel-junction-limited multijunction solar cell performance over concentration,» *Selected Topics in Quantum Electronics, IEEE Journal of,* vol. 19, nº 5, pp. 1-8, 2013.

[39] A. Luque y V. Andreev, Concentrator Photovoltaics, Springer, 2007.

[40] M. Yamaguchi, T. A. K. Takamoto y N. Ekins-Daukes, «Multi-junction III-V solar cells: Current status and future potential,» *Solar Energy,* vol. 79, nº 1, pp. 78-85, 2005.

[41] R. R. King, D. Bhusari, D. Larrabee, X. Liu, E. Rehder, K. Edmondson, H. Cotal, R. K. Jones, J. H. Ermer, C. M. Fetzer, D. C. Law y N. H. Karam, «Solar cell generations over 40% efficiency,» *Progress in Photovoltaics: Research and Applications,* vol. 20, nº 6, pp. 801-815, 2012.

[42] F. Dimroth, M. Grave, P. F. U. Beutel, C. Karcher, T. N. Tibbits, ... y A. Bett, «Wafer bonded four-junction GaInP/GaAs//GaInAsP/GaInAs concentrator solar cells with 44.7% efficiency,» *Progress in Photovoltaics: Research and Applications,* vol. 22, nº 3, pp. 277-282, 2014.

[43] M. A. Green, K. Emery, Y. Hishikawa, W. Warta, E. Dunlop, D. H. Levi y A. W. Y. Ho-Baillie, «Solar cell efficiency tables (version 49),» *Progress in Photovoltaics: Research and Applications,* vol. 25, nº 1, pp. 3-13, 2017.

[44] Censolar, Sistemas de conversión eléctrica, Sevillla: PROGENSA, 2016.

[45] G. Zubi, J. Bernal-Agustín y G. Fracastoro, «High concentration photovoltaic systems applying III-V cells,» *Renewable and Sustainable Energy Reviews,* vol. 13 , nº 9, pp. 2645-2652, 2009.

[46] W. Xie, Y. Dai, R. Wang y K. Sumathy, «Concentrated solar energy applications using Fresnel lenses: A review,» *Renewable and Sustainable Energy Reviews,* vol. 15, nº 6, pp. 2588-2606, 2011.

[47] M. Victoria, C. Dońminguez, I. Anťon y G. Sala, «Comparative analysis of different secondary optical elements for aspheric primary lenses,» *Optics Express,* vol. 17, nº 9, pp. 6487-6492, 2009.

[48] G. Prinsloo, Solar Tracking, Sun Tracking, Sun Tracker, Solar Tracker, Follow Sun, Sun Position, eBook, 2015.

[49] I. Luque-Heredia, G. Quéméré, R. Cervantes, O. Laurent, E. Chiappori y J. Chong, The Sun Tracker in Concentrator Photovoltaics. Next Generation of Photovoltaics, Springer Berlin Heidelberg, 2012.

[50] K. Ghosal, S. Burroughs, K. Heuser, D. Setz y E. Garralaga-Rojas, «Performance results from micro-cell based high concentration photovoltaic research development and demonstration systems,» *Progress in Photovoltaics: Research and Applications, ,* vol. 21, nº 6, pp. 1370-1376, 2013.

[51] K. Ghosal, D. Lilly, J. Gabriel, M. Whitehead, S. Seel, B. Fisher, J. Wilson y S. Burroughs, «Semprius field results and progress in system development,» *Photovoltaics, IEEE Journal of,* vol. 4, nº 2, pp. 703-

708, 2014.

[52] F. Dimroth, T. Roesener, S. Essig, C. Weuffen, A. Wekkeli, E. Oliva, G. Siefer, K. Volz, T. Hannappel, D. Haussler, W. Jager y A. Bett, «Comparison of direct growth and wafer bonding for the fabrication of GaInP/GaAs dual-junction solar cells on silicon,» *Photovoltaics, IEEE Journal of ,* vol. 4, nº 2, pp. 620-625, 2014.

[53] M. Robert, «Concentrator photovoltaic technologies: Review and market prospects,» *Refocus,* vol. 6, nº 4, p. 35–39, 2005.

[54] D. Talavera, J. Fernández-Ferrer, P. Pérez-Higueras, J. Terrados y E. Fernández, «A worldwide assessment of levelised cost of electricity of HCPV systems,» *Energy Conversion and Management,* vol. 127, pp. 679-692, 2016.

[55] E. Fernández, P. Pérez-Higueras, A. Garcia Loureiro y P. Vidal, «Outdoor evaluation of concentrator photovoltaic systems modules from different manufacturers: First results and steps,» *Progress in Photovoltaics: Research and Applications,* vol. 21, nº 4, pp. 693-701, 2013.

[56] S. Kurtz, M. Muller, D. Jordan, K. Ghosal, B. Fisher, P. Verlinden, J. Hashimoto y D. Riley, «Key parameters in determining energy generated by CPV modules,» *Progress in photovoltaics,* vol. 23, nº 10, pp. 1250-1259, 2015.

[57] J. A. Ruiz-Arias, E. F. Fernández, Á. Linares-Rodríguez y F. Almonacid, « Analysis of the Spatiotemporal Characteristics of High Concentrator Photovoltaics Energy Yield and Performance Ratio,» *IEEE Journal of Photovoltaics,* vol. 7, nº 1, pp. 359-366, 2017.

[58] P. Faine, S. Kurtz, C. Riordan and J. M. Olson, “The influence of spectral solar irradiance variations on the performance of selected single-junction and multi-junctions solar cells,” *Solar Cells,* vol. 31, pp. 259 - 278, 1991.

[59] E. Fernández, G. Siefer, F. Almonacid, A. Loureiro y P. Pérez-Higueras, «A two subcell equivalent solar cell model for III–V triple junction solar cells under spectrum and temperature variations,» *Solar Energy,* vol. 92, pp. 221-229, 2013.

[60] W. McMahon, K. Emery, D. Friedman, L. Ottoson, M. Young, J. Ward, C. Kramer, A. Duda y S. Kurtz, «Fill factor as a probe of current-matching for GaInP/GaAs tandem cells in a concentrator system during outdoor operation,» *Progress in Photovoltaics: Research and Applications,* vol. 16, nº 3, pp. 213-224, 2008.

[61] H. Baig, E. Fernández y T. Mallick, «Influence of spectrum and latitude on the annual optical performance of a dielectric based BICPV system,» *Solar Energy,* vol. 124, pp. 268-277, 2015.

[62] N. Chan, T. B. Young, H. E. Brindley, N. Ekins-Daukes, K. Araki, Y. Kemmoku y M. Yamaguchi, «Validation of energy prediction method for a concentrator photovoltaic module in Toyohashi Japan,» *Progress in Photovoltaics: Reserch and Applications,* 2012.

[63] M. Steiner, G. Siefer, T. Hornung, G. Peharz y A. Bett, «YieldOpt, a model to predict the power output and energy yield for concentrating photovoltaic modules,» *Progress in photovoltaics,* vol. 23, nº 3, pp. 385-397, 2015.

[64] M. Theristis, E. Fernández, M. Sumner y T. O'Donovan, «Multiphysics modelling and experimental validation of high concentration photovoltaic modules,» *Energy Conversion and Management,* vol. 139, pp. 122-134, 2017.

[65] P. Rodrigo, E. Fernández, F. Almonacid y P. Pérez-Higueras, «Models for the electrical characterization of high concentration photovoltaic cells and modules: A review,» *Renewable and Sustainable Energy Reviews,* vol. 26, pp. 752-760, 2013.

[66] M. Muller, B. Marion, S. Kurtz y J. Rodriguez, «An investigation into spectral parameters as they impact CPV module perfromance,» *AIP conference proceedings,* vol. 1, pp. 307-311, 2010.

[67] N. Chan, H. Brindley y N. Ekins-Daukes, «Impact of individual atmospheric parameters on CPV system power, energy yield and cost of energy,» *Progress in Photovoltaics: Research and Applications,* vol. in press, 2013.

[68] M. Iqbal, An introduction to solar radiation, Academic Press, 1983.

[69] «ASTM E2527. Standard test method for electrical performance of concentrator,» *American Society of Testing and Materials,* 2009.

[70] E. Fernández, F. Almonacid, P. Rodrigo y P. Pérez-Higueras, «Model for the prediction of the maximum power of a high concentrator photovoltaic module,» *Solar Energy,* vol. 97, pp. 12-18, 2013.

[71] D. L. King, W. E. Boyson y J. A. Kratochvil, «Sandia National Laboratories. Photovoltaic array performance model SAND2004-3535,» Albuquerque, New Mexico, USA, 2004.

[72] F. Almonacid, E. F. Fernández, P. Rodrigo, P. Pérez-Higueras y C. Rus-Casas, «Estimating the maximum power of a High Concentrator Photovoltaic (HCPV) module using an Artificial Neural Network,» *Energy,* vol. 53, pp. 165-172, 2013.

[73] IEC-60904-7, «Photovoltaic devices - Part 7: Computation of the spectral mismatch correction for measurements of photovoltaic devices,» 2008.

[74] C. R. Osterwald, K. A. Emery y M. Muller, «Photovoltaic module calibration value versus optical air mass: the air mass function,» *Progress in Photovoltaics: Reserch and Application,* 2012.

[75] C. Gueymard, «Simple model of the atmospheric radiative transfer of sunshine (SMARTS) version 2.9.5,» 2009.

[76] A. Amillo, T. Huld, P. Vourlioti, R. Müller y M. Norton, «Application of Satellite-Based Spectrally-Resolved Solar Radiation Data to PV Performance Studies.,» *Energies,* nº 8(5), pp. 3455-3488, 2015.

[77] E. Lorenzo, Radiación solar y dispositivos fotovoltaicos, PROGENSA, 2006.

PARTE II: COMPENDIO

La presente tesis doctoral es un compendio de **cuatro artículos publicados en revistas de calidad reconocida indexadas en el ISI JCR**, las cuales han sido realizadas en el ámbito de la misma. En concordancia a lo que exige el reglamento de doctorado de la Universidad de Jaén, estos artículos deben incluirse obligatoriamente en la memoria y están, por tanto, adjuntados en la segunda parte de la misma. Además, se citan **tres aportaciones relevantes efectuadas en congresos especializados en la tecnología de concentración fotovoltaica** surgidos en el proceso investigador de la presente tesis doctoral.

ARTICULOS PUBLICADOS EN REVISTAS JCR

1. **Soria-Moya, A.**, Almonacid Cruz, F., Fernández, E. F., Rodrigo, P., Mallick, T. K. y Pérez-Higueras, P. (2015). *Performance Analysis of Models for Calculating the Maximum Power of High Concentrator Photovoltaic Modules. Photovoltaics, IEEE Journal of, 5*(3), 947-955.
2. Fernández, E. F., Almonacid, F., Ruiz-Arias, J. A**.** y **Soria-Moya, A.** (2014). *Analysis of the spectral variations on the performance of high concentrator photovoltaic modules operating under different real climate conditions. Solar Energy Materials and Solar Cells, 127*, 179-187.
3. Fernández, E. F., Almonacid, F., **Soria-Moya, A.** y Terrados, J. (2015). *Experimental analysis of the spectral factor for quantifying the spectral influence on concentrator photovoltaic systems under real operating conditions. Energy*, 90, 1878-1886.
4. Fernández, E. F., **Soria-Moya, A.**, Almonacid, F y Aguilera, J. (2016). *Comparative assessment of the spectral impact on the energy yield of high concentrator and conventional photovoltaic technology, Solar Energy Materials and Solar Cells,147, 185-197.*

Referencia / Reference: **Soria-Moya, A.**, Almonacid Cruz, F., Fernández, E. F., Rodrigo, P., Mallick, T. K. y Pérez-Higueras, P. (2015). *Performance Analysis of Models for Calculating the Maximum Power of High Concentrator Photovoltaic Modules. Photovoltaics, IEEE Journal of, 5*(3), 947-955.

Estado / Status: Publicado / Published.

Índice de impacto / Impact Factor: 3.165.

Categoría / Catogory: *Applied Physics*. Ranking: 22/143 (Q1)

Performance Analysis of Models for Calculating the Maximum Power of High Concentrator Photovoltaic Modules

Alberto Soria-Moya, Florencia Almonacid Cruz, Eduardo F. Fernández, Pedro Rodrigo, Tapas K. Mallick, *Member, IEEE*, and Pedro Pérez-Higueras

***Abstract*—Due to its special features, one of the problems of high concentrator photovoltaic (HCPV) technology is the estimation of the electrical output of an HCPV module. Although there are several methods for doing this, only some of them can be applied using easily obtainable atmospheric parameters. In this paper, four models to estimate the maximum power of an HCPV module are studied and compared. The models that have been taken into account are the standard ASTM E2527, the linear coefficient model, the Sandia National Laboratories model, and an artificial neural network-based model. Results demonstrate that the four methods show adequate behavior in the estimation of the maximum power of several HCPV modules from different manufacturers.**

***Index Terms*—High concentrator photovoltaic (HCPV), mathematical methods, maximum power, outdoor measurements.**

I. Introduction

AFTER more than 30 years of research into high concentrator photovoltaics (HCPV), this technology is finally entering the market [1], [2]. Although this technology has not achieved yet the needed momentum, HCPV could be in the power generation market soon because of the high efficiencies already reached and expected for this technology [3]–[8].

HCPV cells and modules operate under concentrations between 300 and 2000 suns. This technology is based on optical devices that focus the light received from the sun on the solar cell surface. A typical HCPV module is composed of multijunction (MJ) solar cells, usually monolithic lattice-matched GaInP/GaInAs/Ge III–V triple-junction solar cells, interconnected in series with one optical device per cell, as well as a Fresnel lens and a secondary optical element that concentrates the light with a ratio of around 500–1000 suns [9]. MJ concentrator solar cells are influenced by changes in irradiance, spectrum, and temperature [10]–[12]. Due to the use of these kinds of cells and optical elements, the performance of HCPV modules are also going to be mainly affected by these parameters [13]–[16].

While there is much experience in the modeling of conventional photovoltaic modules with comparisons among different models having been done, there is a little experience in these kinds of studies in HCPV. Therefore, these kinds of studies present great interest and novelty for HCPV technology. Because of these special features, one of the problems of HCPV technology is the difficulty of finding simple and accurate methods that allow prediction of the output of an HCPV module under real conditions. There are several methods for the estimation of the maximum power of an HCPV module. These models present different levels of complexity and accuracy and require different equipment to be applied [17]. The aim of this paper is to study and compare some of these models. In particular, the models used will be those that estimate the maximum power of an HCPV module from outdoor measurements easy to get or estimate from atmospheric databases in order to facilitate their application. Taking this into account, the only models consider have been the standard ASTM E2527 model [18], the linear coefficient model [19], the Sandia National Laboratories model [20], and an artificial neural network (ANN)-based model [21]. The most of the other methods usually need measurements of specific instruments, detailed information of the materials of the modules which is not always available, and advanced knowledge of semiconductor physics, optics, or different specific software. The analysis and comparison of these models for the prediction of the maximum power of HCPV modules in outdoor conditions is useful to promote this technology. Furthermore, the coefficients of all the studied models for several modules are given in order to have a reference of these values of current HCPV modules. This also allows the application of each model for the modules under study.

This paper is organized as follows. Section II describes the experimental setup used to measure and study the HCPV module. In Section III, the descriptions of the models and results obtained in the estimation of maximum power of HCPV modules under study are presented and commented on. In Section IV,

Manuscript received October 3, 2014; accepted January 25, 2015. Date of publication February 18, 2015; date of current version April 17, 2015. This work was supported by the Engineering and Physical Sciences Research Council through the BioCPV (EP/J000345/1) project. This work is part of the project "Desenvolvemento de novos conceptos baseados en tecnoloxía de concentración fotovoltaica para a produción de enerxía eléctrica adaptados a distintas zonas climáticas," through the program "formación posdoutoral do Plan galego de investigación, innovación e crecemento 2011–2015 (Plan I2C)" funded by the Xunta de Galicia and by the European Social Fund.

A. Soria-Moya, F. Almonacid Cruz, and P. Pérez-Higueras are with the Centre of Advanced Studies in Energy and Environment, University of Jaén, Jaén 23071, Spain (e-mail: tecnico@censolar.org; facruz@ujaen.es; pjperez@ujaen.es).

E. F. Fernández is with the Centre of Advanced Studies in Energy and Environment, University of Jaén, Jaén 23071, Spain, and also with the Environment and Sustainability Institute, University of Exeter, Penryn TR10 9FE, U.K. (e-mail: fenandez@ujaen.es).

P. Rodrigo is with Panamericana University, Aguascalientes 20290, Mexico (e-mail: prodrigo@up.edu.mx).

T. K. Mallick is with the Environment and Sustainability Institute, University of Exeter, Penryn TR10 9FE, U.K. (e-mail: T.K.Mallick@exeter.ac.uk).

Color versions of one or more of the figures in this paper are available online at http://ieeexplore.ieee.org.

Digital Object Identifier 10.1109/JPHOTOV.2015.2397605

TABLE I
MAXIMUM POWER OF THE MODULES UNDER STUDY MEASURED AT THE SAME OUTDOOR REFERENCE CONDITIONS FOR WIND SPEED LOWER THAN 1 M/S

Manufacturer	P (W)	DNI (W/m^2)	T_{air} (°C)	AM
A	57.2	900	20	1.5
B	116.9	900	20	1.5
C	45.7	900	20	1.5

P: Maximum power. DNI: Direct normal irradiance. T_{air}: Air temperature. AM: Air mass.

a comparative study among the models used is presented. The main conclusions of the work are presented in Section V.

II. EXPERIMENTAL SETUP

To conduct this study, three HCPV modules from different manufacturers have been selected. These modules are representative of the current industrialized modules, but for confidentiality reasons, they are named as module A, module B, and module C, respectively. The three modules are made of lattice-matched GaInP/GaInAs/Ge MJ solar cell, a PMMA Fresnel lens as primary optic, and a refractive truncated pyramid as secondary optic. Module A has a geometric concentration of 500 and six cells connected in series. Module B has a geometric concentration of 550 and 25 cells connected in series. Module C has a geometric concentration of 625 and five cells connected in series. All of them have a passive cooling. Table I shows the maximum power of the modules under study, measured at the same outdoor reference conditions, obtained following the procedure described in [13].

HCPV modules were measured at the Centre of Advanced Studies in Energy and Environment (CEAEMA), University of Jaén. The center is located at the south of Spain, Jaén, which has a high direct annual irradiation level [22] and air temperatures that can easily reach 40 °C in summer and 5 °C in winter. Because of this, the solar research center is located in an adequate place for HCPV outdoor evaluation.

To carry out this study, the modules were mounted on a high-accuracy two-axis solar tracker. The *I–V* characteristics of the modules were measured with a four-wire electronic load. In addition, a four-wire PT100 placed in contact with the solar cell on the concentrator receiver for each module to measure the cell temperature was installed. It is important to note that each temperature sensor was located in a receiver between the center and the border of the modules so that the measured temperatures should be considered as the average temperature of a receiver due to the temperature distribution of HCPV modules. This approach has been previously used and has been considered as a useful tool for the estimation of the cell temperature of an HCPV module and for its electrical characterization [23]–[25]. An atmospheric station recorded other outdoor parameters such as global irradiance (G), direct normal irradiance (DNI), wind speed (W_{s}), air temperature (T_{air}), relative humidity (H_{r}), or sun elevation (γ_{s}), among others.

Fig. 1 shows the experimental setup to study the behavior of the HCPV modules described above. All the parameters were recorded every 5 min from January 2011 to December 2012. It is also important to note that the modules were cleaned once a week and also after rainy days to avoid possible power losses.

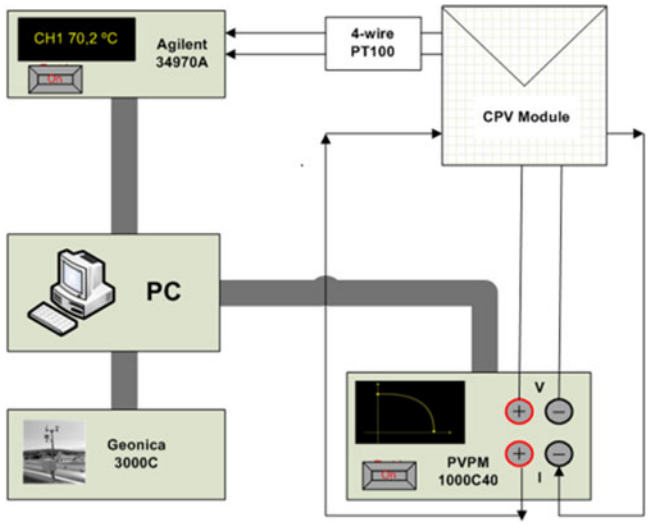

Fig. 1. Scheme of the experimental setup used to study the HCPV modules' behavior at the CEAEMA of the University of Jaén.

Since the MJ solar cells and the HCPV modules are influenced by the incident spectrum, some of the methods that will be studied in next sections use different atmospheric parameters to evaluate its impact. As will be commented, the parameters used are the air mass (AM) and the precipitable water (PW). These parameters are not directly given by the atmospheric station but can be easily calculated. In this case, AM has been determined knowing γ_{s} [26] and PW knowing T_{air} and H_r [27], [28].

Fig. 2 shows the distribution of the main annual atmospheric parameters measured during the experiment at Jaén.

III. HIGH CONCENTRATOR PHOTOVOLTAIC MODULE METHODS

In this section, the models that have been considered will be described and studied. Particularly, the considered models are the standard ASTM E2527 model [18], the linear coefficient model [19], the Sandia National Laboratories model [20], and an ANN-based model [21]. The parameters of each model considered have been obtained from outdoor monitorized data and following the procedure described for each author.

A. Model of the Standard ASTM E2527

The American standard ASTM E2527 [18] defines a simple procedure to predict the maximum power of an HCPV module. The proposed equation is

$$P_{\mathrm{ASTM}} = \mathrm{DNI} \cdot (A_1 + A_2 \cdot \mathrm{DNI} + A_3 \cdot T_{\mathrm{air}} + A_4 \cdot W_s) \tag{1}$$

where A_1, A_2, A_3, and A_4 coefficients are estimated by means of regression analysis from outdoor monitorized data following the procedure described by the authors. Table II shows the values of the coefficients for each module under study. As can be seen, although the HCPV module is influenced by spectral

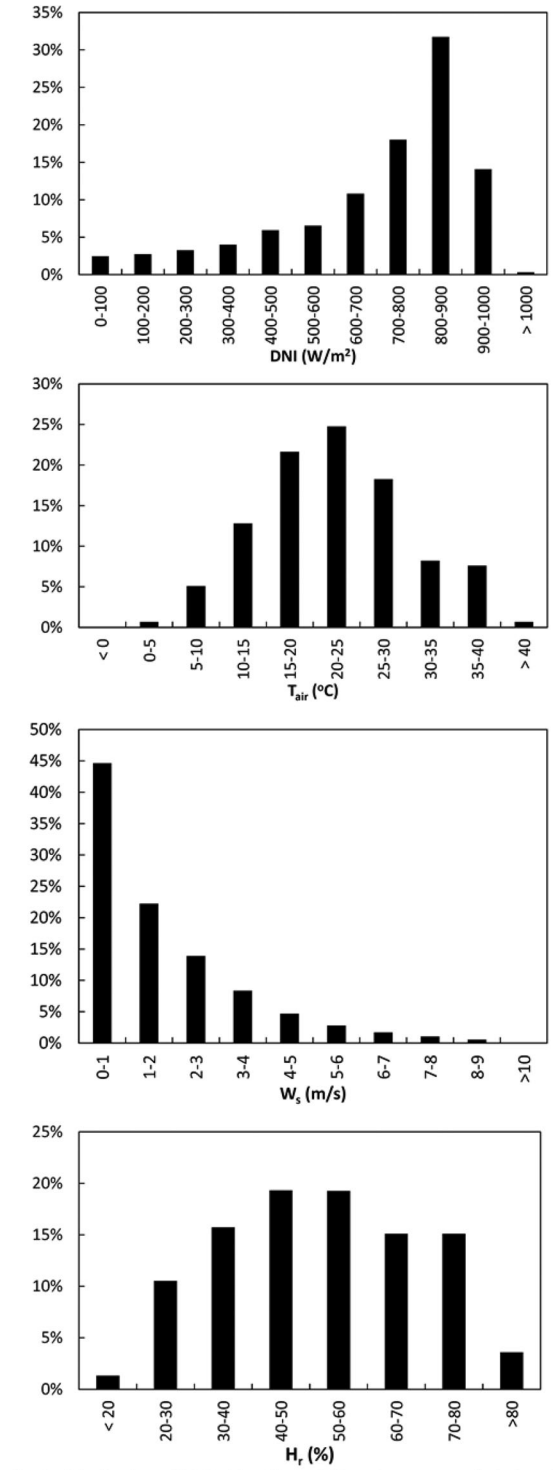

Fig. 2. Distribution of DNI, T_{air}, W_{s}, and H_{r} values measured during the experiment.

changes, this model does not take into account any spectral correction.

B. Model Based on Linear Coefficients

The linear coefficient model [19], [29] uses input parameters DNI, T_{air}, and AM to quantify the spectral influences on the HCPV module. The equation of the model to obtain the maximum power of a HCPV module is

$$P_{\mathrm{Linear}} = \frac{P^{+}}{\mathrm{DNI}^{+}}\mathrm{DNI}(1-\delta(T_{\mathrm{air}}-T_{\mathrm{air}}^{+})) (1-\varepsilon(\mathrm{AM}-\mathrm{AM}_{U})) \quad (2)$$

where P^{+}, DNI^{+}, T_{air} are, respectively, the maximum power, direct normal irradiance, and air temperature at reference conditions (see Table I); δ is the air temperature coefficient of maximum power; ε is the AM coefficient of maximum power of an HCPV module (its value being 0 for $\mathrm{AM} \leq \mathrm{AM_U}$ and the value obtained by the regression analysis of outdoor monitored data for $\mathrm{AM} > \mathrm{AM_U}$); and $\mathrm{AM_U}$ is defined as the umbral AM at which the maximum power begins to be influenced, where its value is about 2, as has been found in [16], [19], and [30].

The temperature coefficients of maximum power (δ) and AM coefficients of maximum power (ε) for the HCPV modules under study are obtained from outdoor monitorized data by means of regression analysis following the procedure described by the authors; results are shown in Table III.

TABLE II
COEFFICIENTS OBTAINED FOR THE THREE MODULES UNDER STUDY OF THE ASTM E2527 MODEL

	A_1	A_2	A_3	A_4
A	3.60905E-02	2.76245E-05	1.42270E-04	2.13138E-04
B	9.56743E-02	3.34642E-05	1.11243E-04	8.00692E-04
C	3.24868E-02	1.61190E-05	0.85932E-04	4.85177E-04

TABLE III
TEMPERATURE COEFFICIENTS OF MAXIMUM POWER (δ) AND AM COEFFICIENTS OF MAXIMUM POWER (ε) OBTAINED FOR THE THREE HCPV MODULES UNDER STUDY OF THE LINEAR COEFFICIENT MODEL

Manufacturer	δ (%/°C)	ε (%)	
		$\mathrm{AM} \leq \mathrm{AM_U}$	$\mathrm{AM} > \mathrm{AM_U}$
A	0.14	0	4.74
B	0.12	0	4.11
C	0.17	0	4.80

C. Model of Sandia National Laboratories

The model of Sandia National Laboratories [20] uses the DNI, the AM and the T_{cell} as inputs. The equations that allow calculating the HCPV module maximum power are

$$f_1(\mathrm{AM}) = a_0 + a_1\cdot\mathrm{AM} + a_2\cdot\mathrm{AM}^2 + a_3\cdot\mathrm{AM}^3 + a_4\cdot\mathrm{AM}^4 \quad (3)$$

$$B_{\mathrm{ef}}(\mathrm{AM}) = (\mathrm{DNI}\cdot f_1(\mathrm{AM}))\,\mathrm{DNI}^{*} \quad (4)$$

$$\delta = (m\cdot k\cdot(T_{\mathrm{cell}}+273.15))/q \quad (5)$$

$$\beta_{V\mathrm{mpp}} = \beta_{V\mathrm{mpp0}} + m_{V\mathrm{mpp}}\cdot(1-B_{\mathrm{ef}}) \quad (6)$$

$$I_{\mathrm{mpp}} = \left(C_0\cdot B_{\mathrm{ef}} + C_1\cdot B_{\mathrm{ef}}^2\right) \times (I_{\mathrm{mpp}}^{*} + \alpha_{\mathrm{Impp}}\cdot(T_{\mathrm{cell}}-T_{\mathrm{cell}}^{*}) \quad (7)$$

TABLE IV
PARAMETERS OBTAINED FOR THE THREE MODULES UNDER STUDY OF THE MODEL OF SANDIA NATIONAL LABORATORIES

Parameter	A	B	C	Units
α_{Impp}	0.0077	0.0009	0.0083	A/°C
$\beta_{\mathrm{Vmpp}}0$	−0.049	−0.140	−0.029	V/°C
m_{Vmpp}	−0.002	−0.004	−0.001	V/°C
a_0	1.0185	0.8841	0.8991	–
a_1	0.00198	0.08849	0.09765	–
a_2	−0.0127	−0.0279	−0.0294	–
a_3	0.00102	0.00201	0.00210	–
a_4	−2.367E-5	−4.575E-5	−4.769E-5	–
I^*_{mpp}	4.12	2.37	4.24	A
V^*_{mpp}	15.92	60.91	12.22	V
m	1.14	5.12	5.59	–
C_0	1.018	0.928	0.950	–
C_1	−0.018	0.072	0.050	–
C_2	−4.33	−0.20	−0.15	–
C_3	−48.93	−1.28	−0.98	1/V

$$V_{\mathrm{mpp}} = V^*_{\mathrm{mpp}} + C_2 \cdot N_S \cdot \delta \cdot \ln(B_{\mathrm{ef}}) + C_3 \cdot N_S \cdot (\delta \cdot \ln(B_{\mathrm{ef}}))^2 + \beta_{V\mathrm{mpp}} \cdot (T_{\mathrm{cell}} - T^*_{\mathrm{cell}}) \quad (8)$$

$$P_{\mathrm{Sandia}} = I_{\mathrm{mpp}} \cdot V_{\mathrm{mpp}}. \quad (9)$$

Equation (3) approximates the spectral correction factor $f_1(\mathrm{AM})$, as defined in the standard ASTM E 973 [31], by a fourth-order polynomial. Equation (4) calculates the effective irradiance (B_{ef}), that is, the irradiance at which the cells actually respond. This irradiance is the DNI corrected with the spectral correction factor, $f_1(\mathrm{AM})$, and normalized to the reference irradiance, DNI*. Equation (5) defines the δ parameter, which is the product of the effective ideality factor of the MJ cell (m) and the thermal voltage. The thermal voltage is obtained from the Boltzmann constant (k), the electron charge (q), and the cell temperature. Equation (6) allows the determination of the temperature coefficient $\beta_{V\mathrm{mpp}}$. This coefficient is used afterward for quantifying the effect of temperature on the module maximum power point voltage. The coefficient is expressed as a linear function of the effective irradiance, i.e., it is allowed to vary with the concentration ratio. Equations (7) and (8) calculate the module maximum power point current (I_{mpp}) and voltage (V_{mpp}) from their values at reference conditions (I^*_{mpp}, V^*_{mpp}). $\alpha_{I\mathrm{mpp}}$ is the temperature coefficient for I_{mpp}, and N_{S} is the number of cells in series for the module. Finally, (9) obtains the maximum power of the HCPV module. The reference conditions are defined as: DNI* = 1000 W/m^2, $T^*_{\mathrm{cell}} = 25$ °C and AM1.5. Every model parameter is obtained from outdoor monitorized data by means of regression analysis, following the procedures described by the authors; results are shown in Table IV.

D. Model Based on Artificial Neural Network

Due to the fact that the relation between atmospheric parameters and module output maximum power is complex, a model that tries to characterize the relation between atmospheric parameters and module output maximum power through ANNs has been proposed in [21]. The model takes into account the spectral influences through easily measurable parameters: the AM and the PW. Inputs of the model are the DNI, the T_{air}, the W_{s}, the AM, and the PW. Therefore, the maximum power is defined by the following function:

$$P_{\mathrm{ANN}} = f(\mathrm{DNI}, \mathrm{AM}, \mathrm{PW}, T_{\mathrm{air}}, W_s). \quad (10)$$

To estimate this function, a feed-forward neural network trained with the Levenberg–Marquardt (LM) back-propagation algorithm was used. The developed ANN has the structure shown in Fig. 3: five nodes in the input layer (DNI, AM, PW, T_{air}, W_{s}), seven nodes in the hidden layer, and one node in the output layer: the maximum power. The number of hidden layer nodes was determined empirically [32]–[35]. To find the final architecture (weights and bias and the number of nodes in the hidden layer), several ANNs with different structures were trained in order to find the ANN that best fitted the network output to the target. The LM training algorithm was used to adjust the weights and bias such that the neural network produces the required output for the given inputs data [36]–[38]. In order to train, validate, and test the ANN, a set of outdoor measurements were used for a wide range of operating conditions following the procedure described by the authors.

Table V shows the configuration and main features of the ANN used to estimate the output of the HCPV modules considered. Tables VI and VII show values of weight and bias for the hidden and output layer neurons obtained for the studied modules.

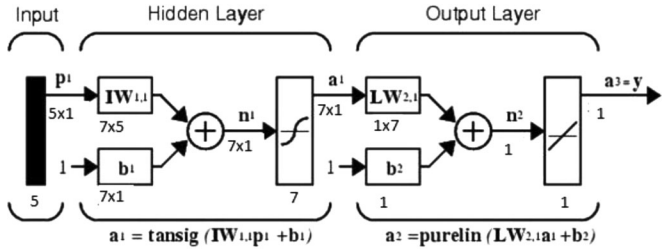

Fig. 3. Structure of the ANN for the prediction of the maximum power of an HCPV module.

TABLE V
CONFIGURATION AND TRAINING PERFORMANCE OF ANN FOR ESTIMATING THE OUTPUT OF THREE MODULES UNDER STUDY

Programing Language	MATLAB 2011b$^{\mathrm{T}}$
Neurons inputs	3
Neurons output layer	1
Neuron hidden layer	5
Maximum iteration limits	500
Training function	Levenberg–Marquardt
Performance function	Mean Square Error
Performance goal	1.00e^{-010}
Minimum gradient	1.00e^{-05}

IV. COMPARATIVE STUDY

To study the behavior of the presented models in detail, the root mean square error (RMSE), the mean bias error (MBE),

TABLE VI
VALUES OF WEIGHTS AND BIAS OBTAINED FOR THE HIDDEN LAYER NEURONS FOR THREE MODULES UNDER STUDY

	Hidden layer					
	Bias	Weights				
A	−1.8429	2.5940	2.2913	2.0389	0.9202	0.2399
	12.7312	−1.1261	−18.5147	−2.7033	0.3902	−0.3920
	−0.7949	0.3861	0.0269	−0.1795	0.0312	0.0682
	2.6424	−2.0327	−1.7782	−1.0675	−0.6628	−0.1742
	−9.2255	−8.7349	13.4286	−5.9909	15.7909	−0.5748
	−1.6165	1.0121	−0.0637	−1.0271	0.1804	0.3708
	1.8776	2.0357	0.5695	1.6886	0.7943	-1.0422
B	−0.0333	−0.8164	−0.0158	0.1841	0.0311	−0.0203
	5.1063	0.8322	−0.3461	5.8053	−1.3989	0.0735
	0.0492	−1.6218	−0.3890	−1.4026	−1.8233	0.7208
	0.8378	−0.2589	−0.4826	0.2493	−0.6977	−2.1617
	0.3880	−1.4806	−0.4486	0.7209	−0.0565	−1.3546
	−2.5878	1.9492	−0.8359	−1.3351	0.1719	1.3480
	1.3662	2.7184	0.9630	−1.3420	−1.1131	1.68329
C	−3.5358	−0.5130	−0.1083	−2.9562	0.6337	−2.4696
	−0.0284	−1.5463	−0.3744	−3.8941	−8.0610	6.2506
	0.8811	−0.7570	−0.0183	−0.0592	0.1353	0.0915
	−1.2296	−1.7805	−0.2535	−2.0785	0.1738	−0.3308
	−0.9498	0.3862	0.0077	−0.2388	−0.0352	−0.0522
	−4.0959	−0.0648	0.4302	−3.0006	0.3828	−0.0756
	4.2547	−0.1722	−2.1945	2.6365	1.1541	0.7253

TABLE VII
VALUES OF WEIGHTS AND BIAS OBTAINED FOR THE OUTPUT LAYER NEURONS FOR THREE MODULES UNDER STUDY

	Output layer							
	Bias	Weights						
A	−2.73	2.73	0.06	4.51	7.67	−0.02	−0.56	0.130
B	−0.14	−1.10	0.14	−0.12	0.07	−0.05	0.113	0.203
C	1.065	−0.08	−0.03	3.42	−0.24	8.02	−2.030	−0.169

TABLE VIII
RMSE, MBE, AND DETERMINATION COEFFICIENT (R^2) OBTAINED FOR THE STUDIED MODELS

	Model	RMSE (%)	MBE (%)	R^2
A	Standard ASTM E2527	4.59	0.00	0.97
	Linear Coefficients	3.22	0.05	0.99
	Sandia National Laboratories	3.35	−0.05	0.99
	Artificial Neural Network	2.11	0.00	0.99
B	Standard ASTM E2527	4.50	0.00	0.97
	Linear Coefficients	3.48	−0.07	0.99
	Sandia National Laboratories	3.60	−0.09	0.99
	Artificial Neural Network	1.96	-0.07	0.99
C	Standard ASTM E2527	5.20	0.00	0.96
	Linear Coefficients	3.55	0.03	0.98
	Sandia National Laboratories	3.60	−0.08	0.98
	Artificial Neural Network	2.56	−0.05	0.98

and the value of determination coefficient (R^2) between predicted and actual data have been calculated (see Table VIII). In addition, as an example, Fig. 4 shows the linear regression analysis between actual data and predicted data for the studied models for module A in order to show their performance

As can be seen, the value of R^2 is close to 1 for the studied models, which indicates a good fit for all of them, as shown in Table VIII. The MBE gives an indication on the average deviation of the predicted values from the corresponding measured data. A positive MBE value indicates the amount of overestimation in the predicted data and *vice versa*. As can be seen in Table VIII, the four studied models have an MBE around 0%, what indicates that all the models are not overestimating or underestimating the maximum power of the HCPV modules under study. The RMSE represents a measure of the variation of predicted values around the measured data. As can be seen in Table VIII, the model with a larger RMSE is the standard ASTM E2527, its value being between 4.50% and 5.20%. This is probably because the model does not introduce any spectral correction. The linear coefficient model and the Sandia National Laboratories model yield similar results, i.e., an RSME around 3.5%. As can also be seen, the model based on ANN has the lowest RMSE, its value being between 1.96 and 2.56%. From this analysis, it can also be concluded that the four models perform effectively in the prediction of the maximum power of HCPV modules: the four models have an R^2 equal to or greater than 0.96, an MBE almost equal to 0%, and a maximum RMSE lower than 5.50% which can be considered as an acceptable margin of error.

In order to study the models in more detail, the RMSE versus the main parameters that affect the performance of an HCPV module is calculated: DNI, cell temperature, and spectrum. It is important to note that the spectral effects on the output of an HCPV module are mainly given by the AM, aerosol optical depth, and PW [15], [39]–[41]. However, the aerosol optical depth values were not available during the measurements. Hence, in order to study the quality of the models versus the spectrum, the only atmospheric parameters taken into account are the AM and PW. Fig. 5 shows an example of the performance of the four models versus these parameters for module A. It is important to note that the behavior found for the other two modules yields to the same conclusions commented below.

Fig. 5(a) shows the RMSE for each DNI level. As can be seen, the ANN model shows the best results with an RMSE almost constant, centered around 2%. The linear and Sandia models show similar results. Both models show the poorest results for low DNI levels with a maximum RMSE around 4% and show a tendency to have a better performance as the DNI increases until an RMSE value around 2%. The ASTM model shows the poorest results with a maximum RMSE around 6% and shows no particular trend.

Fig. 5(b) shows the RMSE for each T_{cell} level. As can be seen, the ANN, the linear, and the Sandia models have a similar behavior with an RMSE almost constant for all T_{cell} values. However, the ANN model shows the best results with an RMSE around 2%, while the linear and Sandia models have an RMSE around 3%. Again, the ASTM model shows the poorest results with an RMSE that shows a clear tendency to increase for high T_{cell} values with a maximum around 6%.

Fig. 5(c) and (d) shows the RMSE for each AM and PW level, respectively. Regarding AM, the ANN shows the best results with an RMSE almost constant, centered around 2%. Again, the linear and the Sandia models have a similar behavior with an RMSE that shows a tendency to increase until AM val-

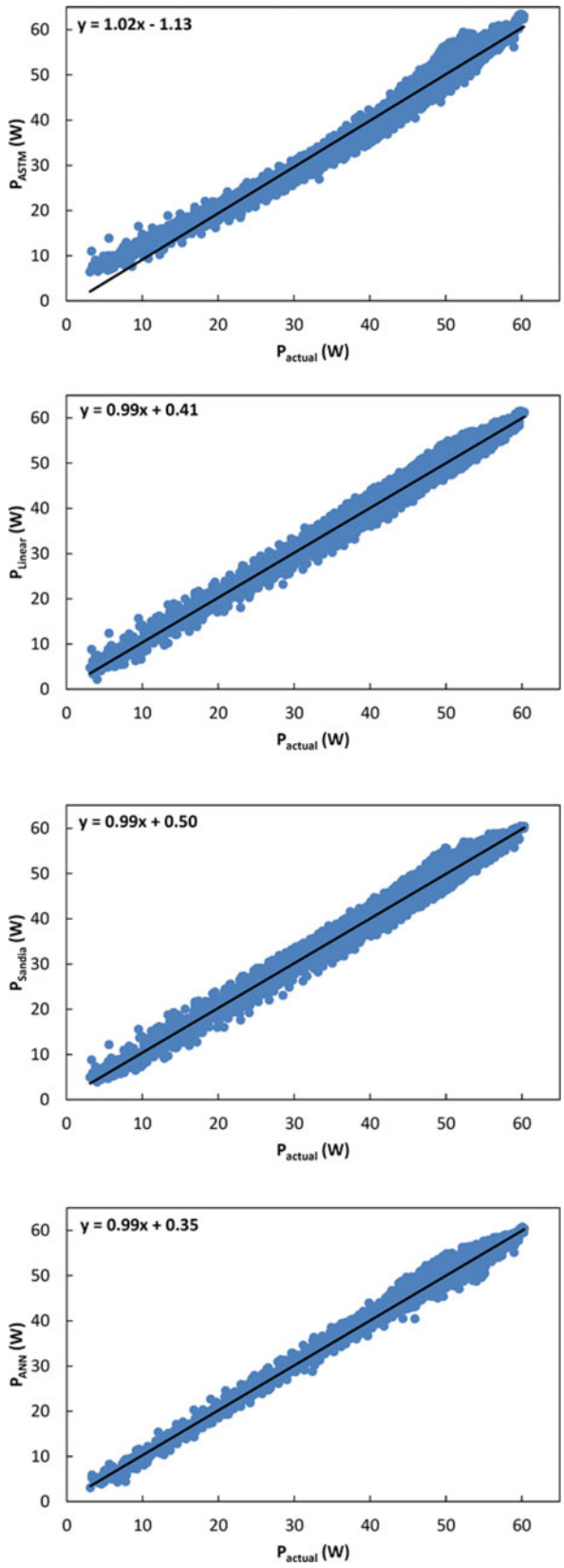

Fig. 4. Linear regression analysis between actual data and predicted data for the studied models for module A.

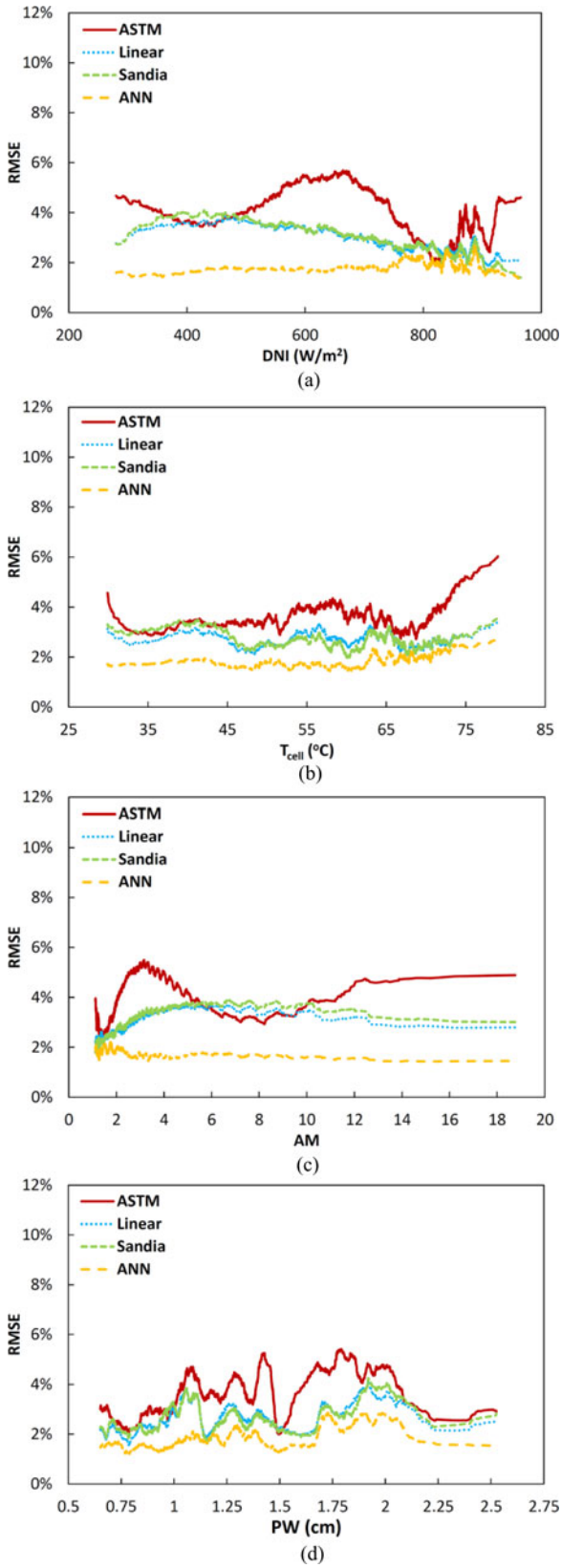

Fig. 5. RMSE for different DNI, T_{cell}, AM, and PW levels for the four studied models for module A.

ues around 5 and keeps almost constant for higher AM values at around 3.5%. The ASTM model shows the poorest results with a maximum RMSE around 5.8% and shows no particular trend. Regarding the PW, all models show the same behavior with a not clear tendency. However, the ANN model provides the best results, while the ASTM model yields the poorest results. The linear and the Sandia models again show similar results.

From the analysis of results, it can be concluded that the model that yields better results is the ANN-based model. This could be explained because the model takes into account a wind speed correction and two spectral corrections (AM and PW) and also to ability of ANN of solving complex problems. However, the model needs advanced knowledge in ANNs. The method based on linear coefficients shows the second best results; furthermore, this model has the advantage that is quite simple to fit and apply. The Sandia National Laboratories model shows a similar behavior to the linear coefficient model. However, this model requires a more complex procedure than other models in order to fit its parameters and needs the cell temperature as input parameter, which is difficult to get, although it is possible to estimate from atmospheric parameters [42]. The ASTM model is also so easy to apply and fit as the linear coefficient model but, because it does not take into account that any spectral correction gives worse results. However, recent works suggest the introduction of spectral correction based on AM and PW in order to improve it [43].

V. Conclusion

A comparative study of four models to estimate the power output of an HCPV module has been undertaken. The studied models estimate the output of HCPV modules from atmospheric parameters that are easy to obtain so that they are useful for a wide variety of HCPV applications. To conduct this study, three HCPV modules from different manufacturers have been selected. These modules are representative of the current industrialized modules; therefore, this study could also allow a further understanding the behavior of this technology in outdoor conditions and promote its application.

From the comparison of the errors of the models, the following conclusions have been found. The ASTM E2527 is the model that gives the poorest results, with an RMSE in the range of 4.50–5.20%. This could be explained because this model does not take into account any spectral correction. The Sandia National Laboratories and the linear coefficient models show similar behavior, with RMSE around 3.5%. The model that shows the best result is the ANN-based model with an RMSE lower than 2.6%. This could be explained because the model includes a wind speed correction and PW as an additional spectral correction. However, results show that the four models can be used to estimate the maximum power of a HCPV module with an RMSE lower than 5%, which can be considered to be an acceptable margin of error. Furthermore, it is important to note that all the models present an MBE around 0%, which means that all of them could be useful to estimate the energy produced by an HCPV module over a year.

In addition, in this paper, all the coefficients obtained for the application of four studied models have been given. This also allows the application of each model for the modules under study. Besides, a significant conclusion could be found from the analysis of coefficients obtained for each model. The coefficients of the ASTM E2527, the Sandia National Laboratories, and the ANNs models have to be considered as fitting parameters without direct physical meaning (with the exception of some coefficients of the Sandia National model). However, the coefficients obtained with the linear model have a physical meaning: relative maximum power losses due to temperature and AM. This means that this model could be used to estimate the maximum power of an HCPV module with similar characteristics to the studied modules, while for the other models, the coefficients need to be adjusted for each different module.

References

[1] M. Robert, "Concentrator photovoltaic technologies: Review and market prospects," *Refocus*, vol. 6, no. 4, pp. 35–39, 2005.

[2] A. Luque, G. Sala, and I. Luque-Heredia, "Photovoltaic concentration at the onset of its commercial deployment," *Prog. Photovoltaics, Res. Appl.*, vol. 14, no. 5, pp. 413–428, 2006.

[3] M. Yamaguchi, T. A. K. Takamoto, and N. Ekins-Daukes, "Multi-junction III-V solar cells: Current status and future potential," *Sol. Energy*, vol. 79, no. 1, pp. 78–85, 2005.

[4] P. Pérez-Higueras, E. Muñoz, G. Almonacid, and P. Vidal, "High concentrator photovoltaics efficiencies: Present status and forecast," *Renewable Sustainable Energy Rev.*, vol. 15, no. 4, pp. 1810–1815, 2011.

[5] F. Dimroth, M. Grave, P. Beutel, U. Fiedeler, C. Karcher, T. N. D. Tibbits, E. Oliva, G. Siefer, M. Schachtner, A. Wekkeli, A. W. Bett, R. Krause, M. Piccin, N. Blanc, C. Drazek, E. Guiot, B. Ghyselen, T. Salvetat, A. Tauzin, T. Signamarcheix, A. Dobrich, T. Hannappel, and K. Schwarzburg, "Wafer bonded four-junction GaInP/GaAs//GaInAsP/GaInAs concentrator solar cells with 44.7% efficiency," *Progress Photovoltaics: Res. Appl.*, vol. 22, no. 3, pp. 277–282, 2014.

[6] K. Ghosal, S. Burroughs, K. Heuser, D. Setz, and E. Garralaga-Rojas, "Performance results from micro-cell based high concentration photovoltaic research development and demonstration systems," *Prog. Photovoltaics, Res. Appl.*, vol. 21, no. 6, pp. 1370–1376, 2013.

[7] K. Ghosal, D. Lilly, J. Gabriel, M. Whitehead, S. Seel, B. Fisher, J. Wilson, and S. Burroughs, "Semprius field results and progress in system development," *IEEE J. Photovoltaics*, vol. 4, no. 2, pp. 703–708, Mar. 2014.

[8] F. Dimroth, T. Roesener, S. Essig, C. Weuffen, A. Wekkeli, E. Oliva, G. Siefer, K. Volz, T. Hannappel, D. Haussler, W. Jager, and A. Bett, "Comparison of direct growth and wafer bonding for the fabrication of GaInP/GaAs dual-junction solar cells on silicon," *IEEE J. Photovoltaics*, vol. 4, no. 2, pp. 620–625, Mar. 2014.

[9] A. Luque and V. Andreev, *Concentrator Photovoltaics*. New York, NY, USA: Springer, 2007.

[10] G. Siefer and A. Bett, "Analysis of temperature coefficients for III-V multijunction concentrator cells," *Prog. Photovoltaics, Res. Appl.*, vol. 22, no. 5, pp. 515–524, 2014.

[11] E. Fernández, G. Siefer, F. Almonacid, A. Loureiro, and P. Pérez-Higueras, "A two subcell equivalent solar cell model for III-V triple junction solar cells under spectrum and temperature variations," *Sol. Energy*, vol. 92, pp. 221–229, 2013.

[12] E. Fernández, G. Siefer, M. Schachtner, A. García Loureiro, and P. Pérez-Higueras, "Temperature coefficients of monolithic III-V triple-junction solar cells under different spectra and irradiance levels," in *Proc. AIP Conf.*, 2012, vol. 1477, pp. 189–193.

[13] E. Fernández, P. Pérez-Higueras, A. Garcia Loureiro, and P. Vidal, "Outdoor evaluation of concentrator photovoltaic systems modules from different manufacturers: First results and steps," *Prog. Photovoltaics, Res. Appl.*, vol. 21, no. 4, pp. 693–701, 2013.

[14] G. Peharz, J. Ferrer Rodríguez, G. Siefer, and A. Bett, "Investigations on the temperature dependence of CPV modules equipped with triple-junction solar cells," *Prog. Photovoltaics, Res. Appl.*, vol. 19, no. 1, pp. 54–60, 2011.

[15] E. Fernández, F. Almonacid, J. Ruiz-Arias, and A. Soria-Moya, "Analysis of the spectral variations on the performance of high concentrator photovoltaic modules operating under different real climate conditions," *Sol. Energy Mater. Sol. Cells*, vol. 127, pp. 179–187, 2014.
[16] E. Fernández, P. Rodrigo, J. Fernández, F. Almonacid, P. Pérez-Higueras, A. García-Loureiro, and G. Almonacid, "Analysis of high concentrator photovoltaic modules in outdoor conditions: Influence of direct normal irradiance, air temperature, and air mass," *J. Renew. Sustainable Energy*, vol. 6, no. 1, art. no. 013102, 2014.
[17] P. Rodrigo, E. Fernández, F. Almonacid, and P. Pérez-Higueras, "Models for the electrical characterization of high concentration photovoltaic cells and modules: A review," *Renew. Sustainable Energy Rev.*, vol. 26, pp. 752–760, 2013.
[18] *Standard Test Method for Electrical Performance of Concentrator*, ASTM E 2527, 2009.
[19] E. Fernández, F. Almonacid, P. Rodrigo, and P. Pérez-Higueras, "Model for the prediction of the maximum power of a high concentrator photovoltaic module," *Sol. Energy*, vol. 97, pp. 12–18, 2013.
[20] D. L. King, W. E. Boyson, and J. A. Kratochvil, *Photovoltaic Array Performance Model SAND2004–3535*, Sandia Nat. Lab., Albuquerque, NM, USA, 2004.
[21] F. Almonacid, E. F. Fernández, P. Rodrigo, P. Pérez-Higueras, and C. Rus-Casas, "Estimating the maximum power of a high concentrator photovoltaic (HCPV) module using an artificial neural network," *Energy*, vol. 53, pp. 165–172, 2013.
[22] P. Pérez-Higueras, P. Rodrigo, E. Fernández, F. Almonacid, and L. Hontoria, "A simplified method for estimating direct normal solar irradiation from global horizontal irradiation useful for CPV applications," *Renew. Sustainable Energy Rev.*, vol. 16, no. 8, pp. 5529–5534, 2012.
[23] E. Fernández, P. Rodrigo, F. Almonacid, and P. Pérez-Higueras, "A method for estimating cell temperature at the maximum power point of a HCPV module under actual operating conditions," *Sol. Energy Mater. Sol. Cells*, vol. 124, pp. 159–165, 2014.
[24] E. Fernández, F. Almonacid, P. Rodrigo, and P. Pérez-Higueras, "Calculation of the cell temperature of a high concentrator photovoltaic (HCPV) module: A study and comparison of different methods," *Sol. Energy Mater. Sol. Cells*, vol. 121, pp. 144–151, 2014.
[25] P. Rodrigo, E. Fernández, F. Almonacid, and P. Pérez-Higueras, "Review of methods for the calculation of cell temperature in high concentration photovoltaic modules for electrical characterization," *Renew. Sustainable Energy Rev.*, vol. 38, pp. 478–488, 2014.
[26] F. Kasten and A. T. Young, "Revised optical air mass tables and approximation formula," *Appl. Opt.*, vol. 28, no. 22, pp. 4735–4738, 1989.
[27] C. Gueymard, "Assessment of the accuracy and computing speed of simplified saturation vapour equations using a new reference dataset," *J. Appl. Meteorol.*, vol. 32, no. 7, pp. 1294–1300, 1993.
[28] C. Gueymard, "Analysis of monthly average atmospheric precipitable water and turbidity in Canada and northern united states," *Sol. Energy*, vol. 53, no. 1, pp. 57–71, 1994.
[29] E. F. Fernández, F. Almonacid, N. Sarmah, T. Mallick, I. Sanchez, J. M. Cuadra, A. Soria-Moya, and P. Pérez-Higueras, "Performance analysis of the lineal model for estimating the maximum power of a HCPV module in different climate conditions," in *Proc. AIP Conf.*, 2014, vol. 1616, pp. 187–190.
[30] E. Fernández, P. Pérez-Higueras, F. Almonacid, A. García Loureiro, J. Fernández, P. Rodrigo, P. Vidal, and G. Airnonacid, "Quantifying the effect of air temperature in CPV modules under outdoor conditions," in *Proc. AIP*, 2012, vol. 1477, pp. 194–197.
[31] *Determination of the Spectral Mismatch Parameter Between a Photovoltaic Device and a Photovoltaic Reference Cell*, ASTM E 973, 2010.
[32] R. Reed, "Pruning algorithms—A survey," *IEEE Trans. Neural Netw.*, vol. 4, no. 5, pp. 740–747, Sep. 1993.
[33] A. Ghosh and D. Lubkeman, "The classification of power system disturbance waveforms using a neural network approach," *IEEE Trans. Power Del.*, vol. 10, no. 1, pp. 109–115, Jan. 1995.
[34] J. Zurada, *Introduction to Artificial Neural Systems*. Eagan, MN, USA: West, 1992.
[35] B. Curry and P. Morgan, "Model selection in neural networks: Some difficulties," *Eur. J. Oper. Res.*, vol. 170, pp. 567–577, 2004.
[36] K. Levenberg, "A method for the solution of certain problems in least squares," *Quart. Appl. Math.*, vol. 2, pp. 164–168, 1944.
[37] D. Marquardt, "An algorithm for least-squares estimation of nonlinear parameters," *SIAM J. Appl. Math.*, vol. 11, pp. 431–441, 1963.
[38] K. Funahashi, "On the approximate realisation of continuous mappings by neural networks," *Neural Netw.*, vol. 2, pp. 183–192, 1989.
[39] E. F. Fernandez and F. Almonacid, "Spectrally corrected direct normal irradiance based on artificial neural networks for high concentrator photovoltaic applications," *Energy*, vol. 74, pp. 941–949, 2014.
[40] N. Chan, T. B. Young, H. E. Brindley, N. Ekins-Daukes, K. Araki, and Y. Y. Kemmoku, "Validation of energy prediction method for a concentrator photovoltaic module in Toyohashi Japan," *Prog. Photovoltaics, Res. Appl.*, vol. 21, pp. 1598–1610, 2012.
[41] N. Chan, H. Brindley, and N. Ekins-Daukes, "Impact of individual atmospheric parameters on CPV system power, energy yield and cost of energy," *Prog. Photovoltaics, Res. Appl.*, vol. 22, pp. 1080–1095, 2013.
[42] F. Almonacid, P. Pérez-Higueras, E. Fernández, and P. Rodrigo, "Relation between the cell temperature of a HCPV module and atmospheric parameters," *Sol. Energy Mater. Sol. Cells*, vol. 105, pp. 322–327, 2012.
[43] M. Muller, B. Marion, and J. K. S. Rodriguez, "Minimizing variation in outdoor CPV power ratings," in *Proc. AIP Conf.*, 2011, vol. 1407, pp. 336–340

Alberto Soria-Moya received the M.S. degree in physics from University of Seville, Seville, Spain, in 2010. He has been working toward the Ph.D. degree with the University of Jaén, Jaén, Spain, since 2013.

He has been a Researcher with Censolar (Solar Energy Training Centre), Spain, since 2010. From 2008 to 2009, he was a Research Assistant with the Fraunhofer Institute for Solar Energy Systems ISE. His research interests include solar energy, photovoltaics, electrical modeling, and spectral characterization.

Florencia Almonacid Cruz received the M.S. degree in electronic engineering from the University of Granada, Granada, Spain, in 2002 and the Ph.D. degree in electronic engineering from the University of Jaén, Jaén, Spain, in 2009.

She is currently an Associate Professor with the Department of Electronic and Automatic Engineering, University of Jaén. Her research interests include the application of the artificial neural networks in the field of the photovoltaic technology, as well as the characterization and modeling of conventional and concentrator photovoltaic devices and systems.

Eduardo F. Fernández received the B.S. degree in physics from the University of Oviedo, Oviedo, Spain, in 2004 and the M.S. degree in physics, the M.S. degree in renewables energies, and the Ph.D. degree in the area of solar energy from the University of Santiago de Compostela, Santiago de Compostela, Spain, in 2006, 2008, and 2012, respectively.

He is currently a Research Associate with the Environment and Sustainability Institute, University of Exeter, Penryn, U.K., where he is conducting a project funded by the Spanish/Galician government and European Union in the field of concentrator photovoltaics. His research interests include the development, characterization, and modeling of concentrator photovoltaic devices and systems.

Pedro Rodrigo received the M.S. degree in industrial engineering from Navarra University, Pamplona, Spain, in 1998 and the Ph.D. degree in electronic engineering from Jaén University, Jaén, Spain, in 2013.

From 2009 to 2014, he was a Research Assistant with the Center of Advanced Studies in Energy and Environment and with the Solar Energy and Automation Research and Development Group (IDEA), University of Jaén. Since 2014, he has been a Researcher with the Engineering Faculty, Panamericana University, Aguascalientes, México. His research interests include the characterization of concentrator photovoltaic modules and systems.

Tapas K. Mallick (M'14) received the Ph.D. degree from the University of Ulster, Coleraine, U.K., in 2003.

From 2007 to 2012, he was a Lecturer with Heriot-Watt University, Currie, U.K. He is currently a Professor with the Renewable Energy and Chair in Clean Technologies with the Environment and Sustainability Institute, University of Exeter, Penryn, U.K. His research interests include renewable energies, concentrating photovoltaics, building integrated photovoltaics, integration of renewables, heat transfer, optics, and electrical modeling.

Pedro Pérez-Higueras received the Ph.D. degree in industrial engineering from the University of Jaén, Jaén, Spain, in 2003.

He is currently a Professor with the Department of Electronic and Automatic Engineering, University of Jaén. He has collaborated on more than 30 R&D projects with different companies and institutions, and he has published more than 100 papers in the most prestigious peer-reviewed journals and congresses related to solar energy. His research interests include the development, characterization, and modeling of concentrator photovoltaic devices and the optimal design of power plants.

Referencia / Reference: Fernández, E. F., Almonacid, F., Ruiz-Arias, J. A. y **Soria-Moya, A.** (2014). *Analysis of the spectral variations on the performance of high concentrator photovoltaic modules operating under different real climate conditions. Solar Energy Materials and Solar Cells, 127*, 179-187.

Estado / Status: Publicado / *Published.*

Índice de impacto / Impact Factor: 5.030.

Categoría / Catogory: *Energy and Fuels*. Ranking: 10/88 (Q1).

Solar Energy Materials & Solar Cells 127 (2014) 179–187

Contents lists available at ScienceDirect

Solar Energy Materials & Solar Cells

journal homepage: www.elsevier.com/locate/solmat

Analysis of the spectral variations on the performance of high concentrator photovoltaic modules operating under different real climate conditions

Eduardo F. Fernández [a,b,*], F. Almonacid [b], J.A. Ruiz-Arias [b,c], A. Soria-Moya [b,d]

[a] Environment and Sustainability Institute, University of Exeter, Penryn, Cornwall TR10 9FE, United Kingdom
[b] Center of Advanced Studies in Energy and Environment (CEAEMA), University of Jaen, Spain
[c] Solar Radiation and Atmosphere Modeling Group, Physics Department, University of Jaen, Spain
[d] Solar Energy Training Centre (Censolar), Spain

ARTICLE INFO

Article history:
Received 9 March 2014
Received in revised form
24 April 2014
Accepted 29 April 2014
Available online 21 May 2014

Keywords:
High concentrator photovoltaic
Spectral effects
Climate conditions

ABSTRACT

Multi-junction (MJ) solar cells show an important dependence on the incident spectrum due to the internal series connection of several cells with different band gap energies. The influence of spectral variations on the performance of HCPV modules or systems is different from that in MJ solar cells since they use optical devices to concentrate the light on the solar cell surface. The spectral distribution of irradiance is affected by atmospheric parameters and changes during the course of day, month or year. Because of this, several authors have done different studies to analyse and quantify the spectral effects on the performance of HCPV modules. However, there are still important issues that have not been addressed. In this paper, a deep analysis of the spectral effects on the performance of different HCPV modules with different multi-junction solar cells and Fresnel lenses on an annual time scale and their study and comparison at locations with different climate conditions is conducted. In order to address this issue, ground-based climatologies at the locations studied, spectra simulations with the SMARTS model and the spectral factor of a HCPV module have been used. Results show that the annual spectral losses vary from 6% to 51% depending on the climate conditions of the location and the HCPV module.

1. Introduction

Photovoltaic devices are influenced by the spectral distribution of the incident solar irradiance. But, due to the internal series connection of several cells with different band gap energies, multi-junction (MJ) solar cells show a significantly greater spectral dependence than single-junction solar cells [1,2].

The spectral distribution of solar irradiance is determined by multiple time-varying atmospheric factors, and several methods have been proposed to quantify the influence of the spectral variations of solar irradiance on the performance of MJ solar cells under real operating conditions [1,3–6].

Nowadays, high concentrator photovoltaic (HCPV) modules and systems are largely based on the use of MJ solar cells [7]. HCPV modules use optical devices, usually Fresnel lenses, to concentrate the light on the solar cell surface and may use secondary optical elements such as homogenizers [8]. The assembly of optical devices alters the spectral distribution of the solar irradiance that strikes the solar cell surface. Hence, the influence of incoming spectral variations on the performance of HCPV modules is inherently different to that in MJ solar cells [9].

Recently, the influence of spectral variations in the incident solar irradiance on the performance of HCPV modules has been evaluated by different authors. The spectral effects on various HCPV mono-modules and systems during a clear and a very clear day have been studied by Hashimoto et al. [9] in Okayama (Japan) from measurements gathered with a spectro-radiometer. However, as is pointed out in [10], the use of spectro-radiometers is complex and presents multiple disadvantages for long-term analyses. As a consequence, an alternative method based on isotype cells has been proposed by Peharz et al. [10]. Isotype cells register the solar irradiance spectral variations and quantify their effects on the electrical parameters of the HCPV modules. This approach has also been used in [11] to gauge the annual spectral losses of different HCPV systems in Madrid (Spain). However, although the methods based on isotype cells are robust and simple, they are difficult to apply in remote sites for long-term studies. The use of ground-based long-term observations of atmospheric properties in conjunction with the Simple Model of the Atmospheric Radiative Transfer of Sunshine (SMARTS [12–14]) poses an alternative

* Corresponding author. Tel.: +34 953213518; fax: +34 953212183.
E-mail address: fenandez@ujaen.es (E.F. Fernández).

http://dx.doi.org/10.1016/j.solmat.2014.04.026
0927-0248/

modelling approach for long-term studies. It allows evaluating the spectral effects at different locations if the atmospheric parameters are available. This approach has been used to study the influence of air mass, aerosol optical depth and precipitable water on the performance of different HCPV modules in Golden (USA) over 9 months [15] and in a HCPV module in Toyohashi (Japan) over a year [16].

Nonetheless, a deeper analysis of the influence of the time-varying solar irradiance spectrum on the performance of HCPV modules at locations with disparate climate conditions is required. This is crucial to leverage our understanding of the annual performance of HCPV modules under real operating conditions [17]. To address this issue, the effects of solar irradiance spectral variations on the annual performance of different HCPV modules at five locations with different climate conditions have been analysed based on high-quality ground-based climatologies at the sites studied and spectra simulations with the SMARTS model. A detailed analysis of the influence of air mass, aerosol optical depth and atmospheric water vapour content is presented.

2. Method and materials

2.1. The spectral factor of a HCPV module

The spectral factor of a single-junction PV device can be defined as [18–20,17]

$$SF = \frac{\int E(\lambda)\mathrm{SR}(\lambda)d\lambda \int E_{ref}(\lambda)d\lambda}{\int E_{ref}(\lambda)\mathrm{SR}(\lambda)d\lambda \int E(\lambda)d\lambda} \quad (1)$$

where $E(\lambda)$ is the incident spectrum on the PV device, $E_{ref}(\lambda)$ is the reference spectrum and $SR(\lambda)$ is the spectral response of the PV device. The spectral factor quantifies the differential performance of a PV device between the incident and reference spectra: an SF higher than 1 represents a better performance (spectral gains) and an SF lower than 1 (spectral losses) indicates a worse performance.

The spectral factor as defined in Eq. (1) is not valid for HCPV modules since the combined use of MJ solar cells and optical devices modifies the incident spectral distribution [9,21,22]. Therefore, the spectral factor needs to be reformulated for use in HCPV modules.

The short-circuit current density of each junction of a MJ solar cell can be expressed as

$$J_{sc,i} = \int E_b(\lambda)\eta(\lambda)SR_i(\lambda)d\lambda \quad (2)$$

where the index i represents the junction considered, $E_b(\lambda)$ is the spectral distribution of direct normal irradiance (E_b) or direct normal spectrum (HCPV modules react only to direct normal irradiance due to the use of lenses), and $\eta(\lambda)$ is the optical efficiency of the HCPV module.

As junctions of a MJ solar cell are interconnected in series, the short-circuit current density of the whole device is given by [23]

$$J_{sc} = \min(J_{sc,i}) \quad (3)$$

From Eqs. (1)–(3), the spectral factor of a HCPV module should be rewritten as

$$SF = \frac{\min(\int E_b(\lambda)\eta(\lambda)SR_i(\lambda)d\lambda) \int E_{b,ref}(\lambda)d\lambda}{\min(\int E_{b,ref}(\lambda)\eta(\lambda)SR_i(\lambda)d\lambda) \int E_b(\lambda)d\lambda} \quad (4)$$

where $E_{b,ref}(\lambda)$ is the reference spectrum AM1.5d ASTM G-173-03 at which MJ solar cells and HCPV modules are rated [24].

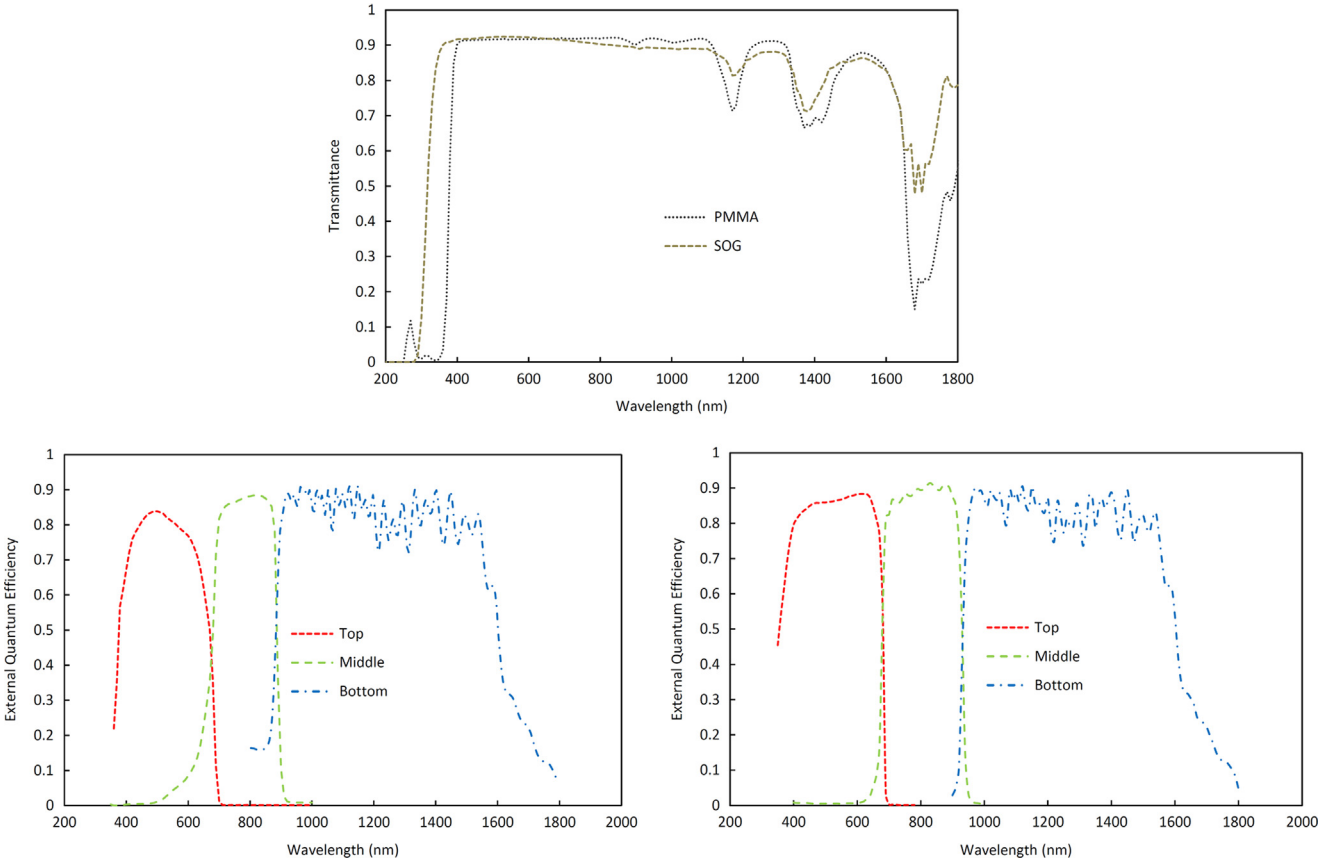

Fig. 1. External Quantum Efficiency of the lattice-matched (bottom left) and the metamorphic (bottom right) multi-junction solar cells at 298 K. (Top) Transmittance of the Fresnel lenses (PMMA and SOG) at 293 K.

Table 1
Average transmittance in the response region of each junction of the lattice-matched and the metamorphic multi-junction solar cells of the studied modules.

Cell	Lens	Average transmittance (%)		
		Top	Middle	Bottom
LM	PMMA	73	92	74
	SOG	87	91	82
MM	PMMA	73	92	76
	SOG	87	90	81

Finally, the spectral effects on the performance of a HCPV module with respect to the reference conditions are computed as

$$\Delta SF(\%) = (SF(E_b(\lambda)) - SF(E_{b,ref}(\lambda)))100 = (SF(E_b(\lambda)) - 1)100 \quad (5)$$

where ΔSF is defined as the relative spectral factor. This equation estimates the performance of a HCPV module as a function of the mismatch among the short-circuit current densities relative to the value under the reference spectrum of the different junctions of the respective MJ solar cell. This approach has already been used by different authors and is considered as a good tool to quantify the spectral impacts on the energy output of HCPV devices [4–6,25,26].

2.2. HCPV modules under study

Four different HCPV module prototypes have been considered for this study. Two modules are equipped with latticed-matched (LM) monolithic triple-junction solar cells with areas of 0.763 cm^2 each and the other two are equipped with metamorphic (MM) monolithic triple-junction solar cells with areas of 0.765 cm^2 each. Fig. 1 (bottom) shows the External Quantum Efficiencies (EQEs) of the cells at 298 K, which are formed by the following materials and band gap energies:

- LM cell: top: GaInP (1.88 eV), middle: GaInAs (1.41 eV), bottom cell: Ge (0.67 eV)
- MM cell: GaInP (1.82 eV), middle: GaInAs (1.33 eV), bottom cell: Ge (0.67 eV)

The four modules are made up of 20 MJ solar cells with a bypass diode per cell and use passive cooling to reduce the cell temperature. One of the modules equipped with LM/MM monolithic triple-junction solar cells uses Fresnel lenses based on poly(methylmethacrylate) (PMMA) material and the other uses Fresnel lenses based on silicon on glass (SOG) material as primary optics to concentrate the light. No secondary optical elements (SOE) have been considered. Both Fresnel lenses have an area of 23×23 cm^2, so the modules have a geometric concentration of around 700. Fig. 1(right) shows the spectral transmittance of the two Fresnel lenses at 293 K and Table 1 shows the average transmittance of the four modules in the response region of each junction of the cells. As can be seen, the modules that use SOG lenses have a higher transmittance on the response regions of the top and bottom junctions while it is similar in the response region of the middle junction.

3. Individual impact of atmospheric parameters

In order to achieve a better understanding of the influence of the spectral variations of the incident solar irradiance on the performance of HCPV modules, it is appropriate to perform an individualized analysis for each of the atmospheric parameters. The atmospheric parameters with the highest influence on the performance of HCPV modules are, in order of importance, air mass, aerosol optical depth, and precipitable water [1,16].

Optical mass is a measure of the length and amount of substance traversed by the solar rays in their course through the atmosphere. It has a differentiated spectral impact on the incoming solar irradiance at the earth surface. When the substance is dry air molecules, optical mass is known as optical air mass. Usually, it is given as the ratio with respect to the optical air mass in the zenith direction. In such a case, it is known as relative optical air mass, whose minimum value is always 1. For further references, see [27]. In this study, we used the relative optical air mass, and we will refer to it hereinafter as simply air mass or AM. For dry air molecules, air mass approximately reduces to a purely geometrical parameter that gives account of the solar position.

Aerosols are small particles suspended in the air with diameters in the range from few nanometres to tenths of microns. Aerosol optical depth, hereinafter noted as AOD, is the physical magnitude to account for the amount of radiation attenuated by aerosol particles. The bigger the AOD the more the radiation that attenuates. Its value changes with solar irradiance wavelength meaning that attenuation by aerosols depends on wavelength. This dependency is often represented with the Ångström law: $\tau = \beta\lambda^{-\alpha}$, where λ is the wavelength in microns, β is the AOD at $\lambda = 1$ μm, and α is the so-called Ångström exponent [28]. The latter represents the spectral incidence of aerosols in the solar flux: small values of α are typical of big particles, such as desert dust, and produce flat spectral responses. Large values of α are typical of small particles such as those found in polluted areas. Under such conditions, the extinction at large solar wavelengths gets smaller and the spectrum becomes redder. Further information can be referred to in [29]. Although the Ångström law represents the spectral dependence of AOD in terms of β, it can be re-formulated as $\tau = \tau_{0.55}(\lambda/0.55)^{-\alpha}$, so that the spectral dependence is now described in terms of the AOD at 0.55 μm ($\tau_{0.55}$) for the wavelength λ given in μm. The reference value at 0.55 μm is appropriate because it is a common observed value in different aerosol data bases, including ground-based and remotely-sensed data sources.

The water vapour content of a cloudless atmosphere also matters in the whole atmospheric spectral response. Water vapour content can be summarized in several ways, one of them being the precipitable water amount (w). It is the total amount of water vapour in the zenith direction, between the surface and the top of the atmosphere. Its unit is mass per unit of area. However, precipitable water is often described as the thickness of the liquid water that would be formed if all the vapour in the zenith direction were condensed at the surface of a unit area. See Ref. [27] for further information.

To analyse the individual influence of each atmospheric parameter, several spectra have been generated with the SMARTS radiative transfer model by varying one of the parameters while keeping the rest fixed at the reference values defined by the standard AM1.5d ASTM G-173-03 (air mass = 1.5, aerosol optical depth at 500 nm = 0.084, aerosol model = rural, precipitable water = 1.42 cm) [5,6,16,15]. The spectral effects on the performance of HCPV modules have been computed following the procedure described in Section 2.1.

3.1. Spectral influence of air mass

Fig. 2 (left) shows ten simulated solar irradiance spectra from AM = 1 to AM = 10. Although increasing AM values yield increasing attenuation of solar irradiance for the entire short-wave spectrum, the relative attenuation is larger in the spectral region of the top junction. Fig. 2 (right) shows ΔSF for the studied HCPV modules as a function of AM. The modules have similar behaviour, with absolute maxima at different AM values between 1 and 2.

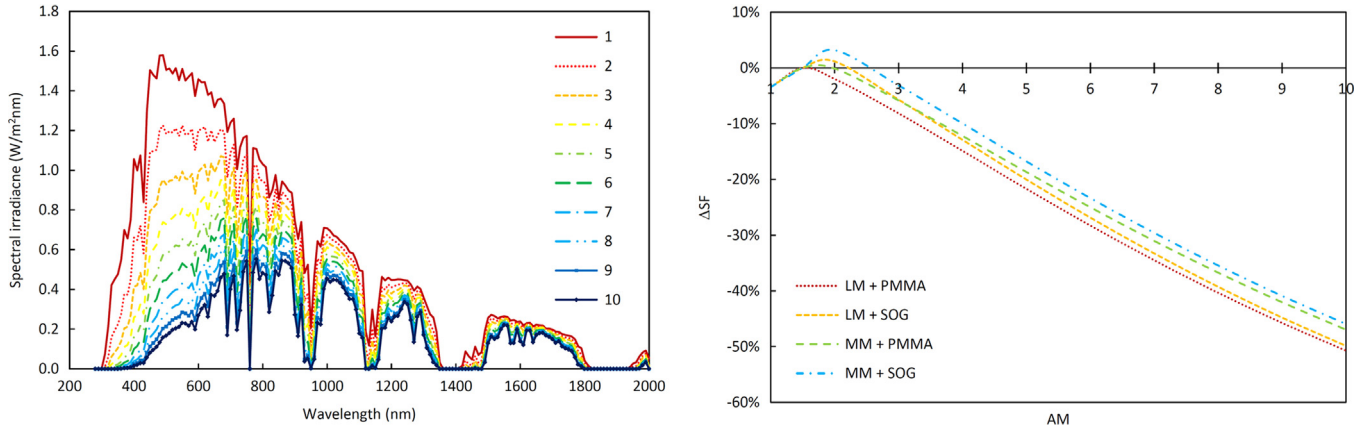

Fig. 2. Effect of air mass on the spectral irradiance (left) and on the HCPV modules performance (right). The other parameters are kept constant at the reference values defined by the AM1.5d ASTM G-173-03 reference spectrum.

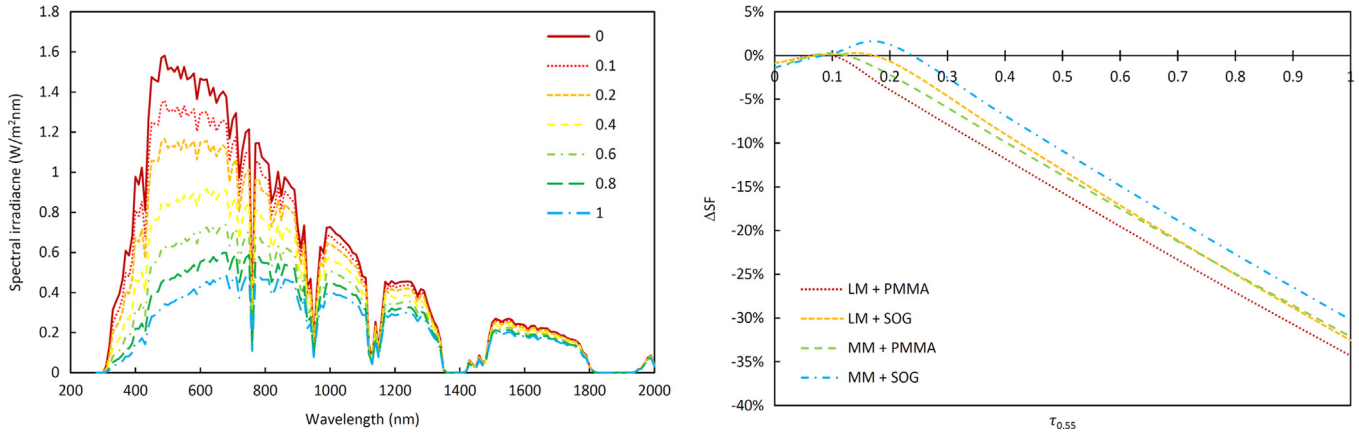

Fig. 3. Effect of aerosol optical depth on the spectral irradiance (left) and on HCPV modules performance (right). The other parameters are kept constant at the reference values defined by the AM1.5d ASTM G-173-03 reference spectrum. (For interpretation of the references to colour in this figure, the reader is referred to the web version of this article.)

This maximum represents the operating point at which the top and middle junctions generate the same current in each module. Around this point, the performance of the HCPV modules decreases due to the limited current by one of the junctions. On the left side the current is limited by the middle junction while on the right side the current is limited by the top junction. Like the absolute maximum, the air mass influence when the top junction is limiting the current is different in the four modules. The rationale behind is the fact that the transmittance of the SOG Fresnel lens is higher than the transmittance of the PMMA Fresnel lens in the spectral region of the top junction and also because the band gap of this junction is narrower in the MM cell than in the LM cell. Hence, the spectral losses due to AM when the current is limited by the top junction are lower for the HCPV module based on SOG Fresnel lenses and MM cells.

3.2. Spectral influence of aerosol optical depth at 0.55 μm

Fig. 3 (left) shows seven simulated solar irradiance spectra between $\tau_{0.55}=0$ and $\tau_{0.55}=1$. As in the previous case, the increase of $\tau_{0.55}$ reduces the incoming solar irradiance at all wavelengths, but removes more energy from the blue region, which is the spectral region where the top junction responds. Aerosol optical depth shows a significantly greater extinction than AM on the spectral region where the middle junction responds. Fig. 3 (right) shows the ΔSF values against $\tau_{0.55}$ for the HCPV modules considered in this study. As for the AM case, the modules have similar behaviour. There is an absolute maximum at $\tau_{0.55}$ values between 0.08 and 0.18 which are reasonable typical values for rural aerosols. Again, the maximum represents the operating point at which the top and middle junctions generate the same current. Around it, the performance of the HCPV modules decreases due to the limiting current by one of the junctions. On the left side the current is limited by the middle junction while on the right side the current is limited by the top junction. Note again that, as in the previous case, the point at which the relative spectral factor is maximum and the decay of the relative spectral factor when the top junction is limiting the current is different in both modules. This is due to the fact that the transmittance of the SOG Fresnel lens is higher than the transmittance of the PMMA Fresnel lens in the spectral region of the top junction and also because the band gap of this junction is narrower in the MM cell than in the LM cell. Because of this, the spectral losses due to $\tau_{0.55}$ when the current is limited by the top junction are lower for the HCPV module based on SOG Fresnel lenses and MM cells.

3.3. Spectral influence of Ångström exponent

Since aerosol particles have a large range of sizes, the aerosol spectral responsivity on the incident solar flux is highly variable and dependent on the size distribution of the particular aerosol arrangement. The Ångström exponent is a lumped parameter to describe this spectral responsivity. Fig. 4 (left) shows five simulated solar irradiance spectra with α values between 0.5 and 2.5.

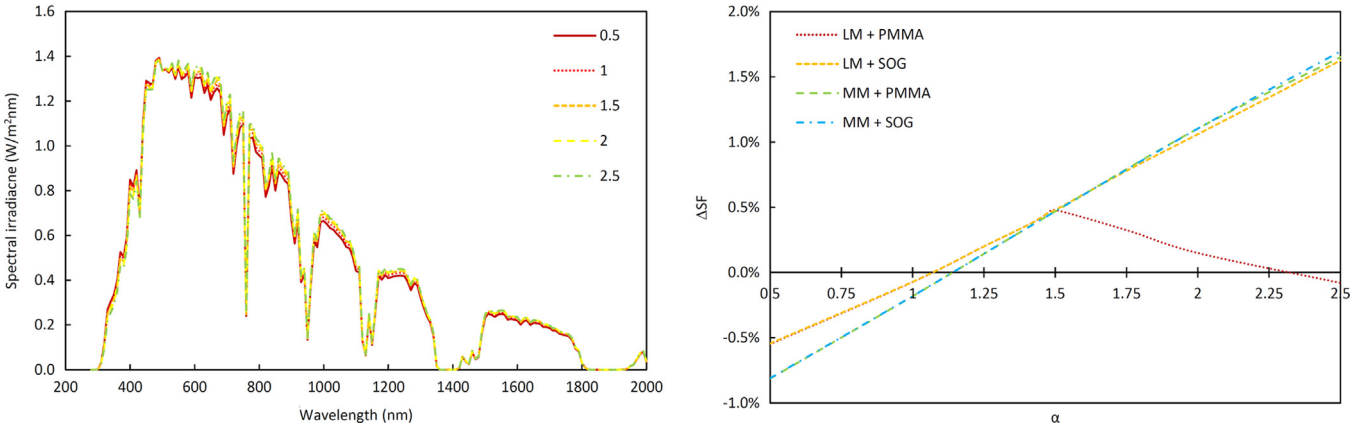

Fig. 4. Effect of the Ångström exponent on the spectral irradiance (left) and on HCPV modules' performance (right). The rest of parameters are kept constant at the reference values defined by the AM1.5d ASTM G-173-03 reference spectrum.

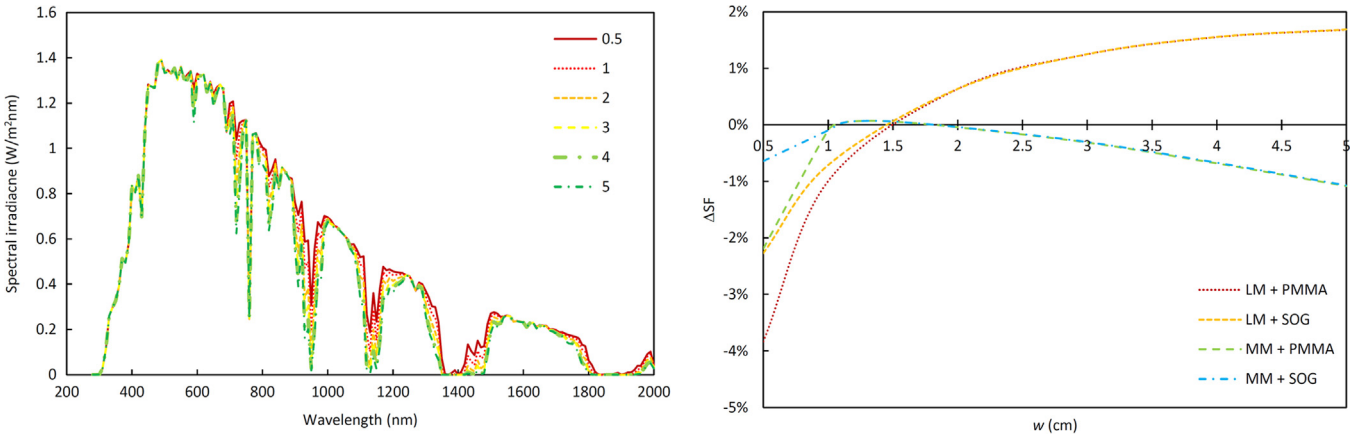

Fig. 5. Effect of precipitable water on the spectral irradiance (left) and on HCPV modules' performance (right). The other parameters are kept constant at the reference values defined by the AM1.5d ASTM G-173-03 reference spectrum.

Overall, the spectral effect is small, but as α increases the solar irradiance at wavelengths greater than 0.55 increases. For smaller wavelengths, solar irradiance decreases. In terms of the MJ cells, the effect of an increasing Ångström exponent is to increase the incident irradiance on the middle and bottom junctions whereas the irradiance stays about the same on the top junction. Fig. 4 (right) shows the ΔSF values for the HCPV modules against α. Unlike for AM and $\tau_{0.55}$, now the behaviour of the modules is distinct. The relative spectral factor of the module based on LM solar cells and PMMA Fresnel lenses reaches an absolute maximum at α of about 1.5, where the top and middle junctions generate the same current. The middle junction limits the current for smaller values of α and the top junction limits the opposite. On the contrary, the performance of the other modules always increases linearly within the range from α=0.5 up to α=2.5 because the top junction never limits the current due to the higher transmittance of the SOG Fresnel lens in the spectral region of the top junction and/or because the band gap of this junction in the MM cell is narrower.

3.4. Spectral influence of precipitable water

Fig. 5 (left) shows six simulated solar irradiance spectra with w values between 0.5 and 5. As can be seen, an increase of w decreases the amount of solar irradiance received in the near-infrared spectral region, where the bottom junction responds. The irradiance in the spectral region of the middle junction also decreases although to a lesser extent. Fig. 5 (right) shows the ΔSF against w for the HCPV modules considered in this study. The behaviour of the modules based on LM and MM solar cells is different. The modules based on LM solar cells have a similar behaviour. Their performance increases with an increase of w. This can be explained considering that although an increase of w produces a decrease of the current throughout the bottom junction, it never limits the current because of its narrow band gap. At the same time, the top junction current stays roughly constant and the current through the middle junction decreases slightly. Therefore, the current throughout the whole HCPV module is kept approximately constant for any value, resulting in an overall increase of the performance in the two modules. The modules based on MM solar cells have a similar behaviour. Their performance increases with an increase of w until a value around 1.2 and decreases slightly for higher values. The different behaviour found between modules based on MM solar cells and LM solar cells can be explained due to the more narrow band gap of the middle junction on the MM solar cells. So, an increase of w produces a decrease of the current throughout the middle junction. Therefore, the current throughout the whole HCPV modules decreases, resulting in an overall decrease of the performance in the two modules. The small difference found among the four modules for values below 1.2 (modules based on MM solar cells) and 1.5 (modules based on LM solar cells) is due to the fact that in this region the top junction is limiting the current, so that the modules based on SOG Fresnel lenses have a better performance because of their higher transmittance on the spectral region of the top junction.

From the analyses conducted in this section, it can be concluded that AM has the largest impact on the performance of HCPV modules. It may give rise to spectral losses of around 50%. The second parameter by order of influence on the performance of a HCPV module is $\tau_{0.55}$. It may give rise to spectral losses of about 35%. In third place, w may explain spectral losses of up to around 2% (module based on MM solar cells and PMMA Fresnel lenses) and 4% (module based on LM solar cells and SOG Fresnel lenses) and spectral gains about 2% for modules based on LM solar cells. The influence of Ångström exponent is small, with relative spectral factors within $\pm 2\%$.

4. Analysis of the spectral effects under different climate conditions

In this section, the expected annual influence of the spectral solar radiation variations at five different locations on the performance of the HCPV modules is evaluated. First, the main climate conditions at the selected locations and the procedure to compute the annual spectral factor are described. Then, the analysis results are presented and discussed.

4.1. Sites studied

The following five sites were chosen from the Aerosol Robotic Network (AERONET, [30]): Solar Village in Saudi Arabia (N 24°54′25″, E 46°23′49″), Alta Floresta in Brazil (S 09°52′15″, W 56°06′14″), Frenchman Flat in USA (N 36°48″32″, W 115°56′06″), Granada in Spain (N 37°09′50″, W 03°36′18″) and Beijing in China (N 39°58′37″, E 116°22′51″). The five sites represent different climate conditions over different continents. Long-term monthly average values of AOD at 0.55 μm, Ångström exponent obtained from AOD observations between 0.44 and 0.87 μm, and precipitable water were gathered from the AERONET data set. AM was calculated as

$$AM = \frac{1}{\cos\theta + 0.45665\theta^{0.07}(96.4836-\theta)^{-1.697}} \quad (6)$$

where θ is the Sun's zenith angle [31].

Fig. 6 shows the annual average values of AM during sunshine hours, $\tau_{0.55}$, α and w at the five sites studied. Solar Village is a desert location with low-to-medium annual average values of AM, high $\tau_{0.55}$ values, small α values and medium w values. Alta Floresta is a tropical location characterized by low annual average values of AM, high values of $\tau_{0.55}$ and medium α values, with a marked seasonal signal due to biomass burning, and the typical high values of w at any tropical site. Frenchman Flat is a desert location with medium annual average values of AM, characterized by very low values of $\tau_{0.55}$, and medium values of α and w. Granada is a non-industrialized medium-size city in southern Spain with medium annual average values of AM. Although it may be affected occasionally by Saharian dust intrusion events, Granada presents medium annual average values of $\tau_{0.55}$, α and w. Beijing site is a highly-polluted urban location with annual average medium values of AM, extremely high values of $\tau_{0.55}$, and medium α and w values.

4.2. Computation of the annual spectral factor

First, the value of AM was computed every minute during daylight times for a whole year at each site. From these values, the particular frequency distribution of AM (P(AM)) at each site was obtained. Then, the solar irradiance spectrum was computed for 200 AM values evenly distributed between 1 and 38 (a solar zenith angle about 90°) using SMARTS and the yearly average values of the atmospheric parameters retrieved from AERONET at each site. The spectral factor SF(AM) was then computed for 200 solar irradiance spectra at each site using Eq. (4) for the HCPV modules

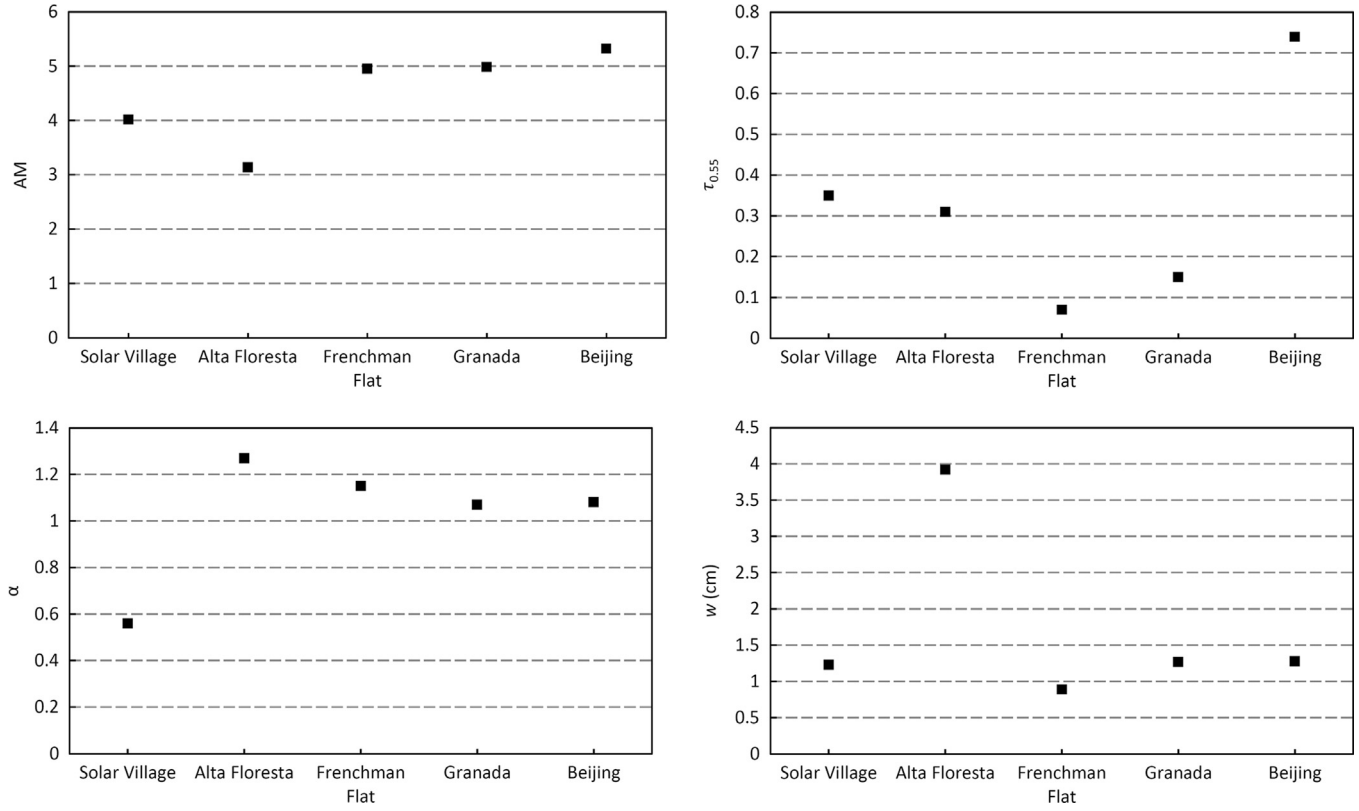

Fig. 6. Annually-averaged values of air mass (top-left), aerosol optical depth at 550 nm (top-right), Ångstrom exponent (bottom-left) and precipitable water (bottom-right) at the five sites studied considered.

studied here. Finally, the annual spectral factor was obtained as

$$SF_{annual} = \frac{\int P(AM)SF(AM)dAM}{\int P(AM)dAM} \quad (7)$$

It represents the annual impact of the spectral variations of the incoming solar irradiance on the performance of each HCPV module at a specific location. From the annual spectral factor, the annual relative spectral factor is calculated using Eq. (5). It is important to note that the annual relative spectral factor estimated is based on the EQE of the MJ solar cells and transmittance of the lenses at the given temperatures shown in Fig. 1. This assumption may affect the results since under real operation conditions the temperature of the cells and that of the lenses is going to be different. This is beyond the scope of this paper but should be studied in future work to better understand and quantify the spectral losses of a HCPV module under real operating conditions.

4.3. Results

Fig. 7 shows the annual spectral impact at the five sites studied for the HCPV modules considered in this study. For all the sites, the modules present losses with respect to the reference spectrum. The site with the lowest losses is Alta Floresta, with annual spectral losses ranging from 7% to 9%. Alta Floresta has the lowest annual average AM value. Similar results are found at Frenchman Flat, with losses ranging from 6% to 11%. At this location, although the annual average AM value is larger, $\tau_{0.55}$ is very small. The results at Granada and Solar Village are very similar to each other, with losses ranging from 10% to 15%. At Solar Village, the annual average AM value is smaller, but $\tau_{0.55}$ is larger. At Beijing, the exceptionally high $\tau_{0.55}$ values produce annual spectral losses ranging from 48% to 51% in the HCPV modules. Overall, the module based on MM solar cells and SOG Fresnel lenses has the lowest spectral losses at all the locations considered here. The reason is that the losses on the performance of the HCPV modules are mainly caused by the limitation of the current of the top junction and taking into account the more narrow band gap of the top junction of the MM solar cell and the higher transmittance of the SOG Fresnel lens in the spectral region of this junction. The module based on LM solar cells and PMMA Fresnel lenses has highest losses while the other two modules show a similar behaviour at all the locations considered here.

AM has proven to have the highest impact on the performance of a HCPV module. Because of this, it is the one parameter used by many authors to account for the spectral influence of the incident

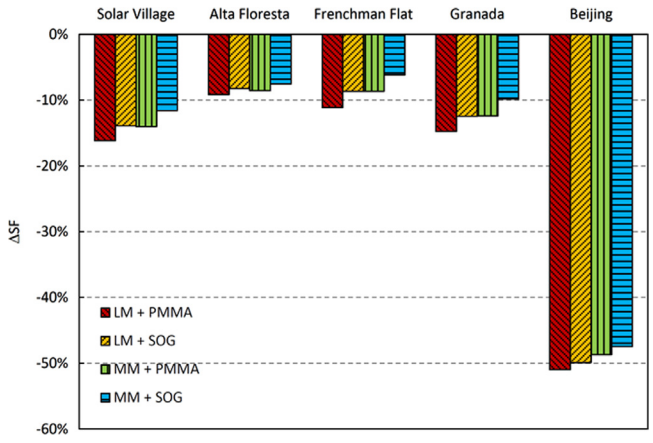

Fig. 7. Annual impact of the spectral variations on the performance of the HCPV modules under study at the five sites studied.

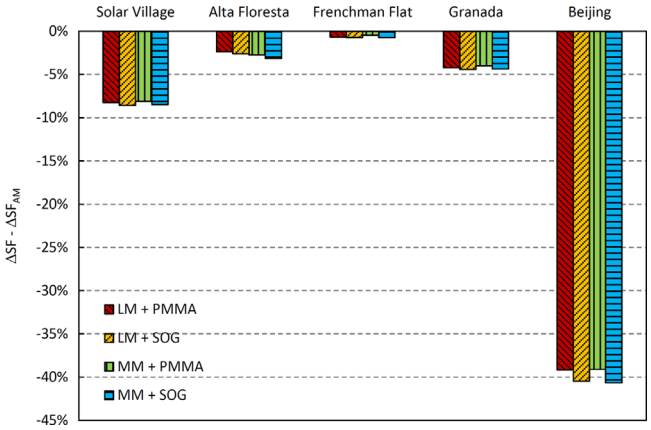

Fig. 8. Annual difference between the spectral impact taking into account the variations of AM, $\tau_{0.55}$, α and w and the spectral impact taking into account only the variations of AM (the rest of parameters are kept constant at the reference values defined by the AM1.5d ASTM G-173-03 reference spectrum) at the five sites studied for the HCPV modules considered in this study.

solar irradiance on the electrical output of a HCPV module or system [32–39]. Therefore, we have conducted the next validating experiment to evaluate the appropriateness of this approach. Fig. 8 shows the difference between the annual spectral impact taking into account the variations of AM, $\tau_{0.55}$, α and w (Fig. 7) and the annual spectral impact taking into account only the variations of AM (ΔSF_{AM}) at the five sites studied for the HCPV modules considered in this study. As is shown, Frenchman Flat is the place with the lowest annual differences with values ranging from 0.5% to 0.7% due to the low annual average $\tau_{0.55}$ value which means that the annual losses are mainly given by AM. Low annual differences are also found in Alta Floresta and Granada with values ranging from 3% to 4%. Both places show a larger annual average $\tau_{0.55}$ value than Frenchman Flat. This also explains the reason of the annual differences found in Solar Village with values ranging from 8% to 9%. Extreme annual differences are found in Beijing with values ranging from 39% to 41% because of the high annual average $\tau_{0.55}$ value which means that the annual losses are mainly given by $\tau_{0.55}$. From this analysis it can be concluded that AM is a good tool to quantify the spectral impacts on the performance of a HCPV module in places with low $\tau_{0.55}$ values. However, places with high values of $\tau_{0.55}$ should include an additional correction to take into account the spectral influence of this atmospheric parameter in order to accurately quantify the influence of the incident spectrum on the performance of a HCPV module.

5. Conclusions and future work

An analysis of the annual influence of the spectral variations on the performance of four HCPV modules under real and different climate conditions has been conducted. In particular the locations chosen are: Solar Village, Alta Floresta, Frenchman Flat, Granada and Beijing. Also, an analysis of the individual impact of the atmospheric parameters with the highest influence on the performance of a HCPV module has been carried out in order to better understand the influence of the spectral effects under real operating conditions.

From the analysis of the individual impact of the atmospheric parameters it can be concluded that the parameters with the largest influence on the performance of a HCPV module are AM and $\tau_{0.55}$ respectively, while α and w have a small influence. This means that the spectral behaviour of a HCPV module under real operating conditions can be explained with an acceptable margin of error taking into account only the influence of AM and $\tau_{0.55}$.

From the analysis of the annual effects of the spectral variations on the performance of the HCPV modules considered, it can be concluded that Alta Floresta is the place with the lowest annual spectral losses (7–9%) due to the low annual average value of AM and Beijing is the place with the highest annual spectral losses (48–51%) due to the extreme annual average value of $\tau_{0.55}$. Also, a spectral correction based only on AM to quantify the influence of the incident spectrum on the electrical output of a HCPV module or system is only valid for locations with low values of $\tau_{0.55}$. This means that locations with high values of $\tau_{0.55}$ should include an additional correction to take into account the spectral influence of this atmospheric parameter. Finally, it is important to note that the module based on MM solar cells and SOG Fresnel lenses has the lowest spectral losses at all the locations here considered due to the narrower band gap of the top junction of the MM solar cell and the higher transmittance of the SOG Fresnel lens in the spectral region of the this junction.

It is important to note that this study is based on the EQE of the MJ solar cells and transmittance of the lenses at the given temperatures as shown in Fig. 1. However, under real operation conditions the temperature of the cells and lenses is going to be different because it will be affected by the changes of direct normal irradiance, air temperature and wind speed [40,41]. Also, other effects such as the possible influence of secondary optical elements and the possible effects of the non-uniform illumination on the solar cell surface produced by the chromatic aberration of the lenses have not been taken into account [42]. Despite the fact that these approximations have been discussed by different authors and are widely considered as a good approach to quantify the spectral influence and the electrical output of a HCPV device [4,5] [9,10] [15,16] [25,26] [34] [36,37] [41] [43,44], authors plan to include them in future works.

Acknowledgements

This work is part of the project “Desenvolvemento de novos conceptos baseados en tecnoloxía de concentración fotovoltaica para a produción de enerxía eléctrica adaptados a distintas zonas climáticas”, through the programme “formación posdoutoral do Plan galego de investigación, innovación e crecemento 2011–2015 (Plan I2C)” funded by the Xunta de Galicia and by the European Social Fund.

References

[1] P. Faine, S. Kurtz, C. Riordan, J.M. Olson, The influence of spectral solar irradiance variations on the performance of selected single-junction and multi-junctions solar cells, Sol. Cells 31 (1991) 259–278.
[2] E. Fernández, A. García-Loureiro, P. Pérez-Higueras, G. Siefer, Monolithic III–V triple-junction solar cells under different temperatures and spectra, in: Proceedings of the Spanish Conference on Electron Devices (CDE), Palma de Mallorca, 2011.
[3] K. Araki, M. Yamaguchi, Influence of spectum change to 3-junction solar cells, Sol. Energy Mater. Sol. Cells 75 (3–4) (2003) 707–714.
[4] G. Kinsey, K.M. Edmondson, Spectral response and energy output of concentrator multijunction solar cells, Prog. Photovolt.: Res. Appl. 17 (2009) 279–288.
[5] S. Philipps, G. Peharz, R. Hoheisel, T. Hornung, N. Al-Abbadi, F. Dimroth, A. Bett, Energy harvesting efficiency of III–V triple-junction concentrator solar cells under realistic spectral conditions, Sol. Energy Mater. Sol. Cells 94 (5) (2010) 869–877.
[6] J. Jaus, C.A. Gueymard, Generalized spectral performance evaluation of multi-junction solar cells using a multicore parallelized version of SMARTS, AIP Conf. Proc. 1477 (2012) 122–126.
[7] G. Zubi, J.L. Bernal-Agustín, G. Vincenzo Frascastoro, High concentration photovoltaic systems applying III–V cells, Renew. Sustain. Energy Rev. 13 (2009) 2645–2652.
[8] W.T. Xie, Y.J. Dai, R.Z. Wang, K. Sumathy, Concentrated solar energy applications using Fresnel lenses: a review, Renew. Sustain. Energy Rev. 15 (6) (2011) 2588–2606.
[9] J. Hashimoto, S. Kurtz, S. Keiichiro, M. Muller, K. Otani, Performance of CPV sytem using three different types of III–V multi-junction solar cells, AIP Conf. Proc. 1477 (2012) 372–376.
[10] G. Peharz, G. Siefer, A. Bett, A simple method for quantifying spectral impacts on multi-junction solar cells, Sol. Energy 83 (2009) 1588–1589.
[11] M. Victoria, S. Askins, R. Nuñez, C. Domínguez, R. Herrero, I. Antón, G. Sala, J.M. Ruíz, Tuning the current ration of a CPV system to maximiza the energy harvesting in a particular location, AIP Conf. Proc. (2013) 156–161.
[12] C. Gueymard, Parameterized transmittance model for direct beam and circumsolar spectral irradiance, Sol. Energy 71 (5) (2001) 325–346.
[13] C. Gueymard, Simple model of the atmospheric radiative transfer of sunshine (SMARTS) version 2.9.5 2009.
[14] C. Gueymard, SMARTS. A simple model of the atmospheric radiative transfer of sunshine: algorithms and performance assessment, Florida Solar Energy Center, Cocoa, FL, 1995 (Profesi, Professional paper, Report no. FSEC-PF-270-95).
[15] M. Muller, B. Marion, S. Kurtz, J. Rodriguez, An investigation into spectral parameters as they impact CPV module performance, AIP Conf. Proc. 1 (2010) 307–311.
[16] N. Chan, T.B. Young, H.E. Brindley, N. Ekins-Daukes, K. Araki, Y.Y. Kemmoku, Validation of energy prediction method for a concentrator photovoltaic module in Toyohashi Japan, Prog. Photovolt.: Res. Appl. (2012).
[17] M. Alonso-Abella, F. Chenlo, G. Nofuentes, M. Torres-Ramírez, Analysis of the spectral effects on the energy yield of different PV (photovoltaic) technologies: the case of four specific sites, Energy 67 (2014) 435–443.
[18] G. Nofuentes, B. García-Domingo, J.V. Muñoz, F. Chenlo, Analysis of the dependence of the spectral factor of some PV technologies on the solar spectrum distribution, Appl. Energy 113 (2014) 302–309.
[19] C.R. Osterwald, K.A. Emery, M. Muller, Photovoltaic module calibration value versus optical air mass: the air mass function, Prog. Photovolt.: Res. Appl. (2012).
[20] IEC-60904-7, “Photovoltaic devices – Part 7: Computation of the spectral mismatch correction for measurements of photovoltaic devices,” 2008.
[21] C. Dominguez, I. Anton, G. Sala, S. Askins, Current-matching estimation for multijunction cells within a CPV modules by means of component cells, Prog. Photovol.: Res. Appl. 21 (7) (2013) 1478–1488.
[22] W. McMahon, K. Emery, D. Friedman, L. Ottoson, M. Young, J. Ward, C. Kramer, A. Duda, S. Kurtz, Fill factor as a probe of current-matching for GaInP2/GaAs tandem cells in a concentrator system during outdoor operation, Prog. Photovolt.: Res. Appl. 16 (2008) 213–224.
[23] C. Domínguez, I. Antón, G. Sala, Multijunction solar cell model for translating I–V characteristics as a function of irradiance, spectrum, and cell temperature, Prog. Photovolt.: Res. Appl. 18 (4) (2010) 272–284.
[24] ASTM G. 173-03 Standard tables for reference solar spectral irradiance: direct normal and hemispherical on 37 tilted surface, American society for testing and materials, 2012, pp. 1–20.
[25] J. Leloux, E. Lorenzo, B. Garcia-Domingo, J. Aguilera, Y.C.A. Gueymard, A bankable method for assessing the performance of a CPV plant, Appl. Energy 118 (2014) 1–11.
[26] G. Kinsey, K. Stone, J. Browd, V. Garboushian, Energy prediction of amonix CPV solar power plants, Prog. Photovolt.: Res. Appl. (2010).
[27] M. Iqbal, An Introduction to Solar Radiation, Academic Press, Canada, 1983.
[28] A. Ångstrom, Techniques of determinig the turbidity of the atmosphere I, Tellus 13 (1961) 214–223.
[29] K.-N. Liou, Second ed., An Introduction to Atmospheric Radiation, 84, Academic Press, California, 2002.
[30] Aerosol Robotic Network 2014. [Online]. Available: ⟨http://aeronet.gsfc.nasa.gov/⟩.
[31] F. Kasteny, A.T. Young, Revised optical air mass tables and approximation formula, Appl. Opt. 28 (22) (1989) 4735–4738.
[32] E. Aronova, V. Grilikhes, M. Shvarts and N. Timoshi, On the estimation of hourly power output of solar photovoltaic installations with MJ SCs and sunlight concentrators. In: Proceedings of Photovoltaic Specialist Conference – PVSC'08, 2008.
[33] D. King, W. Boyson, J. Kratochvill, Photovoltaic Array Performance Model, Sandia National Laboratories, Albuquerque, New Mexico, 2004.
[34] E.F. Fernández, F. Almonacid, P. Rodrigo, P. Pérez-Higueras, Model for prediction of the maximum power point of a high concentrator photovoltaic module, Sol. Energy 97 (2013) 12–18.
[35] P. Rodrigo, E. Fernández, F. Almonacid, P. Pérez-Higueras, Models for the electrical characterization of high concentration photovoltaic cells and modules: a review, Renew.Sustain. Energy Rev. 26 (2013) 752–760.
[36] Y. Kim, S.-M. Kang, R. Winston, Modeling of a concentrating photovoltaic system for optimum land use, Prog. Photovolt.: Res. Appl. 21 (2) (2013) 240–249.
[37] E. Strobach, D. Faiman, S. Kabalo, D. Bokobza, V. Melnichak, A. Gombert, T. Gerstmaier, M. Rottger, Modeling a grid-connected concentrator photovoltaic system, Prog. Photovolt.: Res. Appl. (2014), http://dx.doi.org/10.1002/pip.2467.
[38] E. Fernández, P. Pérez-Higueras, A. García Loureiro, P. Vidal, Outdoor evaluation of concentrator photovoltaic systems modules from different manufacturers: first results and steps, Prog. Photovolt.: Res. Appl. 21 (4) (2013) 693–701.
[39] E. Fernández, P. Rodrigo, J. Fernández, F. Almonacid, P. Pérez-Higueras, A. Garcia-Loureiro, G. Almonacid, Analysis of high concentrator photovoltaic modules in outdoor conditions: influence of direct normal irradiance, air temperature and air mass, J. Renew. Sustain. Energy 6 (2014) 013102.

[40] F. Almonacid, P. Pérez-Higueras, E. Fernández, P. Rodrigo, Relation between the cell temperature of a HCPV module and atmospheric parameters, Sol. Energy Mater. Sol. Cells 105 (2012) 322–327.
[41] T. Hornung, M. Steiner, P. Nitz, Estimation of the influence of Fresnel lens temperature on energy generation of a concentrator photovoltaic system, Sol. Energy Mater. Sol. Cells 99 (2012) 333–338.
[42] H. Baig, K. Heasman, T.K. Mallick, Non-uniform illumination in concentrating solar cells, Renew. Sustain. Energy Rev. 16 (2012) 5890–5909.
[43] E. Fernández, G. Siefer, F. Almonacid, A. García-Loureiro, P. Pérez-Higueras, A two subcell equivalent solar cell model for III–V triple junction solar cells under spectrum and temperature variations, Sol. Energy 92 (2013) 221–229.
[44] G. Siefer, A. Bett, Analysis of temperature coefficients for III–V multi-junction concentrator cells, Prog. Photovolt.: Res. Appl. (2012), http://dx.doi.org/10.1002/pip.2285.

Referencia / Reference: Fernández, E. F., Almonacid, F., **Soria-Moya, A.** y Terrados, J. (2015). *Experimental analysis of the spectral factor for quantifying the spectral influence on concentrator photovoltaic systems under real operating conditions. Energy*, 90, 1878-1886.

Estado / Status: Publicado / *Published.*

Índice de impacto / Impact Factor: 4.844.

Categoría / Catogory: *Energy and Fuels*. Ranking: 12/88 (Q1).

Energy 90 (2015) 1878–1886

Contents lists available at ScienceDirect

Energy

journal homepage: www.elsevier.com/locate/energy

Experimental analysis of the spectral factor for quantifying the spectral influence on concentrator photovoltaic systems under real operating conditions

Eduardo F. Fernández [a, b, *], Florencia Almonacid [b], Alberto Soria-Moya [a], Julio Terrados [b]

[a] Centre of Advanced Studies in Energy and Environment (CEAEMA), University of Jaen, Las Lagunillas Campus, Jaen 23071, Spain
[b] IDEA Solar Energy Research Group, University of Jaen, Las Lagunillas Campus, Jaen 23071, Spain

ARTICLE INFO

Article history:
Received 25 February 2015
Received in revised form
1 July 2015
Accepted 4 July 2015
Available online 29 July 2015

Keywords:
Spectral factor
Concentrator photovoltaics
Outdoor measurements

ABSTRACT

The spectral dependence of concentrator photovoltaic devices shows a larger and more complex behaviour than conventional photovoltaic devices due to the use of multi-junction solar cells and optical elements. The spectral factor is a widely used index for evaluating the spectral influence on the performance of conventional photovoltaics in outdoors. However, the experimental analysis of this index as a tool to evaluate the spectral influence on the performance of concentrator devices has not been undertaken and still remains unknown. The aim of this paper is to analyse the spectral factor as an index for estimating the spectral influence on the power and energy output of concentrator photovoltaic systems. The final goal is to contribute to the development of new procedures for predicting the performance of this technology under real operating conditions. To achieve this goal, two concentrator modules have been monitored over the course of two years in Southern Spain. Results show that the spectral factor has a larger and different spectral sensitivity than the power output. However, this index can be used as a good first approximation for quantifying the spectral influence on the maximum power and energy yield of a concentrator photovoltaic system under real operating conditions.

1. Introduction

HCPV (high concentrator photovoltaic) technology is based on the use of cheap optical elements to collect direct sunrays and concentrate them around 300–1200× on a high efficiency MJ (multi-junction) solar cell [1,2]. The optical devices usually consist of a POE (primary optical element) and a SOE (secondary optical element). The POE (usually a Fresnel lens) concentrates the sunrays on the solar cell surface, and the SOE (optional) receives the light from the primary one to homogenize the light and improve the angular acceptance angle [3,4]. The aim is to decrease the cost of electricity reducing the semiconductor material by the use of cheap optical elements [5–7]. In particular, the LCOE (levelised cost of electricity) of HCPV systems shows a clear tendency to decrease and is expected to be able to reach values in the range of 0.035–0.080 €/kWh in 2020 [8].

The electrical output of photovoltaic devices is sensible to the spectral distribution of the incident irradiance. MJ solar cells have a larger and a more complex spectral dependence than SJ (single-junction) solar cells due to the series connection of several subcells with different energy gaps [9]. Furthermore, the optical devices used modify the spectral distribution of the incident irradiance that falls on the solar cell [10]. Because of this, the spectral influence on the electrical output of HCPV devices is inherently different and more complex than in conventional PV (photovoltaic) devices.

In order to address this issue, different specific indexes tailored to the special features of HCPV devices such as the SMR (spectral matching ratio) or the spectral parameter Z have been recently introduced [11,12]. These indexes expressed with a single parameter a particular incident spectrum as function of the current mismatch between two component cells, usually the top and the middle. The component solar cells have a similar architecture to MJ solar cells, however each component cell has only one active subcell. Because of this, it is possible to measure the current of each individual junction [13]. These methods are widely used since avoid the use of spectroradiometers and offer a simple and useful tool for quantifying the spectral influence on the electrical output of HCPV

* Corresponding author. IDEA Solar Energy Research Group, University of Jaen, Las Lagunillas Campus, Jaen 23071, Spain. Tel.: +34 9543213518.
E-mail address: fenandez@ujaen.es (E.F. Fernández).

http://dx.doi.org/10.1016/j.energy.2015.07.015
0360-5442/

devices in outdoor conditions. The values of SMR and Z indexes gathered with components cells cannot be directly related with the electrical output of a HCPV device under real operating conditions. On the one hand, the SMR and Z indexes characterize the incident direct spectral irradiance distribution, but not its effect on the performance of a particular HCPV device. On the other hand, the absorption band of the active subcell of each component cell is different than the one of MJ solar cells. Furthermore, the component cells do not include any optical element, so that they do not quantify the influence of the optical elements on the spectral distribution that strikes on the MJ solar cells of a HCPV device. Because of this, it is necessary to perform long-term outdoor analysis in order to relate the measured values of SMR and Z and the electrical parameters of each particular HCPV device [12,14].

The mismatch or *SF* (spectral factor) defined in the IEC (International Electronic Commission) 60904-7 [15,16] standard is a widely used index for the spectral evaluation of conventional PV devices in outdoors [17–23]. The *SF* evaluates the impact of an incident spectrum on a particular PV device relative to its electrical characteristics under the reference conditions. The advantage of this parameter is that the spectral influence on the performance of a PV device can be directly evaluated by solving the *SF* with a satisfactory degree of accuracy. The *SF* as defined for conventional PV is not valid for HCPV due to the use of MJ solar cells and optical devices. Taking this into account, this index has been reformulated and introduced for HCPV applications in Ref. [24]. However, the experimental validation of the *SF* as a parameter to evaluate the spectral influence on the power and energy output of HCPV devices has not been undertaken and still remains unknown.

This paper aims to analyse the *SF* as an index for quantifying the spectral impact on the power output of HCPV devices under real operating conditions. So that, the spectral effects on the performance of HCPV systems could be directly evaluated by solving this index, as in the case of conventional PVs. The goal is contribute to the development of new methods to achieve a better knowledge of the behaviour of HCPV system in outdoors. The validation of the *SF* for quantifying the spectral impact on HCPV systems would also allow their power or energy output to be estimated by using the well-known procedures applied in conventional PV systems. Taking this into account, the study of the accuracy in the estimation of the maximum power of a HCPV module as a linear function of the irradiance, thermal factor and spectral factor is also conducted. Furthermore, the analysis of the annual spectral impact on the energy yield of two HCPV modules depending on latitude is carried out. The analysis of the annual spectral effects is useful to better evaluate the potential and to leverage our understanding of performance of HCPV technology in outdoors. In order to achieve this goal, this paper is divided in different sections. Section 2 introduces the spectral factor as a parameter to evaluate the influence of the incident spectrum on the power output of a HCPV device. Section 3 describes the different materials used and experimental measurements gathered to conduct this study. Section 4 describes the procedure followed to obtain the incident spectral distribution. The analyses of the results of the *SF* as an index for quantifying the spectral impact on the power output of HCPV devices are discussed in Section 4. In Section 5, the estimation of the spectral impact on the energy yield of the HCPV modules considered is carried out. Finally, the main conclusions of this work are outlined in Section 6.

2. Spectral factor and power output

The electrical output of a PV or HCPV device is mainly given by the incident irradiance, cell temperature and spectral distribution [23,25–30]. Taking this into account, the following expression has proven to be valid to estimate the maximum power (P) of a conventional PV device with a satisfactory margin of error [31,32]:

$$P \approx \frac{P^*}{G^*} \cdot G \cdot TF \cdot SF \tag{1}$$

where P^* and G^* are the maximum power and global irradiance under the STC (standard test conditions), G is the incident global irradiance, TF is the thermal factor and SF is the spectral factor.

The thermal factor quantifies the influence of cell temperature on the power output of a PV device as [31]:

$$TF = 1 - \gamma\left(T_c - T_c^*\right) \tag{2}$$

where γ is the maximum power temperature coefficient, T_c is the cell temperature and T_c^* is the cell temperature under STC.

The spectral factor quantifies the influence of the spectrum on the power output of a single-junction PV device as [20]:

$$SF = \frac{\int E(\lambda)SR(\lambda)d\lambda \int E_{ref}(\lambda)d\lambda}{\int E_{ref}(\lambda)SR(\lambda)d\lambda \int E(\lambda)d\lambda} \tag{3}$$

where λ is the wavelength, $E(\lambda)$ is the incident global spectral distribution, $E_{ref}(\lambda)$ is reference spectrum and $SR(\lambda)$ is the spectral response of the PV device. This factor evaluates the spectral impact as the ratio of the short-current density at operating conditions relative to the value under STC and is widely regarded as a good approach to quantify the spectral gains or losses on the power output of a conventional PV device [33,34].

HCPV devices only respond to the direct normal component of the irradiance due to the use of optical devices [35]. Hence, following the same approach than in equation (1), the maximum power of a HCPV system may be estimated as:

$$P \approx \frac{P^*}{DNI^*} \cdot DNI \cdot TF \cdot SF \tag{4}$$

where DNI^* is the direct normal irradiance under STC and DNI is the incident direct normal irradiance.

The thermal factor defined in equation (2) has been demonstrated to be valid for HCPV devices since the influence of the cell temperature on their electrical output can be quantified with linear temperature coefficients as discussed in Ref. [36]. So that, the maximum power of a HCPV system can be estimated as function of DNI and T_c as [37]:

$$P \approx \frac{P^*}{DNI^*} \cdot DNI \cdot \left(1 - \gamma\left(T_c - T_c^*\right)\right) \tag{5}$$

However, the spectral factor as expressed in equation (3) is not valid for HCPV devices due to the use of MJ solar cells and optical devices. Because of this, this factor has to be rewritten for HCPV applications as [24]:

$$SF = \frac{\min\left(J_{sc,i}(E_b(\lambda))\right) \int E_{b,ref}(\lambda)d\lambda}{\min\left(J_{sc,i}\left(E_{b,ref}(\lambda)\right)\right) \int E_b(\lambda)d\lambda} \tag{6}$$

where the short-circuit current density of each *i*-junction is given by:

$$J_{sc,i}(E_b(\lambda)) = \int E_b(\lambda)\eta(\lambda)SR_i(\lambda)d\lambda \quad (7)$$

and $E_b(\lambda)$ is the incident direct normal spectral distribution, $E_{b,ref}(\lambda)$ is the direct reference spectrum AM1.5d ASTM G-173-03 at which MJ solar cells and HCPV modules are rated [38] and $\eta(\lambda)$ is the spectral optical efficiency.

The *SF* defined in equation (6) is related with the concept of spectrally corrected direct normal irradiance (DNI_c) previously discussed in Ref. [39]. The *DNIc* represents the portion of the incident spectrum that a HCPV module is able to convert into electricity and can be expressed as:

$$DNIc = DNI \cdot SF \quad (8)$$

However, the use of the *DNIc* to quantify the spectral impact on the power output as formulated in equation (4) has not been undertaken.

Equation (6) estimates the influence of the spectrum of a HCPV device as a function of the minimum short-circuit current of the *i*-junction of the respective MJ solar cell. Because of this, this equation does not take into account the possible spectral influence on the maximum power of the *i*-junctions which are not limiting the current of the device. Also, the indoor characterization of MJ solar cells by using solar simulators has demonstrated that the short-circuit current has a slightly larger and different spectral influence than the maximum power [40–42]. Because of this, the analysis of the *SF* defined in equation (6) as an index for estimating the spectral influence of the power output of a HCPV module or system has to be undertaken. The validation of this index would allow equation (4) for estimating the power or energy output of a HCPV system under different irradiances, temperatures and spectra, to be used. Bearing this in mind, the use of equation (4) for predicting the maxim power of a HCPV system has not been addressed yet and its accuracy needs to be also analysed.

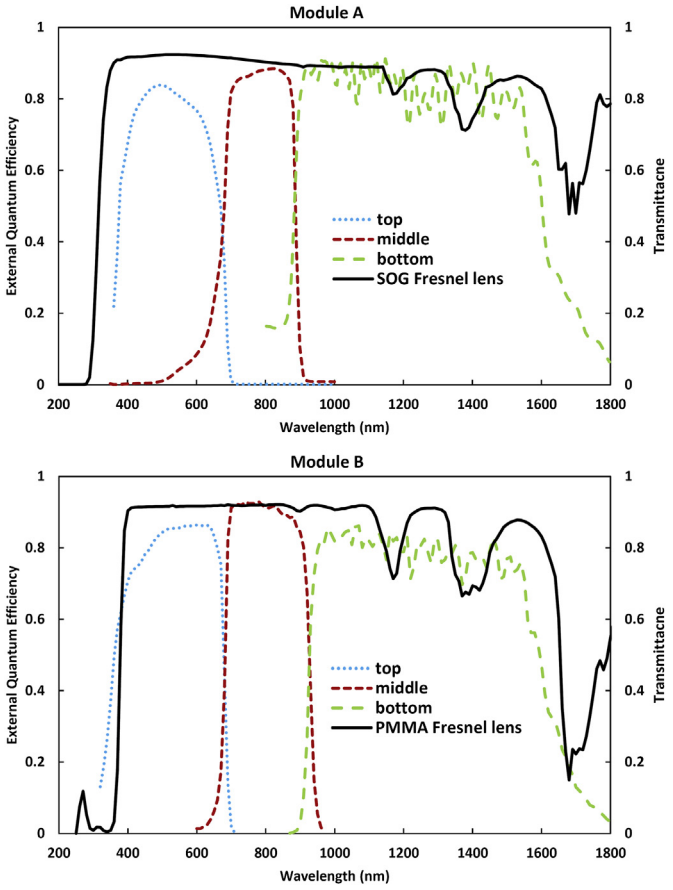

Fig. 1. External quantum efficiency of the MJ cells and transmittance of the Fresnel lenses of the high concentrator photovoltaic modules A and B.

3. Experimental set-up and data available

Two different concentrator photovoltaic modules, denoted as A and B, have been used in this study. The module A is made up of 20 triple-junctions lattice-matched GaInP/GaInAs/Ge solar cells interconnected in series. The module uses SOG (silicon-on-glass) Fresnel lenses as primary optical element. The secondary optical element consists of reflexive truncated pyramids made up of an aluminium film layer to enhance the reflectivity. The module has an optical efficiency of 80%, a geometric concentration of 700 and uses passive cooling to ensure that MJ solar cells operate on their optimal operation range. The module B is made up of 25 triple-junctions lattice-matched GaInP/GaInAs/Ge solar cells interconnected in series. In this case, the module uses PMMA (poly(-methylmethacrylate)) Fresnel lenses as primary optical element and glass refractive truncated pyramids as secondary optical element. The module has an optical efficiency of 85%, a geometric concentration of 550 and also uses passive cooling. The EQE (external quantum efficiency) of the cells and transmittance of the primary optics of each module are plotted in Fig. 1. In addition, Table 1 shows the maximum power of both modules under STC.

Both modules have being under study at the CEAEMA (Centre of Advanced Studies in Energy and Environment) at the University of Jaen in Southern Spain (N 37°27′36″, W 03°28′12″) since January 2013. The HCPV modules were mounted on a high precise two axis-solar tracker located on the roof of the research centre. The electrical parameters of the modules were measured with a high accuracy four-wire electronic load. Also, a four-wire PT100 placed on the back of each module to measure their heat-sink temperature were installed. These thermometers were connected to a data logger to record both temperatures. It is worth mention that these sensors were located in a receiver between the centre and the border of each module in order to avoid differences in temperature due to the temperature distribution of a HCPV module [43–45]. The cell temperature of each module is estimated from its back surface temperature following the procedure introduced in Ref. [37,46]. In addition, an atmospheric station recorded the main atmospheric parameters such as direct normal irradiance, air temperature, wind speed or humidity. All the parameters commented above were recorded daily every 5 min. The days on which the system was stopped, either by failure, maintenance or because a research experiment was conducted have not been taken into account to avoid distorting the study object of this work. Also, modules were cleaned once a week and after rainy days, and the alignment of the tracker was periodically calibrated to avoid possible electrical losses and noise in the data.

Table 1
Maximum power of the concentrator photovoltaic modules considered under standard test conditions (STC).

Module	P (W)	DNI (W/m^2)	T_{cell} (°C)	Spectrum
A	280	1000	25	AM1.5d
B	150	1000	25	AM1.5d

4. Spectra simulation

In order to obtain the spectral factor defined in equation (6) is necessary to know the spectral distribution of the incident direct normal irradiance. The spectra for the whole period of measurement commented in last section have been simulated using the SMARTS (Simple Model of the Atmospheric Radiative Transfer of Sunshine) [47]. This model accurately predicts the spectral distribution of the incident solar irradiance at any given set of atmospheric parameters and is commonly used for the spectral characterization of HCPV devices. As has been widely discussed, the main atmospheric parameters that affect the spectrum and power output of a HCPV module in order of importance are: the *AM* (air mass), the aerosol optical depth, usually quantified at 500 or 550 nm, and the precipitable water [48,49,24]. Taking this into account, the *AM* was calculated as a function of Sun's zenith angle (θ) as [50]:

$$AM = \frac{1}{cos\theta + 0.50572(96.07995 - \theta)^{-1.6364}} \quad (9)$$

and the daily values of aerosol optical depth at 550 nm (AOD_{550}) and *PW* (precipitable water) were obtained from MODIS Daily Level-3 data source [51], following the same approach previously used in Ref. [39]. Also, Jaen is a non-industrialized medium-size city, so that the rural aerosol model was selected. The rest of inputs parameters of SMARTS model were held constant at the reference values defined by the standard AM1.5d ASTM G-173-03 at which MJ solar cells and HCPV modules are rated [38].

Once the spectral distribution is available, the *SF* for the two HCPV modules considered were obtained using equations (6) and (7), and the data of the EQE of MJ solar cells and lens transmittance shown in Fig. 1. Figs. 2 and 3 show two example days of the simulated spectral factor and short-circuit current densities of each junction for both modules. In order to show an extreme variation between data, the summer and winter solstices were selected since these days represent the minimum and maximum daily average *AM* values respectively. As can be seen, the behaviour of the spectral factor is similar for both modules and days. The maximum spectral losses are produced at the sunrise and sunset when the *AM* values are higher, and the minimum spectral losses are produced at middle day when the *AM* values are lower. However, although the behaviour of the spectral factor is similar in both days, the spectral losses are significantly higher in the winter solstice than in summer solstice with average *SF* values around 0.7 and 0.8 respectively for both modules. This difference can be explained taking into account that the *AM* values are significantly higher in the winter solstice than in the summer solstice with average *AM* values of 4.41 and 2.61, maximum values of 18.90 and 14.90, and minimum values of 2.05 and 1.03 respectively. This can be also observed from the analysis of the short-circuit current densities of the top and middle junction of the MJ solar cells of both modules. As can be seen, for low *AM* values the top and middle junctions yield similar currents while for high *AM* values the top junction strongly limits the current resulting in an overall decrease of the *SF* of the modules.

5. Analysis of results

In this section the results of the analysis of the *SF* as an index for estimating the spectral influence of the power output of a HCPV system are presented. First of all, the spectral factor is estimated using equation (4) from the experimental measurements of the maximum power, direct normal irradiance and cell temperature. This spectral factor will be denoted as SF_P. The values of SF_P are compared with the values of *SF* obtained using equation (6) and the procedure commented in section 4. Fig. 4 shows the relative difference between the SF_P and the *SF* expressed as:

$$\Delta SF(\%) = \frac{(SF_P - SF)}{SF} \times 100 \quad (10)$$

This figure shows the average ΔSF versus the *SF* for each module. As can be seen, the ΔSF is positive for *SF* values lower than around 1 and is negative for higher *SF* values with a clear tendency to decrease with an approximate linear behaviour as the *SF* increases. For *SF* values lower than 1, the ΔSF is positive with a maximum value of around 6% ($SF = 0.60$ and $SF_P = 0.64$) and 7% ($SF = 0.55$ and $SF_P = 0.59$) for modules A and B respectively. This indicates that the *SF* predicts higher spectral losses than the ones produced in the power output. For *SF* values higher than 1, the ΔSF is negative with a minimum value of around −1% ($SF = 1.10$ and $SF_P = 1.09$) and 1.5% ($SF = 1.05$ and $SF_P = 1.04$) for modules A and B respectively. This indicates that the *SF* predicts higher spectral gains than the ones produced in the power output. Hence, it can be concluded that the *SF* has a different and larger spectral sensitivity than the power output. Because of this, the spectral effects quantified by the *SF* are different than those produced on the power. It is important to note that the maximum and minimum values of the *SF* will depend on the atmospheric parameters of each location. As was shown in Figs. 2 and 3, the *SF* can reach values of around 0 at sunset and sunrise when the *AM* values are higher. However, the minimum values of the *SF* gathered during the experiment were 0.60 and 0.55 for modules A and B respectively. This is due to the fact that at high *AM* values (low DNI), the sun elevation is low and the HCPV

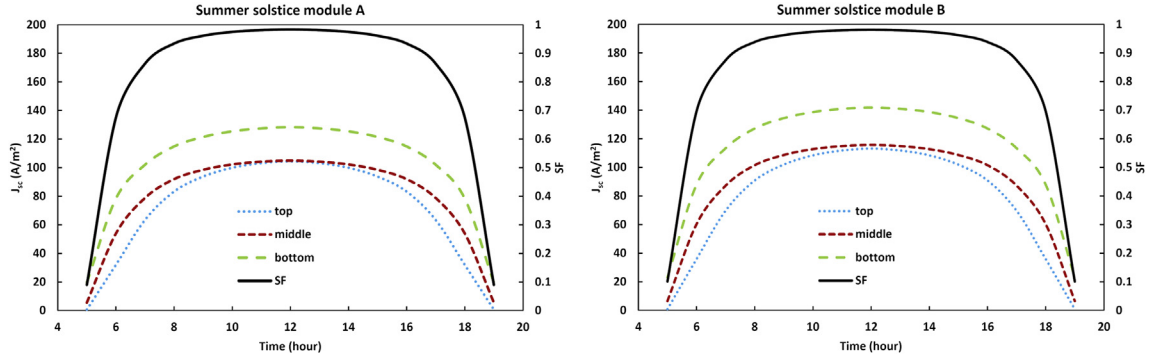

Fig. 2. Simulated spectral factor and short-circuit current densities of each junction for the two modules considered at the summer solstice 2013 ($AOD_{550} = 0.23$, $PW = 1.86$, average $AM = 2.61$).

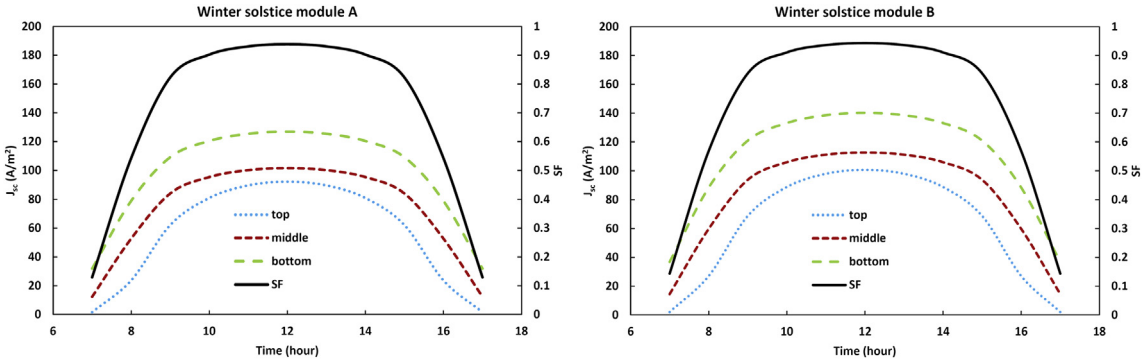

Fig. 3. Simulated spectral factor and short-circuit current densities of each junction for the two modules considered at the winter solstice 2013 ($AOD_{550} = 0.10$, $PW = 1.00$, average $AM = 4.41$).

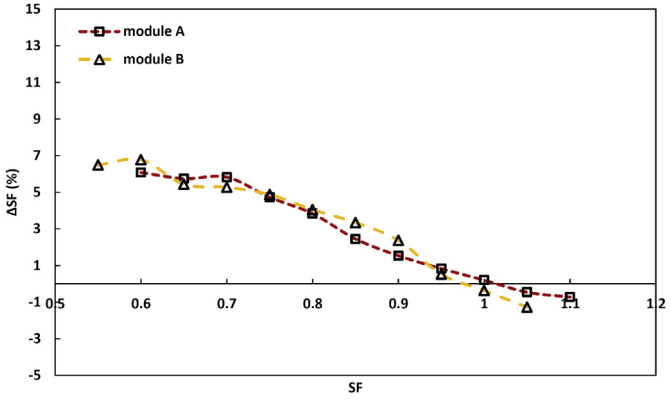

Fig. 4. Average relative difference between the SF_P obtained using equation (4) and the experimental data, and the simulated SF obtained using equation (6) at different the SF levels for modules A and B.

modules are not receiving DNI because of the presence of mountains and buildings.

As can be seen in Fig. 4, there is an almost linear dependence between the average ΔSF and SF. This means that the spectral effects predicted with the SF could be related with the spectral effects produced in the maximum power with a linear mathematical relationship. In order to analyse this in more detail, Fig. 5 shows the linear regression analysis between SF and SF_P. As can be seen, there is a good linear agreement between the two magnitudes with a

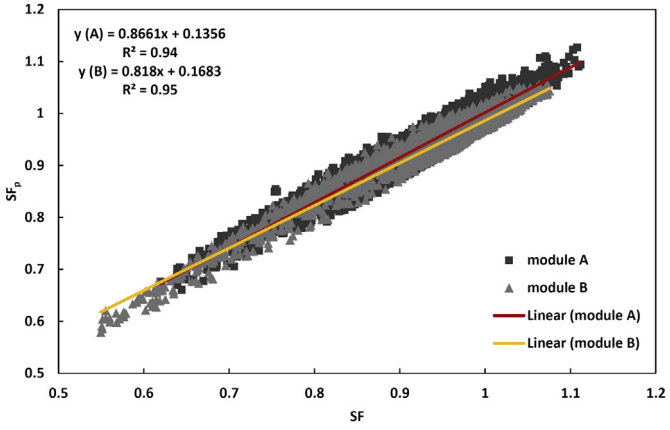

Fig. 5. Linear regression analysis between the SF and SF_p for modules A and B.

determination coefficient of $R^2 = 0.94$ and $R^2 = 0.95$ for modules A and B respectively. This indicates that the SF and SF_p can be related with a low margin of error as:

$$SF_P = aSF + b \tag{11}$$

So that, equation (4) can be more accurately expressed for HCPV systems as:

$$P \approx \frac{P^*}{DNI^*} \cdot DNI \cdot TF \cdot (aSF + b) \tag{12}$$

where a and b are specific coefficients of the concentrator that will be given by the characteristics of the MJ solar cells and optical devices used.

The analysis of the errors in the estimation of the maximum power using equation (4) based on the SF as a spectral corrections is also conducted. Table 2 shows the RMSE (root means square error), the MBE (mean bias error) and the determination coefficient between actual and predicted power using different methods for the two modules considered. As can be seen, the power output estimated using the spectral correction based on the SF significantly improves the results obtained without considering any spectral correction. The RMSE decreases at around 1.1% and the R^2 increases and is closer to 1. Regarding to the MBE, the procedure based on the SF trends to slightly underestimate the power as was expected from the analysis above. The procedure based on the SF_P using equation (12) and the coefficients of Fig. 5 yields better results than the procedure based on the SF. The RMSE decreases at around 0.5% and the MBE is close to 0% that indicates that this method neither underestimates nor overestimates the power output. However, it can be concluded that the SF is a good tool in order to correct the spectral influence on the power output of a HCPV system in a first approximation.

As an example, the simulated power spectral losses estimated by using the SF and the SF_p for the modules A and B at the summer

Table 2
Root mean square error (RMSE), mean bias error (MBE) and determination coefficient (R^2) between actual and predicted power for the three methods considered.

Method	Module	RMSE (%)	MBE (%)	R^2
$P = \frac{P^*}{DNI^*} \cdot DNI \cdot TF$	A	4.82	1.40	0.94
	B	4.85	1.18	0.95
$P = \frac{P^*}{DNI^*} \cdot DNI \cdot TF \cdot SF$	A	3.64	−1.25	0.98
	B	3.72	−1.10	0.99
$P = \frac{P^*}{DNI^*} \cdot DNI \cdot TF \cdot SF_P$	A	3.26	0.22	0.99
	B	3.20	0.15	0.99

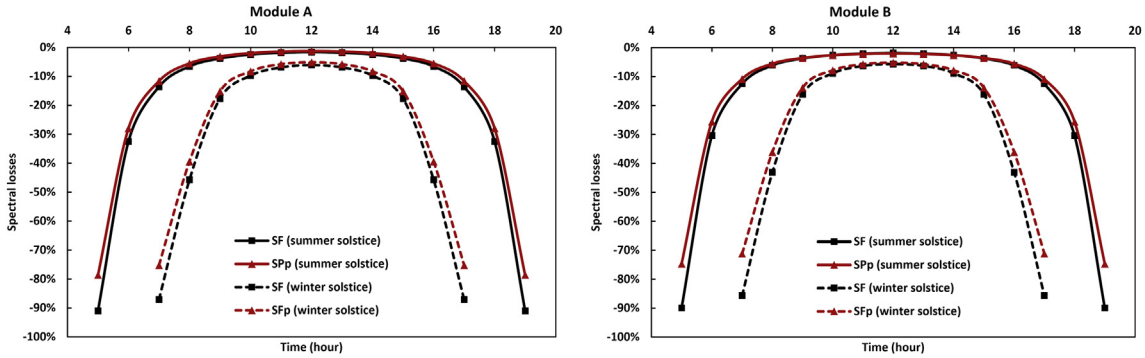

Fig. 6. Simulated power spectral losses as a function of the *SF* and SF_p for modules A and B at the winter and summer solstices 2013.

and winter solstice are shown in Fig. 6. As can be seen, both indexes show the same behaviour. As expected, the *SF* shows the poorest results at sunset and sunrise when the *AM* values and the spectral losses are higher. Despite of this, this figure shows that the *SF* can considered as a good approximation for quantifying the instantaneous power spectral effects of a HCPV module.

As was proved, the *SF* and SF_P exhibit different values under spectral changes, with an average recorded relative difference of around 3% for the two modules under study. Despite of this, the use of SF_P or *SF* as spectral correction for estimating the power output of HCPV devices under real operating has demonstrated to have a similar accuracy with a difference in the RMSE of 0.5%. The rationale behind this can be found in Figs. 7 and 8. These figures show the data distribution as function of the *SF* and the *DNI* for modules A and B. As can be seen, the maximum of this distribution is located at around $SF = 1$ and approximately the 85% of the cases are obtained for *SF* values in the range of 0.90–1.10 and a *DNI* higher than 400 W/m^2. Within this interval, the relative difference between *SF* and SF_P is in the range of around ±2%, as shown in Fig. 4. Furthermore, it is important to note that the 95% of the direct energy received from the sun is usually obtained for *DNI* values higher than 400 W/m^2 [35]. Bearing this in mind, the *SF* is expected to be close to SF_P in the majority of the cases and when the contribution to the final energy yield of the system is at maxima. Therefore, the *SF* could be considered as a good index for evaluating the spectral influence on the power or energy output of a HCPV system under real operating conditions with a satisfactory degree of accuracy. The analysis of the *SF* for quantifying the spectral impact on the energy yield is addressed in more detail in next section.

6. Annual energy spectral losses depending on latitude

The analysis of the spectral impact on the annual energy yield of the two HCPV modules considered as a function of latitude is conducted. The *SF* and SF_p commented above are only valid to estimate the instantaneous spectral impact on the power output. Both indexes must be weighted with the irradiance for estimating the spectral impact on the energy yield for a desired period of time. This has been noted by different authors and new procedures for estimating the spectral impact on the monthly and annual energy yield of conventional PVs have been introduced, i.e. [20,21]. These methods need a very high computation performance and they are not suitable for studies that implicate a large number of detailed simulations. However, following the same approach, the spectral impact on the energy yield for any desired period of time can be estimated as:

$$\Delta E(\%) = \left(\frac{\sum_j^N P(AM_j) DNI(AM_j) SF(AM_j)}{\sum_j^N P(AM_j) DNI(AM_j)} - 1 \right) \times 100 \qquad (13)$$

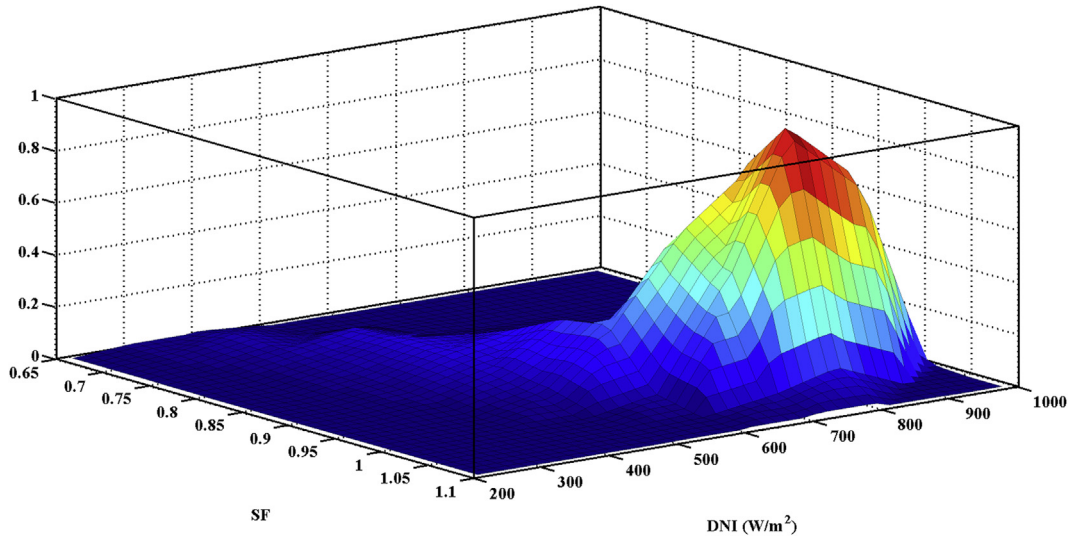

Fig. 7. Normalised data distribution as function of the *SF* and the DNI for module A.

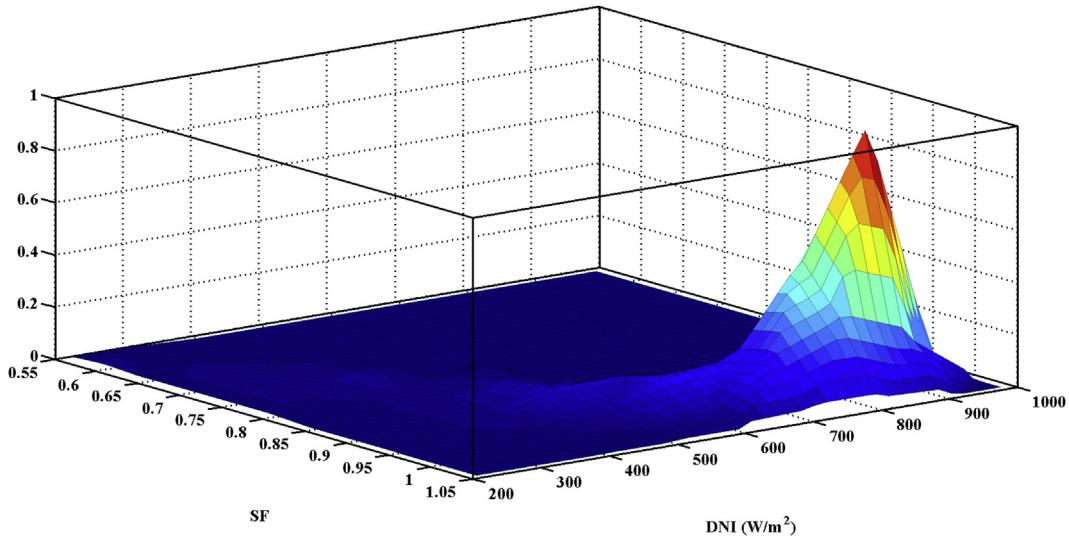

Fig. 8. Normalised data distribution as function of the *SF* and the DNI for module B.

where *ΔE(%)* represents the spectral impact on the energy yield for a given period of time, *P(AM)* is the frequency distribution of *AM*, the *j*-index represents each *AM* value of this distribution and *N* is the total number of bins of *AM* considered. In order to obtain *ΔE(%)* is necessary to know the value of the *SF* at any instant of time during the whole year. Hence, the estimation of the spectral distribution of the *DNI* is required. To conduct this, the *AM* has been calculated every minute during daylight time for the whole year at all latitudes using equation (9). After that, *P(AM)* evenly distributed in 1500 values between 1 and 38 (a zenith angle of 90°) for each latitude were obtained. Then, the solar spectrum was simulated for the 1500 *AM* values using the SMARTS model. The rest of the parameters required for the SMARTS model were kept fixed at the values defined by the standard AM1.5d ASTM G-173-03 spectrum. Then, every *SF* value has been calculated for the two modules considered using the data shown in Fig. 1 and equation (6). Finally, the *ΔE(%)* at all latitudes for the two modules was obtained using equation (13), where the *DNI* has been estimated from the spectrum. Following the same procedure, the *ΔE(%)* as a function of SF_p at all latitudes for the two modules has been also estimated. The aim is to analyse the accuracy of the *SF* as an index for quantifying the spectral impact on the energy yield of HCPV systems.

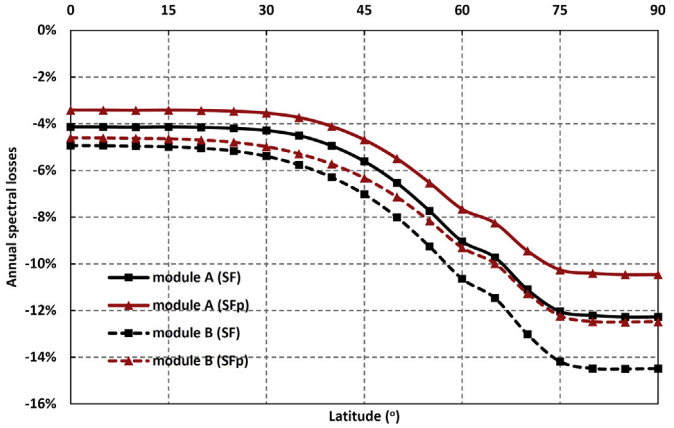

Fig. 9. Simulated annual energy spectral losses as a function of latitude for modules A and B by using equation (13) and the *SF* and SF_p.

Fig. 9 shows the results of the *ΔE(%)* for the two modules following the two procedures commented above. As can be seen, both modules show annual spectral losses for all latitudes and have a similar behaviour. The spectral losses can be considered independent of latitude until approximately 30° with a value at around −4% and −5% for modules A and B respectively. For higher latitudes, the spectral losses strongly increase until around 75° where they reach a value at around −12% and −14% for modules A and B respectively. For higher latitudes than 75°, the spectral losses kept almost constant. As expected, the spectral losses predicted with the *SF* are higher than the ones estimated with the SF_p. This is due to the fact that the spectral losses simulated with the *SF* are higher than the ones produced in the maximum power, as was already commented. Despite of this, it can be concluded that both indexes predict similar spectral losses for all latitudes. In particular, the maximum, minimum and average difference between the *SF* and SF_p is around −2%, −0.5% and −1% respectively. The deviation found between the *SF* and SF_p is small because the maximum difference between both indexes is produced at low values of the *SF*. At these low values, the *AM* is high and therefore the incident *DNI* is low. As was commented and shown in equation (13), the spectral losses are weighted with the incident *DNI* to quantify their impact on the annual energy yield. Because of this, the annual energy spectral losses produced by low *SF* values are small since they are produced at low *DNI* values. This also explains the increase of the error in the estimation of the annual spectral losses with the latitude by using the *SF* observed in Fig. 9. The *AM* values increases with latitude, so that the *SF* and *DNI* values decreases as the latitude is increased.

7. Conclusions

In this paper, the analysis of the spectral factor for estimating the spectral influence on the power and energy output of concentrator photovoltaic systems under real operating conditions is conducted. Two HCPV modules have been measured over the course of two years in order to analyse the spectral influence of their power output at the University of Jaen in Southern Spain. At the same time, the spectral factor is obtained from the simulated direct normal spectral irradiance and the characteristics of the MJ solar cells and optical devices of each module for the whole period

of measurements. The spectral distribution is obtained using different atmospheric parameters (air mass, aerosol optical depth and precipitable water) and the SMARTS (Simple Model of the Atmospheric Radiative Transfer of Sunshine).

Results show that the spectral factor has a higher spectral sensitivity than the power output of HCPV modules. For *SF* values lower than 1, this index predicts higher spectral losses than the ones produced in the power output. For *SF* values higher than 1, this index predicts higher spectral gains than the ones produced in the power output. Despite this difference, the results in the estimation of the maximum power of the two HCPV modules considered show that the *SF* could be considered as a useful tool for evaluating the spectral influence on the maximum power as a first approximation. The estimation of the power output using the *SF* as a spectral corrections significantly improves the results obtained without considering any spectral correction. In particular, the root mean square error decreases at around 1.1% and the determination coefficient increases and is closer to 1. Results also show that the spectral influence on the power output and the spectral factor can be more accurately related with an approximated linear equation. Based on these results, a new mathematical relationship for estimating the maximum power of a HCPV system is also proposed. The study of the *SF* as an index to evaluate the annual energy spectral losses of a HCPV system as a function of latitude is also conducted. The analysis of results show that the *SF* can be used to estimate the annual spectral losses with a maximum, minimum and average deviation of around −2%, −0.5% and −1% respectively. Based on this analysis can be concluded that the *SF* could be considered as a good index for evaluating the spectral influence on the maximum power and energy yield of a HCPV system under real operating conditions. Further researches should compare this index with other indexes currently used by the HCPV community such as the SMR (spectral matching ratio) or the spectral parameter Z. This would be useful to better understand the *SF* index and its relation with other spectral characterization procedures.

References

[1] Cotal H, Fetzer C, Boisvert J, Kinsey G, King R, Hebert P, et al. III-V multijunction solar cells for concentrating photovoltaics. Energy Environ Sci 2009;2(2):174–92.

[2] Pérez-Higueras P, Muñoz E, Almonacid G, Vidal P. High concentrator photovoltaics efficiencies: present status and forecast. Renew Sustain Energy Rev 2011;15(4):1810–5.

[3] Xie W, Dai Y, Wang R, Sumathy K. Concentrated solar energy applications using Fresnel lenses: a review. Renew Sustain Energy Rev 2011;15(6):2588–606.

[4] Victoria M, Domínguez C, Antón I, Sala G. Comparative analysis of different secondary optical elements for aspheric primary lenses. Opt Express 2009;17(9):6487–92.

[5] Zubi G, Bernal-Agustín J, Fracastoro G. High concentration photovoltaic systems applying III-V cells. Renew Sustain Energy Rev 2009;13(9):2645–52.

[6] Luque A, Sala G, Luque-Heredia I. Photovoltaic concentration at the onset of its commercial deployment. Prog Photovolt Res Appl 2006;14(5):413–28.

[7] Swanson RM. The promise of concentrators. Prog Photovolt Res Appl 2000;8(1):93–111.

[8] Talavera D, Pérez-Higueras P, Ruíz-Arias J, Fernández E. Levelised cost of electricity in high concentrated photovoltaic grid connected systems: spatial analysis of Spain. Appl Energy 2015;151:49–59.

[9] Faine P, Kurtz S, Riordan C, Olson JM. The influence of spectral solar irradiance variations on the performance of selected single-junction and multi-junctions solar cells. Sol Cells 1991;31:259–78.

[10] McMahon W, Emery K, Friedman D, Ottoson L, Young M, Ward J, et al. Fill factor as a probe of current-matching for GaInP/GaAs tandem cells in a concentrator system during outdoor operation. Prog Photovolt Res Appl 2008;16(3):213–24.

[11] Domínguez C, Anton I, Sala G, Askins S. Current-matching estimation for multijunction cells within a CPV module by means of component cells. Prog Photovolt Res Appl 2013;21(7):1478–88.

[12] Peharz G, Ferrer Rodríguez J, Siefer G, Bett A. A method for using CPV modules as temperature sensors and its application to rating procedures. Sol Energy Mater Sol Cells 2011;95(10):2734–44.

[13] Helmers H, Schachtner M, Bett A. Influence of temperature and irradiance on triple-junction solar subcells. Sol Energy Mater Sol Cells 2013;116:144–52.

[14] García-Domingo B, Aguilera J, de la Casa J, Fuentes M. Modelling the influence of atmospheric conditions on the outdoor real performance of a CPV (concentrated photovoltaic) module. Energy 2014;70:239–50.

[15] IEC-60904-7. Photovoltaic devices – part 7: computation of the spectral mismatch correction for measurements of photovoltaic devices. 2008.

[16] Osterwald CR, Emery KA, Muller M. Photovoltaic module calibration value versus optical air mass: the air mass function. Prog Photovolt Res Appl 2014;22(5):560–73.

[17] Pérez-López J, Fabero F, Chenlo F. Experimental solar spectral irradiance until 2500 nm: results and influence on the PV conversion of different materials. Prog Photovolt Res Appl 2007;15(4):303–15.

[18] Tsutsui J, Kurokawa K. Investigation to estimate the short circuit current by applying the solar spectrum. Prog Photovolt Res Appl 2008;16(3):205–11.

[19] Nikolaeva-Dimitrova M, Kenny R, Dunlop E, Pravettoni M. Seasonal variations on energy yield of a-Si, hybrid, and crystalline Si PV modules. Prog Photovolt Res Appl 2010;18(5):311–20.

[20] Alonso-Abella M, Chenlo F, Nofuentes G, Torres-Ramírez M. Analysis of spectral effects on the energy yield of different PV (photovoltaic) technologies: the case of four specific sites. Energy 2014;67:435–43.

[21] Dirnberger D, Blackburn G, Müller BRC. On the impact of solar spectral irradiance on the yield of different PV technologies. Sol Energy Mater Sol Cells 2014;132:431–42.

[22] Senthilarasua S, Fernandez EF, Almonacid F, Mallick TP. Effects of spectral coupling on perovskite solar cells under diverse climatic conditions. Sol Energy Mater Sol Cells 2015;133:92–8.

[23] Ishii T, Otani K, Takashima T, Xue Y. Solar spectral influence on the performance of photovoltaic (PV) modules under fine weather and cloudy weather conditions. Prog Photovolt Res Appl 2013;21(4):481–9.

[24] Fernández E, Almonacid F, Ruiz-Arias J, Soria-Moya A. Analysis of the spectral variations on the performance of high concentrator photovoltaic modules operating under different real climate conditions. Sol Energy Mater Sol Cells 2014;179–187:127.

[25] Katsumata N, Nakada Y, Minemoto T, Takakura H. Estimation of irradiance and outdoor performance of photovoltaic modules by meteorological data. Sol Energy Mater Sol Cells 2011;95(1):199–202.

[26] Minemoto T, Nagae S, Takakura H. Impact of spectral irradiance distribution and temperature on the outdoor performance of amorphous Si photovoltaic modules. Sol Energy Mater Sol Cells 2007;91(10):919–23.

[27] Nagae S, Toda M, Minemoto T, Takakura H, Hamakawa Y. Evaluation of the impact of solar spectrum and temperature variations on output power of silicon-based photovoltaic modules. Sol Energy Mater Sol Cells 2006;90(20):3568–75.

[28] Kinsey G, Edmondson KM. Spectral response and energy output of concentrator multijunction solar cells. Prog Photovolt Res Appl 2009;17:279–88.

[29] Philipps S, Peharz G, Hoheisel R, Hornung T, Al-Abbadi N, Dimroth F, et al. Energy harvesting efficiency of III–V triple-junction concentrator solar cells under realistic spectral conditions. Sol Energy Mater Sol Cells 2010;94(5):869–77.

[30] Chan NLA, Young TB, Brindley HE, Ekins-Daukes NJ, Araki K, Kemmoku Y, et al. Validation of energy prediction method for a concentrator photovoltaic module in Toyohashi Japan. Prog Photovolt Res Appl 2013;21(8):1598–610.

[31] Ishii T, Otani K, Takashima T. Effects of solar spectrum and module temperature on outdoor performance of photovoltaic modules in round-robin measurements in Japan. Prog Photovolt Res Appl 2011;19(2):141–8.

[32] Nofuentes G, García-Domingo B, Muñoz JV, Chenlo F. Analysis of the dependence of the spectral factor of some PV technologies on the solar spectrum distribution. Appl Energy 2014;113:302–9.

[33] Hibberd C, Plyta F, Monokroussos C, Bliss M, Betts T, Gottschalg R. Voltage-dependent quantum efficiency measurements of amorphous silicon multijunction mini-modules. Sol Energy Mater Sol Cells 2011;95(1):123–6.

[34] Monokroussos C, Bliss M, Qiu Y, Hibberd C, Betts T, Tiwari A, et al. Effects of spectrum on the power rating of amorphous silicon photovoltaic devices. Prog Photovolt Res Appl 2011;19(6):640–8.

[35] Fernández E, Pérez-Higueras P, Garcia Loureiro A, Vidal P. Outdoor evaluation of concentrator photovoltaic systems modules from different manufacturers: first results and steps. Prog Photovolt Res Appl 2013;21(4):693–701.

[36] Peharz G, Ferrer Rodríguez J, Siefer G, Bett A. Investigations on the temperature dependence of CPV modules equipped with triple-junction solar cells. Prog Photovolt Res Appl 2011;19(1):54–60.

[37] Fernández E, Almonacid F, Rodrigo P, Pérez-Higueras P. Calculation of the cell temperature of a high concentrator photovoltaic (HCPV) module: a study and comparison of different methods. Sol Energy Mater Sol Cells 2014;121:144–51.

[38] ASTM G 173-03e1 Standard tables for reference solar spectral irradiance: direct normal and hemispherical on 37 tilted surface. Am Soc Test Mater 2012:1–20.

[39] Fernandez EF, Almonacid F. Spectrally corrected direct normal irradiance based on artificial neural networks for high concentrator photovoltaic applications. Energy 2014;74:941–9.

[40] Fernández E, Siefer G, Almonacid F, García-Loureiro A, Pérez-Higueras P. A two subcell equivalent solar cell model for III–V triple junction solar cells under spectrum and temperature variations. Sol Energy 2013;92:221–9.

[41] Siefer G, Bett AW. Analysis of temperature coefficients for III–V multijunction concentrator cells. Prog Photovolt Res Appl 2014;22(5):515–24.

[42] Domínguez C, Antón I, Sala G. Multijunction solar cell model for translating I-V characteristics as a function of irradiance, spectrum, and cell temperature. Prog Photovolt Res Appl 2010;18(4):272–84.
[43] Ota Y, Nagai H, Araki K, Nishioka K. Temperature distribution in 820X CPV module during outdoor operation. In: AIP Conference Proceedings vol. 1477; 2012. p. 364–7.
[44] Strobach E, Faiman D, Kabalo S, Bokobza D, Melnichak V, Gombert A, et al. Modeling a grid-connected concentrator photovoltaic system. Prog Photovolt Res Appl 2015;23(5):582–92.
[45] Fernández E, Rodrigo P, Almonacid F, Pérez-Higueras P. A method for estimating cell temperature at the maximum power point of a HCPV module under actual operating conditions. Sol Energy Mater Sol Cells 2014;124:159–65.
[46] Rodrigo P, Fernández E, Almonacid F, Pérez-Higueras P. Review of methods for the calculation of cell temperature in high concentration photovoltaic modules for electrical characterization. Renew Sustain Energy Rev 2014;38:478–88.
[47] Gueymard C. Parameterized transmittance model for direct beam and circumsolar spectral irradiance. Sol Energy 2001;71(5):325–46.
[48] Chan NLA, Brindley HE, Ekins-Daukes NJ. Impact of individual atmospheric parameters on CPV system power, energy yield and cost of energy. Prog Photovolt Res Appl 2014;22(10):1080–95.
[49] Muller M, Marion B, Kurtz S, Rodriguez J. An investigation into spectral parameters as they impact CPV module performance. In: AIP conference proceedings vol. 1277; 2010. p. 307–11.
[50] Kasten F, Young AT. Revised optical air mass tables and approximation formula. Appl Opt 1989;28(22):4735–8.
[51] MODIS Daily Level-3 data, [Online]. Available from: http://gdata1.sci.gsfc.nasa.gov/daac-bin/G3/gui.cgi?instance_id=MODIS_DAILY_L3 [accessed 2014].

Referencia / Reference: Fernández, E. F., **Soria-Moya, A.**, Almonacid, F y Aguilera, J. (2016).*Comparative assessment of the spectral impact on the energy yield of high concentrator and conventional photovoltaic technology, Solar Energy Materials and Solar Cells,147,185-197.*

Estado / Status: Publicado / *Published*.

Índice de impacto / Impact Factor: 5.030.

Categoría / Catogory: *Energy and Fuels*. Ranking: 10/88 (Q1).

Solar Energy Materials & Solar Cells 147 (2016) 185–197

Contents lists available at ScienceDirect

Solar Energy Materials & Solar Cells

journal homepage: www.elsevier.com/locate/solmat

Comparative assessment of the spectral impact on the energy yield of high concentrator and conventional photovoltaic technology

Eduardo F. Fernández [a,b,*], Alberto Soria-Moya [a], Florencia Almonacid [b], Jorge Aguilera [b]

[a] Centro de Estudios Avanzados en Energía y Medio Ambiente (CEAEMA), University of Jaen, Jaen, Spain
[b] Grupo IDEA, University of Jaen, Jaen, Spain

ARTICLE INFO

Article history:
Received 6 August 2015
Received in revised form
3 December 2015
Accepted 10 December 2015
Available online 28 December 2015

Keywords:
Spectral impact
Energy yield
High concentrator photovoltaics
Photovoltaics

ABSTRACT

Photovoltaic materials are spectrally selected and their electrical output is affected by the spectral distribution of the incident irradiance. The performance of high concentrator photovoltaic (HCPV) systems is more influenced by the spectral changes than conventional single-junction photovoltaic (PV) systems due to the use of multi-junction (MJ) solar cells and optical devices. Despite this, the detailed comparison of the spectral impact on the electrical output of HCPV and PV technology under the same atmospheric conditions has not been addressed yet. Because of this, this paper aims to compare the spectral impact on the energy yield of both type of devices at a monthly and annual time scale at several locations with disparate climate conditions. The spectral dependence of both technologies is quantified by using the spectral factor (SF) index in conjunction with the Simple Model of Atmospheric Radiative Transfer of Sunshine (SMARTS) at five locations of the Aerosol Robotic Network (AERONET) database. The present paper shows that the current HCPV systems present annual spectral losses of around 5% with respect to PV systems at representative locations.

1. Introduction

From the outset, high concentrator photovoltaic (HCPV) technology has appeared as an alternative power source to produce more cost-effective electricity than conventional photovoltaic (PV) technology [1]. The use of optical devices to concentrate the light on high efficiency multi-junction (MJ) solar cells offers at the same time, high efficiencies and a reduction in the amount of semiconductor material [2]. The limit of the efficiency of MJ solar cells and HCPV systems is far from being reached, and an increase of 10% within the next decade is expected [3]. Taking this into account, the cumulative installed capacity of HCPV technology is tending to grow from a value of 358 MWp at the end of 2014 to more than 1 GWp in 2020 [4]. At the same time, the levelised cost of electricity (LCOE) is tending to decrease, LOCE = 0.035–0.080 €/kW h in 2020, and reach lower values than conventional PV technology at locations with high annual direct normal irradiation [5]. All the above show the great potential of this technology to play an important role in the energy generation market within next decades.

On the other hand, the maturity and understanding of HCPV technology when operating in outdoors is clearly lower than conventional PV technology. Because of this, important efforts are still needed in order to achieve a better understanding, increase the investors' confidence and therefore promote the market expansion of HCPVs as a real alternative energy source to conventional PVs [6]. One of the more relevant differential issues between HCPV and PV technology is related with the influence of the spectral variations on their electrical output [7]. The use of MJ solar cells based on the internal series connection of several subcells with different energy gaps [8], and optical devices which modify the spectral distribution that strikes on the solar cells surface [9], make HCPV devices more sensitive to the incident spectral distribution.

Because of this, the scientific community has devoted great efforts to understand the impact of the input spectrum on the performance of HCPV technology under real operating conditions. The use of the SMARTS model in conjunction with AERONET data source have been used by Muller et al. [10] to evaluate the effect of air mass, aerosol optical depth and precipitable water on the performance of different HCPV modules in Golden (USA) over 9 months. Hashimoto et al. [11] studied the impact of spectral changes on the performance of different HCPV one-cell modules during a clear and a very clear day through the SMR (spectral matching ratio) index measured with a spectroradiometer. An alternative procedure based on isotype solar cells and the spectral parameter *Z* has been proposed by Peharz et al. [12,13] to evaluate the spectral impact on the electrical output of different HCPV modules over several months at Freiburg (Germany). A similar

* Corresponding author. Tel.: +34 9543213520.
E-mail address: fenandez@ujaen.es (E.F. Fernández).

http://dx.doi.org/10.1016/j.solmat.2015.12.003
0927-0248/

approach based on the SMR index registered with isotype solar cells has been also used by García-Domingo et al. [14] to evaluate the spectral impact on the electrical characteristics of various HCPV modules over the course of a year in Jaen (Spain). The contour diagram of the performance ratio of a HCPV system analysed during a year at Miyazaki (Japan), as a function of the cell temperature and spectrum, quantified with the APE (Average Photon Index) index gathered with a spectroradiometer, has been obtained by Husna et al. [15]. The studies above are focused on analysing the instantaneous impact of spectral variations on the performance of HCPV modules or systems. Other recent work addresses the spectral impact on an annual time scale since it is directly related with the annual energy yield of the systems. Victoria et al. [16] quantified the annual spectral losses on the energy yield of different HCPV modules in Madrid (Spain) by the use of the SMR index measured with isotype solar cells. Fernández et al. [17] evaluated the annual average spectral impact on the performance of several HCPV modules made up of different types of MJ solar cells and optical devices through the spectral factor (SF) index with spectra simulated with the SMARTS model and data obtained from AERONET at five locations (Solar Village (Saudi Arabia), Alta Floresta (Brazil), Frenchman Flat (USA), Granada (Spain) and Beijing (China)). The same HCPV modules and a similar approach have also been used by Soria-Moya et al. [18] to estimate the annual energy spectral losses as a function of latitude. Chan et al. [19] quantified the impact of air mass, aerosol optical depth and precipitable water on the annual energy harvested by a HCPV module at five AERONET sites (Rogers Dry Lake (USA), Tamanrasset (Algeria), Sede Boqer (Israel), Solar Village (Saudi Arabia) and Jaipur (India)) by using the Syracuse simulation model [20] and spectra generated with the SMARTS model.

At the same time, single-junction PV devices are also spectrally selected and their power and energy output is also affected by spectral variation under real operating conditions. Because of this, the spectral dependence of these devices is also continuously being analysed by the scientific community and a wide number of studies can be found in the literature. Minemoto et al. [21] analysed the impact of the spectral variations in some PV devices as a function of the APE index measured with a spectroradiometer, as well as the contour diagrams of the performance ratio of several PV devices as a function of APE and module temperature [22–25], over the course of a year at Kusatsu (Japan). The APE and SF indexes gathered with a spectroradiometer have been used by Ishii et al. [26] to evaluate the spectral impact on the performance ratio of a wide number of PV technologies during 17 months at eight selected locations in Japan (Sapporo, Nakatsugawa, Otsu, Kobe, Katsuragi, Tosu, Isahaya and Okinoerabu). A similar approach has been followed by Nofuentes et al. [27] to analyse the spectral dependencies of some commercial PV devices during a year at Jaen (Spain). The work above represent examples of studies concerning the instantaneous impact of spectral changes on the performance of PV devices. As in the case of HCPV technology, other researchers have recently conducted different studies to analyse the spectral impact on an annual or monthly time scale. Alonso-Abella et al. [28] quantified the spectral impact on the monthly and annual energy yield of a wide number of commercial PV devices by using the SEDES2 spectral model and Meteonorm software at four locations (Stuttgart (Germany), Tamanrasset (Algeria), Madrid (Spain) and Jaen (Spain)). Fernández et al. [29,30] evaluated the average annual spectral impact on the performance of various new generation solar cells by also using the SF index in conjunction with the SMARTS model at six AERONET locations (Solar Village (Saudi Arabia), Alta Floresta (Brazil), Frenchman Flat (USA), Granada (Spain), Beijing (China) and Edinburgh (Scotland)). The analysis of the effect of spectral variations on the monthly and annual energy yield of different commercial PV devices, by using the SF index and spectral measurements of around 3.5 years performed with a spectroradiometer, has been also conducted by Dirnberger et al. [31] at Freiburg (Germany).

The examples above represent relevant studies concerning the analysis of the effect of spectral variations on the performance of both technologies. These studies allow different conclusions to be reached. It seems clear that HCPV systems show a higher spectral dependence than conventional PV systems. However, it can be also concluded that the impact of the spectral variations on both technologies depends on the atmospheric characteristics of each particular site (i.e. air mass, aerosol optical depth and precipitable water). Moreover, the procedures and approaches used by the authors to analyse the spectral impact on HCPV and PV technology are different. Hence, based on the current studies, the direct comparison between the spectral impact on the electrical output of HCPV and PV technology under the same climate conditions is not possible and has not been done. At the same time, the energy harvested by photovoltaic systems is directly related with their bankability [32]. Bearing this in mind, this paper is focused on the comparative evaluation of the spectral impact on the energy yield of HCPV and PV technologies under a wide range of atmospheric conditions. In order to achieve this goal, the approach previously used by the authors in [17], where the annual average spectral impact on the performance of several HCPV systems but not on the energy yield was analysed, has been followed. So, the present study allows the analysis and comparison between the performance and potential of HCPV and PV technologies to be done in terms of the spectral behaviour.

2. Methods and materials

2.1. Spectral factor and energy yield

The power output of a HCPV or PV system is mainly determined by the incident irradiance, spectral distribution and the operating cell temperature. Hence, the maximum power (P) of a PV device can be expressed with a low margin of error as [26]:

$$P \approx \frac{P^*}{G^*} \cdot G \cdot \mathrm{TF} \cdot \mathrm{SF} \tag{1}$$

and of a HCPV device as [33]:

$$P \approx \frac{P^*}{\mathrm{DNI}^*} \cdot \mathrm{DNI} \cdot \mathrm{TF} \cdot \mathrm{SF} \tag{2}$$

where P^*, G^* and DNI^* are the maximum power, global irradiance and direct normal under the standard test conditions (STC), G and DNI are the incident global and direct normal irradiance, TF is the thermal factor and SF is the spectral factor.

The TF quantifies the effect of cell temperature of the power output of a PV and HCPV device as [27,34]:

$$\mathrm{TF} = 1 + \gamma (T_c - T_c^*) \tag{3}$$

where γ is the maximum power temperature coefficient, T_c is the cell temperature and T_c^* is the cell temperature under STC.

The spectral factor quantifies the influence of the input spectrum on the power output of a single-junction PV device as [35]:

$$\mathrm{SF} = \frac{\int E_g(\lambda) SR(\lambda) d\lambda \int E_{g,\mathrm{ref}}(\lambda) d\lambda}{\int E_{g,\mathrm{ref}}(\lambda) SR(\lambda) d\lambda \int E_g(\lambda) d\lambda} \tag{4}$$

where λ is the wavelength, $E_g(\lambda)$ is the incident global spectral distribution, $E_{g,\mathrm{ref}}(\lambda)$ is the reference global spectrum and $SR(\lambda)$ is the spectral response of the PV device.

Following the same approach, the impact of the incident spectral distribution on the power output of a HCPV device can be

expressed as [17]:

$$SF = \frac{\min(\int E_b(\lambda)\eta(\lambda)SR_i(\lambda)d\lambda)\int E_{b,ref}(\lambda)d\lambda}{\min(\int E_{b,ref}(\lambda)\eta(\lambda)SR_i(\lambda)d\lambda)\int E_b(\lambda)d\lambda} \quad (5)$$

where the i-index represents the junction of the MJ solar cell, $E_b(\lambda)$ is the incident direct normal spectral distribution, $E_{b,ref}(\lambda)$ is the direct reference spectrum and $\eta(\lambda)$ is the spectral optical efficiency.

The SF quantifies the instantaneous spectral impact as the ratio of the short-current density at operating conditions relative to the short-current density under STC: an SF higher than 1 indicates spectral gains while an SF lower than 1 indicates spectral losses. This index has been experimentally demonstrated to be valid to approximate the spectral gains or losses on the power output of HCPV and conventional single-junction PV devices [33,36,37], and therefore allows the direct comparison of the spectral impact on the maximum power of HCPV and PV devices to be done.

The energy harvested by a PV or HCPV system during a specific period of time T can be estimated from Eqs. (1) to (2) as:

$$E \approx \int_T P(I, T_c, E(\lambda))dT = \frac{P^*}{I^*}\cdot\int_T I\cdot TF(T_c)\cdot SF(E(\lambda))dt \quad (6)$$

where I represents the incident irradiance: I=G for a PV system and I=DNI for a HCPV system, and $E(\lambda)$ represent the incident spectral distribution: $E(\lambda)=E_g(\lambda)$ for a PV system and $E(\lambda)=E_b(\lambda)$ for a HCPV system.

Since the aim is the individual estimation of the spectral impact on the energy produced, the thermal effects have to be neglected in Eq. (6) (TF=1). So, the relative spectral impact on the energy yield for a desired period of time can be expressed as:

$$\Delta E(\%) \approx 100\cdot\left(\frac{\frac{P^*}{I^*}\cdot\int_T I\cdot SF(E(\lambda))dt - \frac{P^*}{I^*}\cdot\int_T I\cdot SF(E_{ref}(\lambda))dt}{\frac{P^*}{I^*}\cdot\int_T I\cdot SF(E_{ref}(\lambda))dt}\right) \quad (7)$$

since $SF(E_{ref}(\lambda))=1$, Eq. (7) becomes:

$$\Delta E(\%) \approx 100\cdot\left(\frac{\int_T I\cdot SF(E(\lambda))dt - \int_T Idt}{\int_T Idt}\right) = 100 \cdot\left(\frac{\int_T I\cdot SF(E(\lambda))dt}{\int_T Idt} - 1\right) \quad (8)$$

and in normalised form as:

$$\Delta E \approx \frac{\int_T I\cdot SF(E(\lambda))dt}{\int_T Idt} \quad (9)$$

The reasoning above that leads to Eqs. (8) and (9) is essentially the same as the procedures discussed in [28,31] and the one based on component cells presented in [38].

2.2. Materials

To conduct this study, four HCPV and five PV typical devices have been considered. Two of the HCPV systems are based on lattice-matched (LM) triple-junction gallium indium phosphide (GaInP)/gallium indium arsenide (GaInAs)/germanium (Ge) solar cells and the other two are based on metamorphic-mismatched (MM) triple-junction gallium indium phosphide (GaInP)/gallium indium arsenide (GaInAs)/germanium (Ge) solar cells. One of the systems formed by LM/MM monolithic triple-junction solar cells uses Fresnel lenses based on poly(methylmethacrylate) (PMMA) material and the other uses Fresnel lenses based on silicon on glass (SOG) material as primary optics to concentrate the light around 700×. Fig. 1 shows the spectral response of the cells and transmittance of the Fresnel lenses considered and Table 1 shows the average transmittance of the four systems in the spectral absorption band of each junction of the LM and MM cells. The five PV technologies consist of monocrystalline silicon (m-Si), polycrystalline silicon (p-Si), amorphous silicon (a-Si), cadmium telluride (CdTe) and copper indium gallium selenide (CIGS). The spectral response of each of these materials is shown in Fig. 2. The data of the PV materials have been taken from [28,31], while further information of the HCPV systems considered can be found in [17]. The technologies above have been selected because they cover virtually all the photovoltaic market share. So, the results of this work could be considered representative of the current HCPV and PV systems.

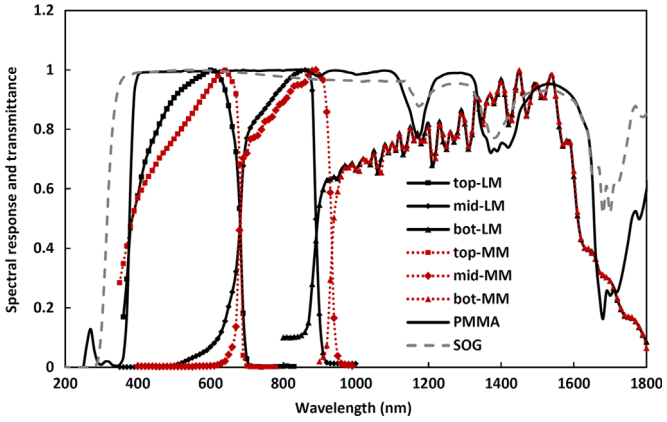

Fig. 1. Normalised spectral response of the lattice-matched and metamorphic-mismatched solar cells, and transmittance of the Fresnel lenses (PMMA and SOG) used for estimating the spectral factor.

Table 1
Average transmittance of Fresnel lenses in the spectral band of each subcell of the lattice-matched and the metamorphic-mismatched multi-junction solar cells of the HCPV systems considered.

		Average transmittance (%)		
Cell	**Lens**	**Top**	**Middle**	**Bottom**
LM	PMMA	73	92	74
	SOG	87	91	82
MM	PMMA	73	92	76
	SOG	87	90	81

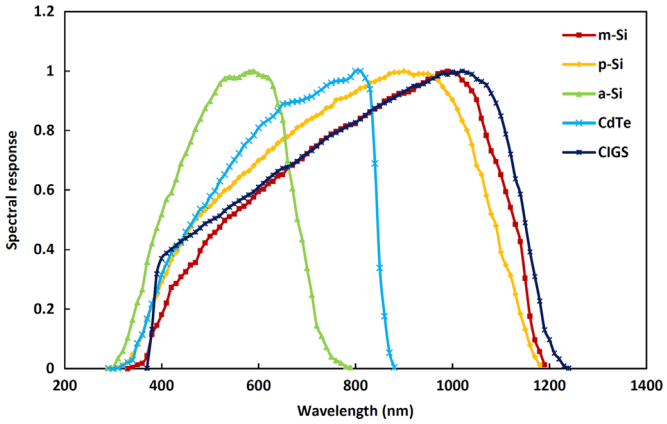

Fig. 2. Normalised spectral response of different single-junction photovoltaics materials used for estimating the spectral factor.

3. Instantaneous impact of atmospheric parameters

The electrical output of HCPV or PV devices is affected by the variations of the incident spectral distribution. The air mass, aerosol optical depth (usually evaluated at 500 or 550 nm) and precipitable water have been demonstrated to be the relevant atmospheric parameters to accurately evaluate the spectral impact on the

electrical characteristics of photovoltaic devices [7,19,35]. The variation of air mass (AM) during the course of a day has a strong impact in the incoming spectral irradiance because of scattering and absorption phenomena. AM can be defined as the relation between the optical path length of the solar beam through the atmosphere and the optical path through a standard atmosphere at sea level with the sun at the zenith. This factor can be approximated to a pure geometrical parameter function of the solar position whose minimum and maximum values are 1 (a solar zenith angle of 0°) and 38 (a solar zenith angle of 90°) [39]. Aerosols are small particles suspended in the air either in solid or liquid state that scatter and absorb sunlight, and aerosol optical depth (AOD) is the physical magnitude to quantify their influence in the solar irradiance. The influence of aerosols in the spectral irradiance can be approximated by the Ångström turbidity formula as $AOD = AOD_{550}(\lambda/0.55)^{-\alpha}$. In this equation, AOD_{550} is the amount of aerosols in a vertical column of the atmosphere at 550 nm, λ is the wavelength and α is the Ångström or wavelength exponent [40]. The presence of water vapour in the atmosphere has an important absorption effect on the incident spectral distribution. Although there are several ways to quantify the water vapour content, the widely used way to evaluate this quantity is through the precipitable water (PW). PW corresponds to the volume of liquid water that would be obtained if all the water vapour aloft were condensed [41].

The influence of AM, AOD_{550} and PW in both the global and direct normal irradiance is plotted in Fig. 3. As can be seen, the higher the atmospheric parameter the higher the attenuation and therefore the lower the irradiance. However, the effect of each atmospheric parameter also has a strong impact on the spectral distribution. Regarding AM, the attenuation is larger in the UV region of the spectrum, so that the increase of AM results in a progressive red-shift of the spectral distribution. Regarding AOD_{550}, the attenuation is also larger at the shorter wavelengths of the spectrum and also produces a red shift of the spectrum. However, in this case that largest attenuation is located in the UV–visible part of the spectrum. Finally, PW produces a clear larger attenuation in the near-infrared part of the spectral distribution. Based on the above, it is obvious to see that the variations of each atmospheric parameter above will produce different effects on the performance of the photovoltaic materials shown in Figs. 1 and 2 since their absorption bands are located in different parts of the spectrum. Moreover, the effect of the variations of each atmospheric parameter affects the global and direct components of the irradiance to a different extent. This can be clearly seen in Fig. 3 (middle) where the attenuation of the direct component of the irradiance is around 3 times higher than in the global component by increasing the value of AOD_{550} from 0.2 to 0.8. Taking this into account, the different impact of spectral variations in HCPV and PV devices will be due to their different abortion bands but also to the different effect of each specific atmospheric parameter in each component of the radiation. To understand this issue better, an individualised analysis of the impact of each atmospheric parameter on the performance of HCPV and PV technologies is conducted. To achieve this goal, several spectra are simulated with the Simple Model of the Atmospheric Radiative Transfer of Sunshine (SMARTS) [42]. These spectra are generated varying one of the atmospheric parameters while the rest are kept constant at the reference values defined by the AM1.5G ASTMG-173-03 reference spectrum [43]. The values of AM, AOD_{550} and PW are varied from a low to an extreme value as observed in more than 350 worldwide sites of the Aerosol Robotic Network (AERONET) database [44]. The instantaneous impact of each generated spectrum is estimated by solving the SF index as defined in Eqs. (4) and (5) and the data shown in Figs. 1 and 2. This allows the performance of HCPV and PV under study to be understood and compared in a wide range of real operating conditions. It should be highlighted that the results

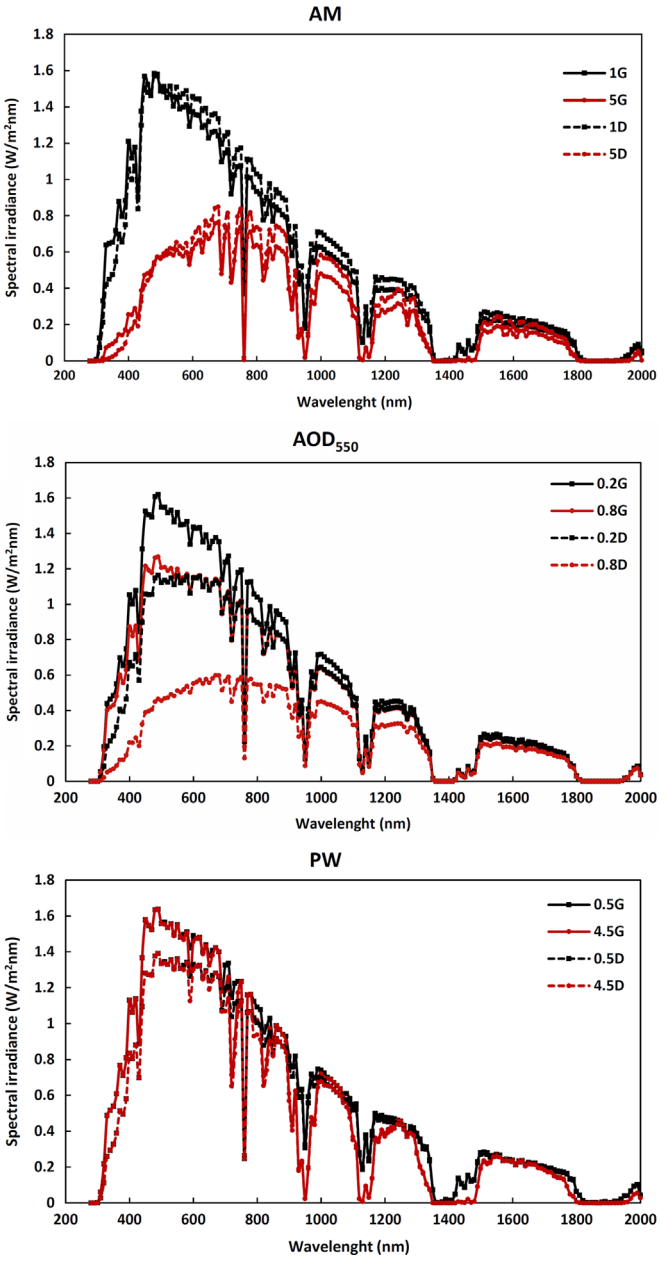

Fig. 3. Impact on the global (denoted as G) and direct (denoted as D) spectral irradiance of air mass (top), aerosol optical depth at 550 nm (middle) and precipitable water (bottom) simulated with the SMARTS model. The other parameters are kept constant at the reference values defined by the AM1.5d ASTMG-173-03 reference spectrum.

regarding the HCPV systems have already been presented in [17]. However, they are also shown below in order to better understand the differential performance between HCPV and PV technologies under the changes of the main atmospheric variables.

3.1. Impact of air mass

Fig. 4 shows the spectral impact of AM variations on the performance of the HCPV (top) and PV (bottom) devices considered. As can be seen, the impact of AM is clearly higher in the performance of the HCPV systems. The four systems show a similar behaviour under AM variations. They have a maximum where the top and middle junctions generate the same current (current-matched condition) that leads to feeble spectral gains for both

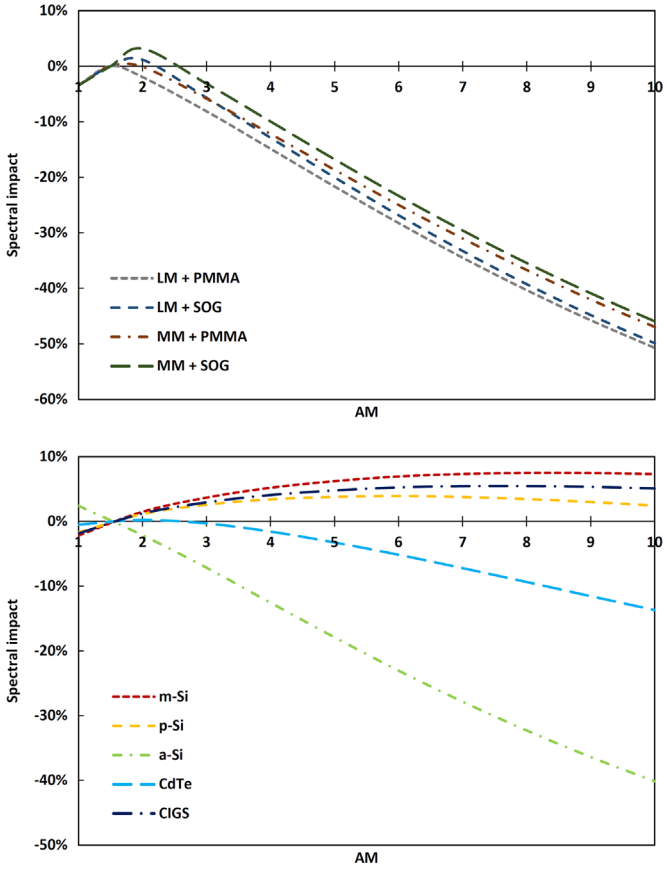

Fig. 4. Individual impact of air mass on the performance of the HCPV (top) and PV (bottom) technologies under study. The other parameters are kept constant at the reference values defined by the AM1.5d ASTMG-173-03 reference spectrum.

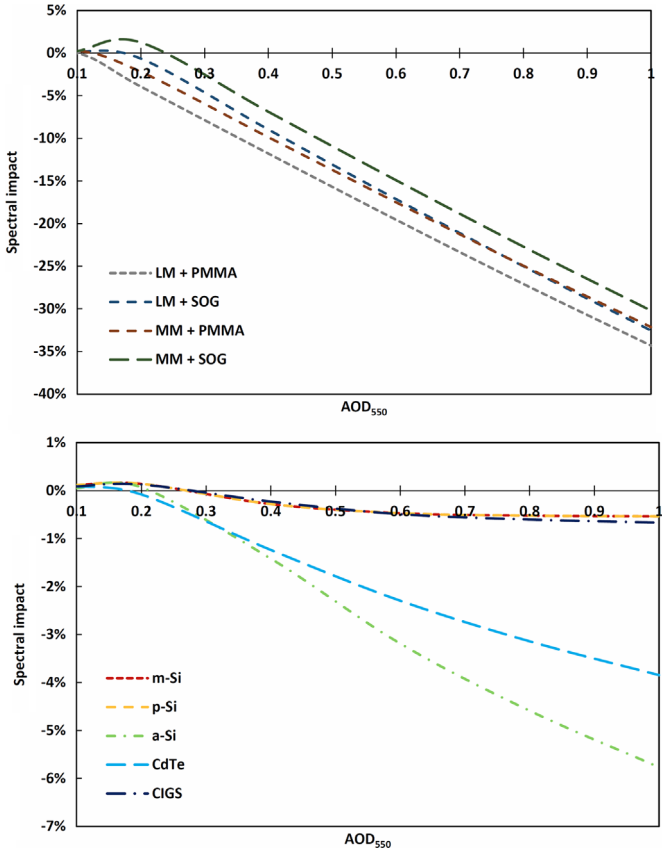

Fig. 5. Individual impact of aerosol optical depth on the performance of the HCPV (top) and PV (bottom) technologies under study. The other parameters are kept constant at the reference values defined by the AM1.5d ASTMG-173-03 reference spectrum.

systems based on SOG lenses. On the left of this maximum, the performance of the HCPV systems decreases by the current limitation of the middle junction until a value around −3.5%, while on the right side it decreases by the current limitation of the top junction until values around −45% and −50%. It is also worth mentioning that the LM+PMMA and MM+SOG devices show the worst and best performance respectively. This can be explained due to the fact that the SOG Fresnel lens has a higher transmittance in the spectral region of the top junction and due to the redshift of the absorption bands of the top and middle junctions of the MM solar cell. This analysis also indicates that spectral losses under real operating conditions of the HCPV devices will be dominated by the limitation of the current of the top junction that can be explained by its higher energy gap. Among the PV devices, the a-Si and CdTe PV materials also present a notable spectral dependence under AM variations since their absorption bands are mainly located in the blue part of the spectrum. Both materials have a similar behaviour and show slight spectral gains for low AM values and significantly spectral losses as AM increases with a maximum around −40% (a-Si) and −14% (CdTe). The worse performance of the a-Si compared with the CdTe material can be explained due to its wider ban gap. The other PV materials show a stable and similar performance under AM variations. As can be seen, these materials have slight spectral losses for low AM values and spectral gains as AM increases with a maximum around 7.5% (m-Si), 3.9% (p-Si) and 5.4% (CIGS). This behaviour can be explained due to their low energy gap and wide absorption band located not only in the blue part of the spectral irradiance.

3.2. Impact of aerosol optical depth

Fig. 5 shows the spectral impact of AOD_{550} variations on the performance of the HCPV (top) and PV (bottom) devices considered. As in the previous case, the impact of AOD_{550} is similar and higher in the performance of the HCPV systems. The systems have a maximum at current-matched condition where the systems based on SOG lenses also present slightly spectral gains. On the left of this maxima, the middle junction is limiting the current, and on the right side the top junction is limiting the current decreasing the performance of the HCPV systems until values around −30% and −35%. Again, the LM+PMMA and MM+SOG systems show the worst and best performance respectively for the same reason mentioned in the previous section. As in the previous case, the a-Si and CdTe devices present the highest spectral dependence under AOD_{550} variations among all the PV materials. Both show slightly spectral gains for low AOD_{550} values and significantly spectral losses for high AOD_{550} values with a maximum around −7% (a-Si) and −4% (CdTe). The worse performance of the a-Si is also explained by its higher energy gap. It is important to highlight that the spectral losses produced in these two devices by the increase of AOD_{550} are significantly lower than by the increase of AM due to the lower impact of aerosols in the global irradiance. The other PV materials show a small influence under AOD_{550} variations due to the low effect of aerosols in the global irradiance and to their narrow ban gap. The three materials have slightly spectral gains for low AOD_{550} values and spectral losses as this factor increases with a maximum around −1%.

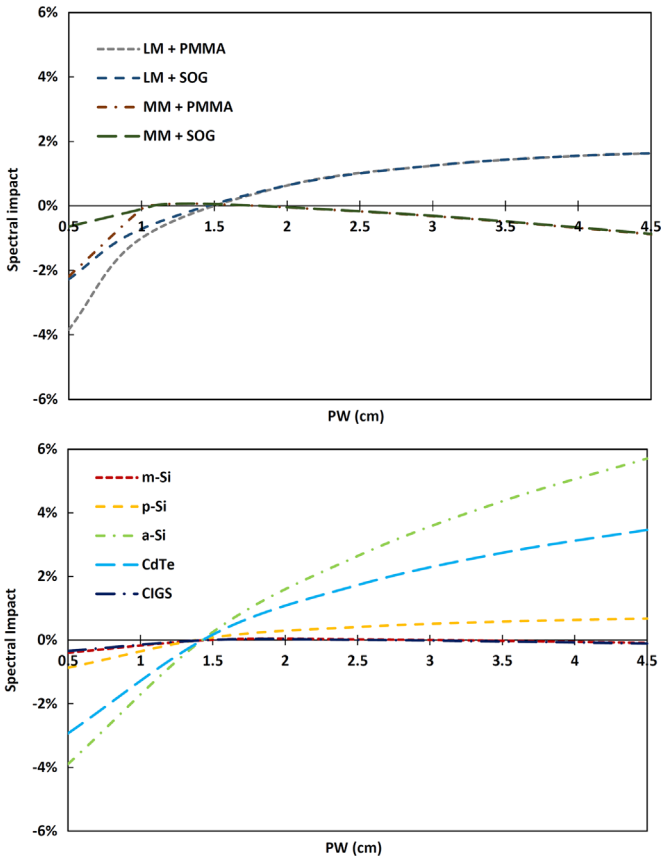

Fig. 6. Individual impact of aerosol optical depth on the performance of the HCPV (top) and PV (bottom) technologies under study. The other parameters are kept constant at the reference values defined by the AM1.5d ASTMG-173-03 reference spectrum.

3.3. Impact of precipitable water

Fig. 6 shows the spectral impact of PW variations on the performance of the HCPV (top) and PV (bottom) devices considered. In this case, the HCPV and PV materials show a similar performance. The HCPV systems based on LM solar cells and the a-Si and CdTe PV devices present spectral losses for low PW values and spectral gains as this parameter increases. This can be explained since the increase of PW mainly decreases the spectral irradiance in the near-infrared region. As a result, the current of the top and middle junctions of the LM solar cells and the a-Si and CdTe materials keep almost constant resulting in an overall increase of the performance of the materials with PW. The top and middle junctions of the MM solar cell and the m-Si, p-Si and CIGS materials can absorb lower energetic photons in the near-infrared region. Because of this, although these materials also show spectral losses for low PW values, the ratio between the effect of PW on the irradiance and the current of these devices keeps almost constant resulting in a more stable performance under PW variations.

From the analysis above it can be concluded that the HCPV systems have a larger spectral sensitivity than the PV devices under spectral variations. Moreover, the air mass has been demonstrated to be the atmospheric parameter with the largest impact on the performance of both the HCPV and PV devices. This suggests that the effects of the spectral variations on the energy yield of both technologies under real operating conditions are going to be mainly dominated by this factor. The aerosol optical depth has been also found to produce a strong impact on the performance of the HCPV systems but not as high on the PV materials. This is due to the different absorption bands of the materials but also to the significantly lower effect of the aerosol optical depth in the global than in the direct component of the radiation. At the same time, the third parameter with the largest impact on the performance of the HCPV systems is PW, but this leads to similar effects to the aerosol optical depth in the PV devices. Moreover, contrary to the other two atmospheric parameters, PW produces a similar impact on the performance of both technologies. This can be mainly explained since PW produces almost equal effects in the global and direct irradiance due to the fact that it mainly absorbs but does not scatter the incoming irradiance. So, contrary to AM and AOD, the presence of PW in the atmosphere does not produce diffuse irradiance that contribute to the global component of the radiation. The results above indicate that the spectral effects in the performance of HCPV and PV materials will be different and determined by the absorption band of each specific device. However, the different influence of each atmospheric parameter in the amount and spectral distribution of the global and direct irradiance is also a key parameter that needs to be considered.

4. Spectral impact on the energy yield

In the last section, the analysis and comparison of the instantaneous impact of each individual atmospheric parameters on the performance of HCPV and PV devices was undertaken. This is useful to achieve a better understanding of the behaviour of both technologies. However, to properly compare the spectral impact on the energy yield of both technologies, is necessary to take into account the effect of all the time-varying atmospheric parameters on the amount and spectral distribution of the irradiance for the desired period of time. In this section, the spectral influence on the energy yield of both technologies at selected locations with disparate climate conditions is conducted. First of all, the chosen sites together with their atmospheric characteristics are listed, as well as the procedure followed to simulate the time-series of the spectral distribution. After that, the analysis of the spectral impact on the energy harvested of all photovoltaic technologies considered at a monthly and annual time scale is conducted.

4.1. Locations and spectra simulation

The following five sites have been selected:

- Solar Village (Saudi Arabia): lat. N 24°54′25″, long. E 46°23′49″
- Alta Floresta (Brazil): lat. S 09°52′15″, long. W 56°06′14″
- Frenchman Flat (USA): lat. N 36°48″32″, long. W 115°56′06″
- Granada (Spain): lat. N 37°09′50″, long. W 03°36′18″
- Beijing (China): lat. N 39°58′37″, long. E 116°22′51″

These locations have been chosen since they represent places with diverse climate conditions over different continents and latitudes. So, it allows the performance of HCPV and PV systems to be studied and compared in a wide range of real operating conditions. Moreover, the atmospheric parameters of these locations can be obtained from the AERONET database. The AERONET programme is a federation of ground-based sun photometer sensors established by NASA and PHOTONS which started in the early 1990s [45]. It offers measurements of aerosol optical depth and other relevant atmospheric parameters at remote sites for three data quality levels (i.e. Level 1, Level 1.5 and Level 2). Hence, high-quality observed values of the relevant atmospheric parameters for these sites were available to accurately estimate the incident spectra. Fig. 7 shows the monthly-average values of the atmospheric parameters gathered from AERONET in order to show the atmospheric characteristics of the locations considered. Solar Village is a desert location with medium values of precipitable water

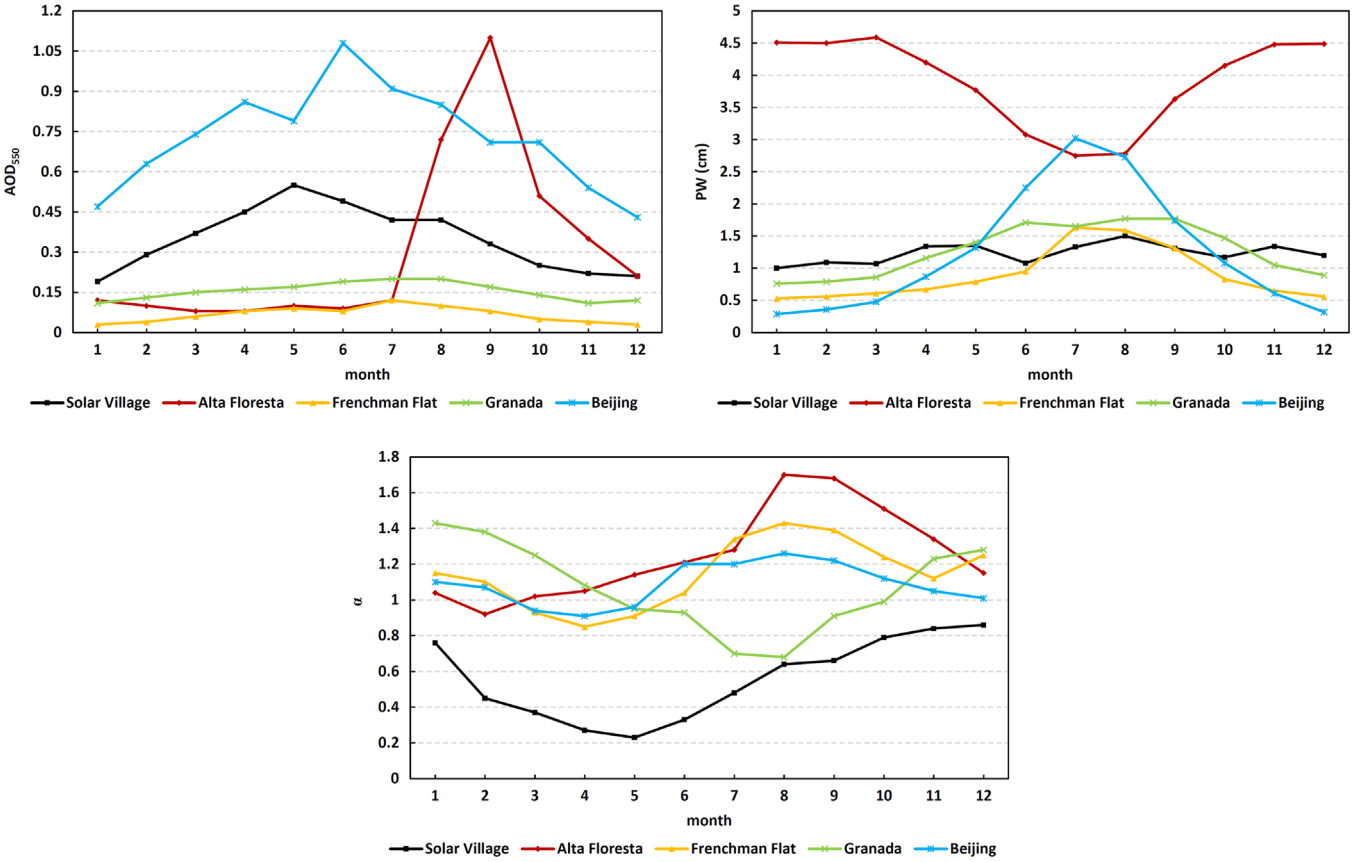

Fig. 7. Monthly-average values of aerosol optical depth at 550 nm (AOD_{550}), Ångström exponent (α) and precipitable water (PW) obtained from AERONET for the five sites considered.

and high values of aerosol optical depth dominated by dust emissions. Alta Floresta is a tropical site with the typical high values of precipitable water of these locations, and high values of aerosol optical depth from August to October produced by biomass burning in the Amazon. Frenchman Flat is a clay desert location with medium values of precipitable water and is characterized by a clear atmosphere with very low values of aerosol optical depth. Granada is a non-industrialised medium city with medium values of precipitable water and aerosol optical depth periodically affected by Saharan dust. Finally, Beijing is an industrialised city with medium values of precipitable water and is characterized by a highly polluted atmosphere with extreme values of aerosol optical depth. Further information about the climatology of these sites can be found for instance in [46–49], as well as at AERONET website.

In order to estimate the spectral impact on the energy yield of each material is necessary to know the spectral distribution of the irradiance at every instant of time. To conduct this, AM was calculated as a function of Sun´s zenith angle (θ) every ten minutes as [50]:

$$AM = \frac{1}{\cos\theta + 0.45665\theta^{0.07}\left(96.4836 - \theta\right)^{-1.697}} \quad (10)$$

and the daily values of AOD_{550}, α and PW were obtained from the AERONET database, [51] while the rest of input parameters of the SMARTS model were kept constant at the reference values (AM1.5G ASTMG-173-03 spectrum). Table 2 shows the number and quality of available data at each specific location. Once the parameters above were available, the daily time-series of the direct and global component of the spectral irradiance for the whole year were simulated with the SMARTS model. Finally, the spectral impact on the energy yield for a desired period of time of each material has been calculated using Eqs. (4), (5) and (9), and the data shown in Figs. 1 and 2.

Table 2
Number of days and quality of observed data available at AERONET database at each location considered.

Location	Available time period (days)	Data quality
Solar Village	3909	Level 2.0 Quality Assured Data (Highest)
Alta Floresta	3045	
Frenchman Flat	1752	
Granada	1707	
Beijing	2959	

The use of high-quality observed data from AERONET in conjunction with the SMARTS model is widely used by the scientific community to evaluate the spectral performance of PV devices, as shown in the different references listed in the introduction. In addition, the analytical expressions discussed in Section 2 and the procedure followed in this work to evaluate the spectral impact on the electrical output of solar devices have been previously validated by the authors in [33,52]. In order to have a sense of the accuracy of the methodology used here, Appendix I has been also included to compare the simulated results with long-term experimental data.

4.2. Monthly impact

Figs. 8 and 9 show the monthly spectral impact on the energy yield of the selected HCPV systems and PV devices for the five sites considered. As was expected from the previous study, the energy yield of the HCPV systems shows a higher monthly spectral dependence than the PV devices. Moreover, the HCPV systems have the same monthly behaviour at each particular site. Among them, the system made up of LM+PMMA and MM+SOG show the worst

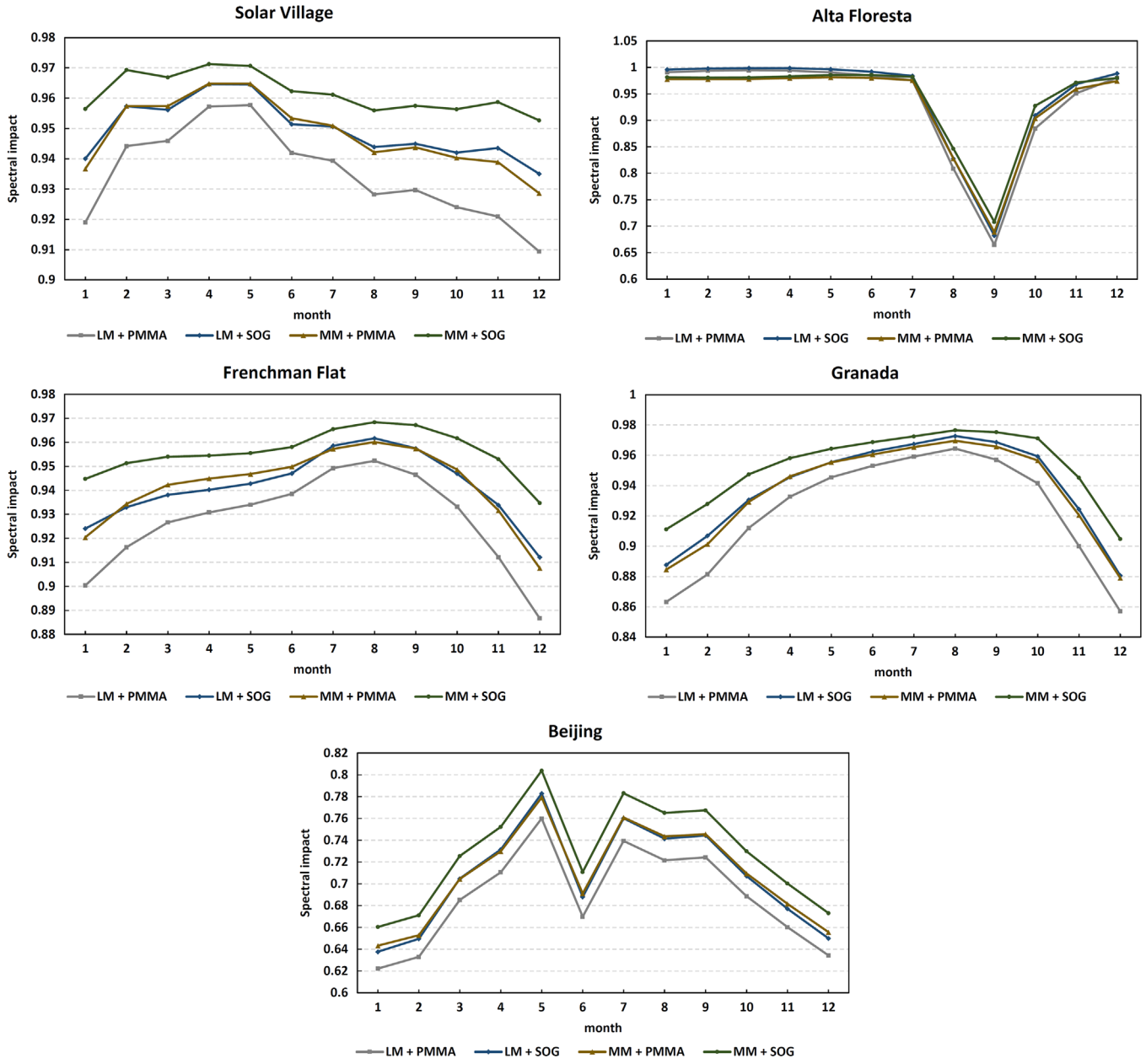

Fig. 8. Impact of the spectral variation on the monthly energy yield of the HCPV materials under study for the five sites considered.

and best performance respectively, while the other two present similar spectral dependences. This is valid at all sites except in Alta Floresta. This site has extremely high values of PW that increase the performance of the systems based on LM solar cells as previously discussed. Taking this into account, and the extreme AOD_{550} values reached from August to October, this place shows the highest monthly variations among the five sites. The maximum difference at this location is produced by the LM+PMMA system with spectral losses ranging from −0.6% to −33.5%, and the minimum by the MM+SOG system with values ranging from −1.4% to −29.2%. The lowest monthly variations are found in Solar Village, where the maximum difference is produced by the LM+PMMA system with spectral losses ranging from −4.2% to −9.1%, and the minimum by the MM+SOG system with values ranging from −2.9% to −4.7%. With regards to the PV materials, the a-Si and CdTe show a similar and clear higher monthly spectral dependence than the others that can be explained by their wider ban gap. The a-Si material shows the highest monthly variations in Alta Floresta, as in the case of HCPV systems, with values ranging from 8.6% to −5.6%. This strong variation is also produced by the high values of PW during all the year and by the extreme values of AOD_{550} from August to October. The CdTe material shows the highest monthly variations in Beijing with spectral losses ranging from −1.8% to −8.5%.The lowest monthly variations for both materials are produced in Solar Village with values ranging from 1.3% to −0.9% for the a-Si and values ranging from −0.6% to −1.5% for the CdTe material. The other PV materials have a stable performance and almost the same monthly variations. The highest and lowest monthly spectral variations are found for the p-Si material in Beijing and Alta Floresta with energy losses ranging from −0.5% to −3% and 0.1% to −0.3%, respectively.

Finally, it can be concluded that all the photovoltaic devices tend to have a seasonal dependence. However, this seasonal variation cannot be explained only taking into account the variation of the Sun´s position during the year, and therefore the AM variations (the parameter with the largest impact). This means that it is necessary to take into account the impact of the other

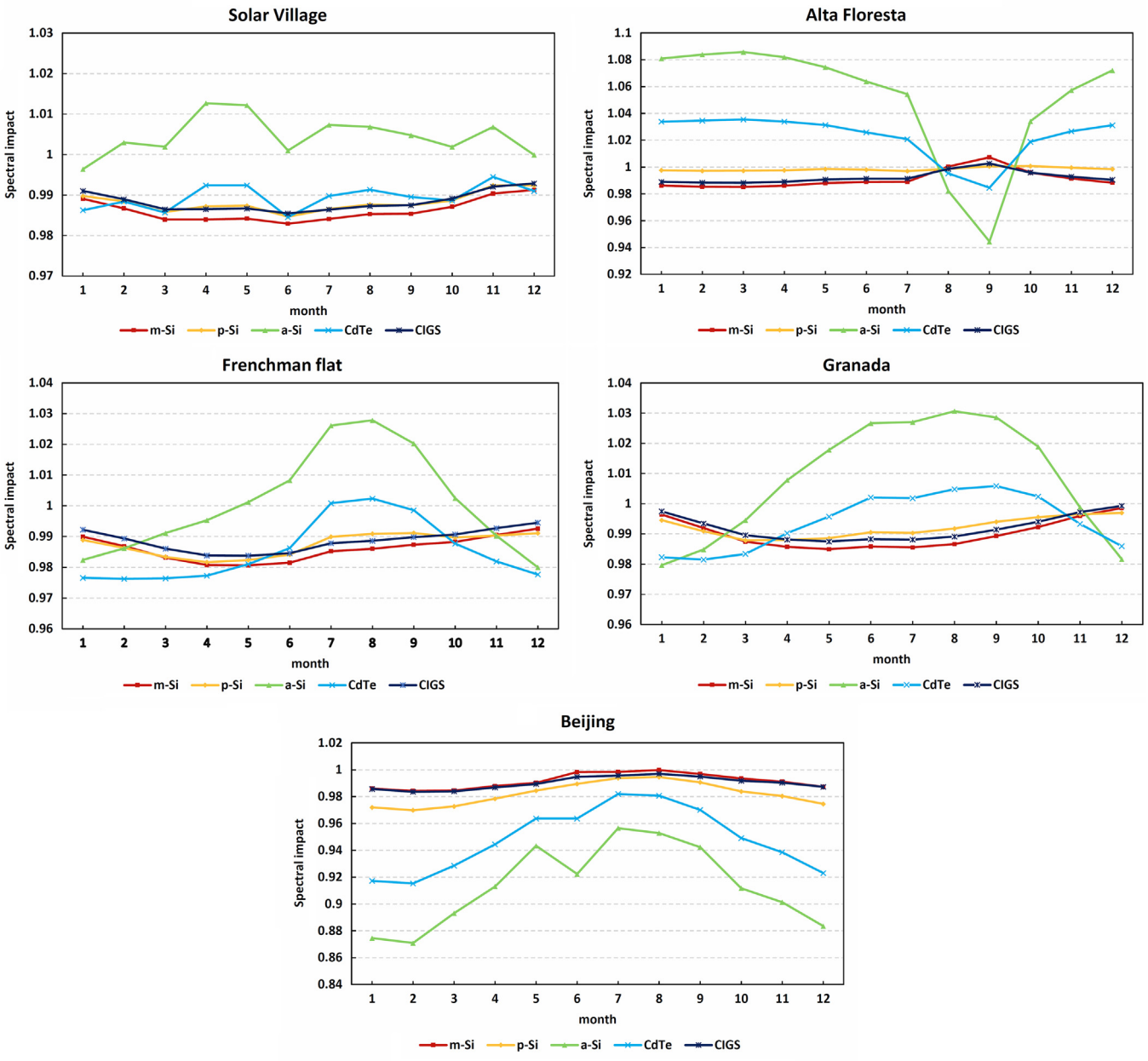

Fig. 9. Impact of the spectral variation on the monthly energy yield of the PV materials under study for the five sites considered.

atmospheric parameters to properly understand the impact of the spectrum on the energy yield of photovoltaics material. A good example of this is the strong variation produced in September in Alta Floresta for both the HCPV and PV devices due to the high AOD_{550} values produced by biomass burning in the Amazon.

4.3. Annual impact

Figs. 10 and 11 show the annual spectral impact on the energy yield of the HCPV and PV devices for all sites studied. As was expected, the energy yield of the HCPV systems shows a higher annual spectral dependence than the PV devices. Furthermore, the HCPV systems present relevant spectral losses and have a similar behaviour at each location. The minimum spectral losses are produced at Alta Floresta since it has the lowest AM (lowest latitude) and highest PW values, with energy losses ranging from −3.9% to −5.2%. The maximum spectral losses are produced at Beijing since it has the highest AM (highest latitude) and AOD_{550} values, with energy losses ranging from −26.5% to −30.6%. As in the monthly analysis, the LM+PMMA and MM+SOG systems have the worst and best performance and the others present similar spectral dependences, expect in Alta Floresta. Although this location has extreme AOD_{550} values from August to October, the high values of PW during all the year yield to a better performance of the systems based on LM solar cells. Among the PV materials, the a-Si and CdTe devices show the largest spectral dependence, due to their higher energy gap, and a similar behaviour for each location. As for the HCPV systems, the best and worst performance of these two materials are found in Alta Floresta and Beijing. Alta Floresta presents spectral gains of 5.4% for the a-Si device and 2.4% for the CdTe device since this location has the lowest and highest AM and PW values. Beijing presents spectral losses of −7.8% for the a-Si device and −4.6% for the CdTe device since this location has the highest AM and AOD_{550} values. As expected, the other PV materials show a stable behaviour for all locations, due to their narrow band gap, and almost the same annual energy losses. The worst and best

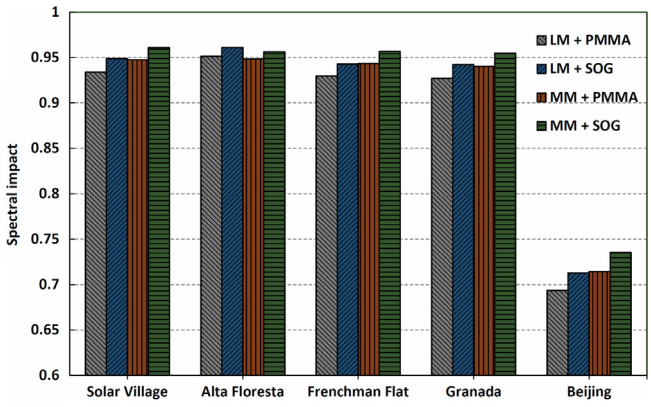

Fig. 10. Impact of the spectral variation on the annual energy yield of the HCPV materials under study for the five sites considered.

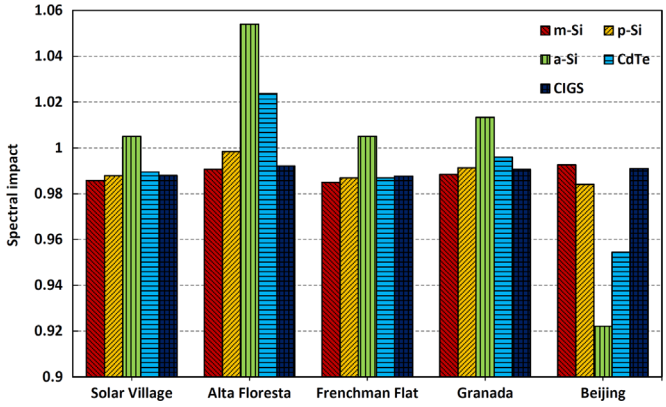

Fig. 11. Impact of the spectral variation on the annual energy yield of the PV materials under study for the five sites considered.

Table 3
Total maximum, minimum and average difference between the spectral impact of the HCPV and the PV technologies considered.

HCPV[a]			
PV material	**Maximum (%) (city)**	**Minimum (%) (city)**	**Average (%)**
m-Si	−6.14 (Granada)	−2.45 (Solar Village)	−4.26
p-Si	−6.42 (Granada)	−2.66 (Solar Village)	−5.86
a-Si	−10.56 (Alta Floresta)	−4.38 (Solar Village)	−6.25
CdTe	−7.53 (Alta Floresta)	−2.83 (Solar Village)	−4.76
CIGS	−6.35 (Granada)	−2.67 (Solar Village)	−4.29
		Average	−5.09

[a] Beijing has not been taken into account.

performance is found for the p-Si materials in Beijing and Alta Floresta with energy losses of −1.6% and −0.2%.

As a summary, Table 3 listed the annual maximum, minimum and average differences found between the annual spectral impact on the energy yield of the HCPV and the PV technologies. In addition, the annual differences between the spectral impact of each HCPV system and the PV materials at all the locations are shown in the Appendix II (Tables B1–B4). It is important to highlight that the case of Beijing has not been considered in Table 3 and for estimating the average values shown in Tables B1–B4. This location has been selected to show an extreme variation between the energy spectral losses of HCPV and PV devices, due to the high impact of aerosols on DNI and HCPV technology. However, this location should not be considered representative of the annual energy spectral losses of HCPV systems. As can be seen in Table 3, the minimum difference is found with respect to the m-Si device with a maximum, minimum and average value of −6.14%, −2.45% and −4.3% respectively. The maximum difference is found with respect to the a-Si device with a maximum, minimum and average value of −10.56%, −4.38 and −6.2% respectively. As also shown, the minimum differences are always produced in Solar Village, while the maximum differences are produced in Granada (m-Si, p-Si and CIGS) and Alta Floresta (a-Si and CdTe). Finally, the annual average difference between all the HCPV and PV devices analysed at all sites considered has found to be about 5%.

5. Conclusions

In this paper, the comparative assessment of the spectral impact on the energy yield at a monthly and annual time scale, of HCPV and PV technologies at several locations with disparate climate conditions has been conducted. In order to achieve this goal, several HCPV systems made up of different multi-junction solar cells and primary optics, and various single-junction commercial PV devices have been selected. The spectral impact of both technologies is evaluated thought the spectral factor index in conjunction with the Simple Model of Atmospheric Radiative Transfer of Sunshine (SMARTS). The comparison of both technologies is performed at five AERONET sites: Solar Village, Alta Floresta, Frenchman Flat, Granada and Beijing.

From the monthly analysis it can be concluded that, although the HCPV devices show a clear greater spectral dependence, both technologies show a seasonal behaviour. The higher and lower monthly variations for HCPV systems are found in Alta Floresta (−0.6 to −33.5% for the LM+PMMA) and Solar Village (−2.9% and −4.7% for the MM+SOG). With regard to the PV materials, the a-Si and CdTe show a similar and higher monthly spectral dependence than the others. The higher and lower monthly variations are found in Alta Floresta (8.6% to –5.6% for the a-Si) and Solar Village (−0.6% to −1.5% for the CdTe). The m-Si, p-Si and CIGS materials show a more stable performance with the higher and lower monthly spectral variations produced in Beijing (−0.5 to −3% for the p-Si) and Alta Floresta (0.1% to −0.3% for the p-Si) respectively. The analysis of the annual spectral impact on the energy yield also indicates that HCPV technology shows a higher spectral dependence. The lower annual spectral losses are produced in Alta Floresta (−3.9 to −5.2%), while the higher are produced at Beijing (−26.5% to −30.6%). Again, the a-Si and CdTe devices show the largest spectral dependence among all the PV materials. The best and worst performance of these devices are found in Alta Floresta (5.4%) and Beijing (−7.8%). The other PV materials show a more stable behaviour, the best and worst performances are found in Alta Floresta (−0.2%) and Beijing (−1.6%) respectively. Finally, it has been found that the current HCPV systems present annual spectral losses of around 5% with respect to PV systems at representative sites. This indicates that the spectral changes are not a crucial limitation for the market expansion of HCPV technology since their conversion efficiencies are significantly higher than PV technology.

Acknowledgements

This work is supported by the Spanish Economy Ministry and the European Regional Development Fund/Fondo Europeo de Desarrollo Regional (ERDF/FEDER) under the Project ENE2013-45242-R, by the Spanish Ministry of Education, Social Policy and Sports under the Project ENE2009-08302 (FEDER Funds) and by the Andalusian Research Plan under the Project P09-TEP-5045 (FEDER Funds). Eduardo F. Fernández is supported by the Spanish Ministry of Economy and Competitiveness through the Juan de la Cierva 2013 fellowship.

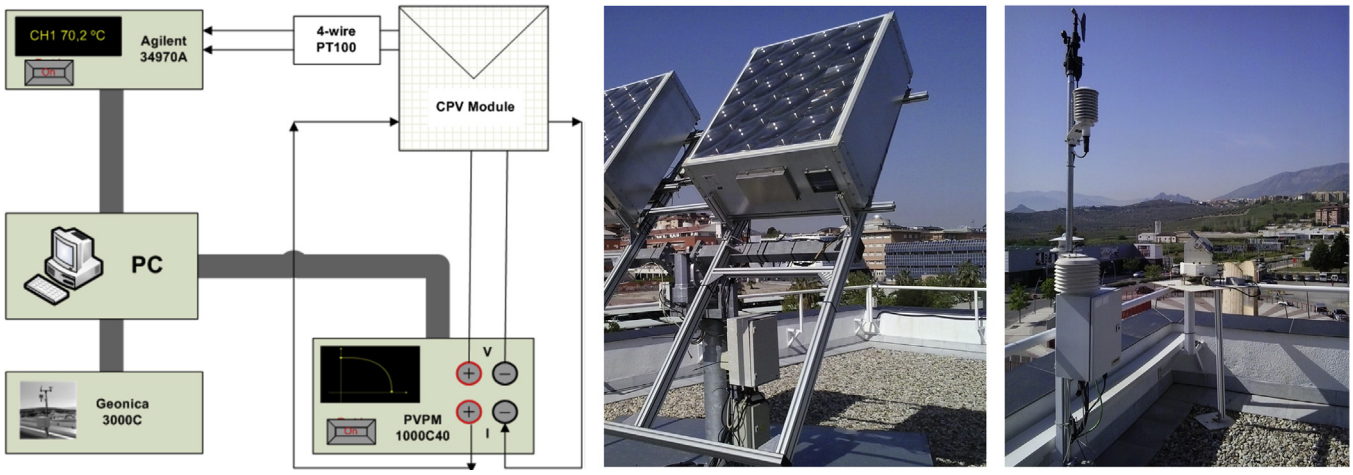

Fig. A1. Experimental set-up to carry out this study at the roof top of the Centro de Estudios Avanzados en Energía y Medio Ambiente in southern Spain.

Appendix A

As mentioned, the complete procedure followed in this paper is based on widely used techniques and mathematical expressions previously validated by the authors. Despite this, in this appendix the comparison between the simulated and actual data of two HCPV systems is conducted. In particular, the LM+PMMA and LM+SOG systems located at the Centro de Estudio Avanzados en Energía y Medio Ambiente (N 37°27′36″, W 03 °28′12″) placed close to the Granada AERONET site, measured since January 2013, have been used. Fig. A1 shows the experimental set-up to carry out the measurements, detailed information about this can be found in [6]. The spectral factor of the two HCPV systems is estimated from the short-circuit current (I_{sc}):

$$SF = \frac{\min(\int E_b(\lambda)\eta(\lambda)SR_i(\lambda)d\lambda)\int E_{b,ref}(\lambda)d\lambda}{\min(\int E_{b,ref}(\lambda)\eta(\lambda)SR_i(\lambda)d\lambda)\int E_b(\lambda)d\lambda} = \frac{I_{sc}(25^{\circ}C)}{I^*_{sc}}\frac{DNI^*}{DNI} \quad (A1)$$

as previously discussed in [53,54], which is essentially the same magnitude as the one described by Sandia national Laboratories to spectrally correct the broadband irradiance [35]. Table A1 shows the simulated and actual impact of the spectral changes on the annual output of the two systems. As can be seen, the procedure followed in this work has a high accuracy with an annual difference lower than 1%.

Table A1
Simulated and experimental impact of the spectral variation on the annual energy yield of the two HCPV systems considered.

System	Simulated ΔE	Experimental ΔE
LM+PMMA	0.934	0.929
LM+SOG	0.949	0.941

Appendix B

Tables B1–B4 show the annual difference between the spectral impact of each HCPV system and the PV materials considered.

Table B1
Annual difference between the spectral impact of the HCPV LM+PMMA system and the PV materials considered.

LM+PMMA[a]						
PV material	**Solar Village (%)**	**Alta Floresta (%)**	**Frenchman Flat (%)**	**Granada (%)**	**Beijing (%)**	**Average (%)**
m-Si	−5.17	−3.91	−5.52	−6.14	−29.90	−5.18
p-Si	−5.38	−4.68	−5.72	−6.42	−29.04	−5.55
a-Si	−7.10	−10.25	−7.53	−8.62	−22.84	−8.37
CdTe	−5.55	−7.22	−5.72	−6.89	−26.08	−6.34
CIGS	−5.39	−4.06	−5.79	−6.35	−29.73	−5.40

[a] Beijing has not been taken into account in the estimation of the average values.

Table B2
Annual difference between the spectral impact of the HCPV LM+SOG system and the PV materials considered.

LM+SOG[a]						
PV material	**Solar Village (%)**	**Alta Floresta (%)**	**Frenchman Flat (%)**	**Granada (%)**	**Beijing (%)**	**Average (%)**
m-Si	−3.68	−2.96	−4.20	−4.61	−27.99	−3.86
p-Si	−3.89	−3.74	−4.40	−4.90	−27.13	−4.23
a-Si	−5.61	−9.30	−6.21	−7.10	−20.93	−7.05
CdTe	−4.05	−6.27	−4.40	−5.36	−24.17	−5.02
CIGS	−3.90	−3.11	−4.47	−4.83	−27.82	−4.08

[a] Beijing has not been taken into account in the estimation of the average values.

Table B3
Annual difference between the spectral impact of the HCPV MM+PMMA system and the PV materials considered.

MM+PMMA[a]						
PV material	**Solar Village (%)**	**Alta Floresta (%)**	**Frenchman Flat (%)**	**Granada (%)**	**Beijing (%)**	**Average (%)**
m-Si	−3.81	−4.22	−4.13	−4.83	−27.83	−4.25
p-Si	−4.02	−4.99	−4.33	−5.11	−26.97	−4.61
a-Si	−5.74	−10.56	−6.13	−7.31	−20.77	−7.44
CdTe	−4.18	−7.53	−4.33	−5.58	−24.01	−5.40
CIGS	−4.03	−4.37	−4.40	−5.04	−27.66	−4.46

[a] Beijing has not been taken into account in the estimation of the average values.

Table B4
Annual difference between the spectral impact of the HCPV LM+SOG system and the PV materials considered.

MM+SOG[a]						
PV material	**Solar Village (%)**	**Alta Floresta (%)**	**Frenchman Flat (%)**	**Granada (%)**	**Beijing (%)**	**Average (%)**
m-Si	−2.45	−3.43	−2.83	−3.37	−25.75	−3.02
p-Si	−2.66	−4.21	−3.03	−3.65	−24.90	−3.39
a-Si	−4.38	−9.77	−4.83	−5.85	−18.70	−6.21
CdTe	−2.83	−6.75	−3.03	−4.11	−21.93	−4.18
CIGS	−2.67	−3.58	−3.10	−3.58	−25.58	−3.23

[a] Beijing has not been taken into account in the estimation of the average values.

References

[1] A. Luque, G. Sala, I. Luque-Heredia, Photovoltaic concentration at the onset of its commercial deployment, Prog. Photovolt.: Res. Appl. 14 (5) (2006) 413–428.
[2] H. Cotal, C. Fetzer, J. Boisvert, G. Kinsey, R. King, P. Hebert, H. Yoon, N. Karam, III-V multijunction solar cells for concentrating photovoltaics, Energy Environ. Sci. 2 (2) (2009) 174–192.
[3] S.P. Philipps, A.W. Bett, K. Horowitz, S. Kurtz, Current Status of Concetrator Photovotailc (CPV) Technology, Fraunhofer ISE and NREL, Springfield, USA, 2015.
[4] Globaldata, Globaldata, Concentrated Photovoltaics (CPV) – Global Market Size, Competitive Landscape and Key Country Analysis to 2020, UK, 2014.
[5] D. Talavera, P. Pérez-Higueras, J. Ruíz-Arias, E. Fernández, Levelised cost of electricity in high concentrated photovoltaic grid connected systems: spatial analysis of Spain, Appl. Energy 151 (2015) 49–59.
[6] E. Fernández, P. Pérez-Higueras, A. Garcia Loureiro, P. Vidal, Outdoor evaluation of concentrator photovoltaic systems modules from different manufacturers: first results and steps, Prog. Photovolt.: Res. Appl. 21 (4) (2013) 693–701.
[7] P. Faine, S. Kurtz, C. Riordan, J.M. Olson, The influence of spectral solar irradiance variations on the performance of selected single-junction and multijunctions solar cells, Sol. Cells 31 (1991) 259–278.
[8] E. Fernández, G. Siefer, F. Almonacid, A. García-Loureiro, P. Pérez-Higueras, A two subcell equivalent solar cell model for III–V triple junction solar cells under spectrum and temperature variations, Sol. Energy 92 (2013) 221–229.
[9] W. McMahon, K. Emery, D. Friedman, L. Ottoson, M. Young, J. Ward, C. Kramer, A. Duda, S. Kurtz, Fill factor as a probe of current-matching for GaInP/GaAs tandem cells in a concentrator system during outdoor operation, Prog. Photovolt.: Res. Appl. 16 (3) (2008) 213–224.
[10] M. Muller, B. Marion, S. Kurtz, J. Rodriguez, An investigation into spectral parameters as they impact CPV module perfromance, in: Proceedings of the AIP Conference, 1 , 2010, pp. 307–311.
[11] J. Hashimoto, S. Kurtz, S. Keiichiro, M. Muller, K. Otani, Performance of CPV sytem using three different types of III-V multi-junction solar cells, in: Proceedings of the AIP Conference, 1477, 2012, pp. 372–376.
[12] G. Peharz, G. Siefer, A. Bett, A simple method for quatifying spectral impacts on multi-junction solar cells, Sol. Energy 83 (2009) 1588–1589.
[13] G. Peharz, J. Ferrer Rodríguez, G. Siefer, A. Bett, A method for using CPV modules as temperature sensors and its application to rating procedures, Sol. Energy Mater. Sol. Cells 95 (10) (2011) 2734–2744.
[14] B. García-Domingo, J. Aguilera, J. de la Casa, M. Fuentes, Modelling the influence of atmospheric conditions on the outdoor real performance of a CPV (Concentrated Photovoltaic) module, Energy 70 (2014) 239–250.
[15] H.A. Husna, Impact of spectral irradiance distribution and temperature on the outdoor performance of concentrator photovoltaic system, in: Proceedings of the AIP Conference, 1556, 2013, pp. 252–255.
[16] M. Victoria, S. Askins, R. Nuñez, C. Dominguez, R. Herrero, I. Antón, G. Sala, J.M. Ruíz, Tuning the current ration of a CPV system to maximiza the energy harvesting in a particular location, in: Proceedings of the AIP Conference, 1556, 2013, pp. 156–161.
[17] E. Fernández, F. Almonacid, J. Ruiz-Arias, A. Soria-Moya, Analysis of the spectral variations on the performance of high concentrator photovoltaic modules operating under different real climate conditions, Sol. Energy Mater. Sol. Cells 179–187 (2014) 127.
[18] A. Soria-Moya, E.F. Fernández, F. Almonacid, T.K. Mallick, Spectral losses of high concentrator photovoltaic modules depending on latitude, in: Proceedings of the AIP Conference, 2015.
[19] N. Chan, H. Brindley, N. Ekins-Daukes, Impact of individual atmospheric parameters on CPV system power, energy yield and cost of energy, Prog. Photovolt.: Res. Appl. 22 (10) (2014) 1080–1095.
[20] N. Chan, T. Young, H. Brindley, N. Ekins-Daukes, K. Araki, Y. Kemmoku, M. Yamaguchi, Validation of energy prediction method for a concentrator photovoltaic module in Toyohashi Japan, Prog. Photovolt.: Res. Appl. 21 (8) (2013) 1598–1610.
[21] T. Minemoto, M. Toda, S. Nagae, M. Gotoh, A. Nakajima, K. Yamamoto, H. Takakura, Y. Hamakawa, Effect of spectral irradiance distribution on the outdoor performance of amorphous Si//thin-film crystalline Si stacked photovoltaic modules, Sol. Energy Mater. Sol. Cells 91 (2–3) (2007) 120–122.
[22] T. Minemoto, S. Nagae, H. Takakura, Impact of spectral irradiance distribution and temperature on the outdoor performance of amorphous Si photovoltaic modules, Sol. Energy Mater. Sol. Cells 91 (10) (2007) 919–923.
[23] S. Nagae, M. Toda, T. Minemoto, H. Takakura, Y. Hamakawa, Evaluation of the impact of solar spectrum and temperature variations on output power of silicon-based photovoltaic modules, Sol. Energy Mater. Sol. Cells 90 (20) (2006) 3568–3575.
[24] Y. Nakada, S. Fukushige, T. Minemoto, H. Takakura, Seasonal variation analysis of the outdoor performance of amorphous Si photovoltaic modules using the contour map, Sol. Energy Mater. Sol. Cells 93 (3) (2009) 334–337.
[25] N. Katsumata, Y. Nakada, T. Minemoto, H. Takakura, Estimation of irradiance and outdoor performance of photovoltaic modules by meteorological data, Sol. Energy Mater. Sol. Cells 95 (1) (2011) 199–202.
[26] T. Ishii, K. Otani, T. Takashima, Effects of solar spectrum and module temperature on outdoor performance of photovoltaic modules in round-robin measurements in Japan, Prog. Photovolt.: Res. Appl. 19 (2) (2011) 141–148.
[27] G. Nofuentes, B. García-Domingo, J.V. Muñoz, F. Chenlo, Analysis of the dependence of the spectral factor of some PV technologies on the solar spectrum distribution, Appl. Energy 113 (2014) 302–309.
[28] M. Alonso-Abella, F. Chenlo, G. Nofuentes, M. Torres-Ramírez, Analysis of spectral effects on the energy yield of different PV (photovoltaic) technologies: the case of four specific sites, Energy 67 (2014) 435–443.
[29] E. Fernandez, F. Cruz, T. Mallick, S. Sundaram, Effect of spectral irradiance variations on the performance of highly efficient environment-friendly solar cells, IEEE J. Photovolt. 5 (4) (2015) 1150–1157.
[30] S. Senthilarasu, E. Fernández, F. Almonacid, T. Mallick, Effects of spectral coupling on perovskite solar cells under diverse climatic conditions, Sol. Energy Mater. Sol. Cells 133 (2015) 92–98.
[31] D. Dirnberger, G. Blackburn, B. Müller, C. Reise, On the impact of solar spectral irradiance on the yield of different PV technologies, Sol. Energy Mater. Sol. Cells 132 (2015) 431–442.
[32] J. Leloux, E. Lorenzo, B. García-Domingo, J. Aguilera, C. Gueymard, A bankable method of assessing the performance of a CPV plant, Appl. Energy 118 (2014) 1–11.
[33] E.F. Fernandez, F. Almonacid, A. Soria-Moya, J. Terrados, Experimental analysis of the spectral factor for quantifying the spectral influence on concentrator

photovoltaic systems under real operating conditions, Energy 90 (2015) 1878–1886.
[34] E. Fernández, F. Almonacid, P. Rodrigo, P. Pérez-Higueras, Calculation of the cell temperature of a high concentrator photovoltaic (HCPV) module: a study and comparison of different methods, Sol. Energy Mater. Sol. Cells 121 (2014) 144–151.
[35] C. Osterwald, K. Emery, M. Muller, Photovoltaic module calibration value versus optical air mass: the air mass function, Prog. Photovolt.: Res. Appl. 22 (5) (2014) 560–573.
[36] C. Monokroussos, M. Bliss, Y. Qiu, C. Hibberd, T. Betts, A. Tiwari, R. Gottschalg, Effects of spectrum on the power rating of amorphous silicon photovoltaic devices, Prog. Photovolt.: Res. Appl. 19 (6) (2011) 640–648.
[37] C. Hibberd, F. Plyta, C. Monokroussos, M. Bliss, T. Betts, R. Gottschalg, Voltage-dependent quantum efficiency measurements of amorphous silicon multi-junction mini-modules, Sol. Energy Mater. Sol. Cells 95 (1) (2011) 123–126.
[38] R. Núñez, C. Domínguez, S. Askins, M. Victoria, R. Herrero, I. Antón y G. Sala, Determination of spectral variations by means of component cells useful for CPV rating and design, Prog. Photovolt.: Res. Appl. (2015) http://dx.doi.org/10.1002/pip.2715, in press.
[39] C. Rigollier, O. Bauer, L. Wald, On the clear sky model of the ESRA-European Solar Radiation Atlas-With respect to the Heliosat method, Sol. Energy 68 (1) (2000) 33–48.
[40] Y.A. Eltbaakh, M. Ruslan, M. Alghoul, M. Othman, K. Sopian, T. Razykov, Solar attenuation by aerosols: an overview, Renew. Sustain. Energy Rev. 16 (6) (2012) 4264–4276.
[41] C. Gueymard, Impact of on-site atmospheric water vapor estimation methods on the accuracy of local solar irradiance predictions, Sol. Energy 101 (2014) 74–82.
[42] C. Gueymard, Parameterized transmittance model for direct beam and circumsolar spectral irradiance, Sol. Energy 71 (5) (2001) 325–346.
[43] ASTM, ASTM G173-03 Standard tables for reference solar spectral irradiances: direct normal and Hemispherical on 37° Tilted Surface, American Society for Testing and Materials, 2012, pp. 1–20.
[44] J. Jaus, C.A. Gueymard, Generalized spectral performance evaluation of multijunction solar cells using a multicore parallelized version of SMARTS, in: Proceedings of the AIP Conference, 1477, 2012, pp. 122–126.
[45] B. Holben, T. Eck, I. Slutsker, D. Tanré, J. Buis, A. Setzer, E. Vermote, J. Reagan, Y. Kaufman, T. Nakajima, F. Lavenu, I. Jankowiak, A. Smirnov, AERONET-A federated instrument network and data archive for aerosol characterization, Remote Sens. Environ. 66 (1) (1998) 1–16.
[46] G. Camponogara, M. Silva Dias, G. Carrió, Relationship between Amazon biomass burning aerosols and rainfall over the la Plata Basin, Atmos. Chem. Phys. 14 (9) (2014) 4397–4407.
[47] M. Chin, T. Diehl, O. Dubovik, T. Eck, B. Holben, A. Sinyuk, D. Streets, Light absorption by pollution, dust, and biomass burning aerosols: A global model study and evaluation with AERONET measurements, Ann. Geophys. 27 (9) (2009) 3439–3464.
[48] I. Sabbah, F. Hasan, Remote sensing of aerosols over the Solar Village, Saudi Arabia, Atmos. Res. 90 (2–4) (2008) 170–179.
[49] A. Sayer, N. Hsu, C. Bettenhausen, M.-J. Jeong, B. Holben, J. Zhang, Global and regional evaluation of over-land spectral aerosol optical depth retrievals from SeaWiFS, Atmos. Meas. Tech. 5 (7) (2012) 1761–1778.
[50] F. Kasten, A.T. Young, Revised optical air mass tables and approximation formula, Appl. Opt. 2 (22) (1989) 4735–4738.
[51] Aerosol Robotic Network, available online: ⟨http://aeronet.gsfc.nasa.gov/⟩, 2015.
[52] E.F. Fernández, A.J. García-Loureiro, y G.P. Smestad, Multijunction concentrator solar cells: analysis and fundamentals, in: Pedro Pérez-Higueras, Eduardo F. Fernández (Eds.), High Concentrator Photovoltaics: Fundamentals, Engineering and Power Plants, Springer, Gewerbestrasse, Switzerland, 2015, pp. 9–37.
[53] E. Fernández, F. Almonacid, Spectrally corrected direct normal irradiance based on artificial neural networks for high concentrator photovoltaic applications, Energy 74 (C) (2014) 941–949.
[54] F. Almonacid, E. Fernández, T. Mallick, P. Pérez-Higueras, High concentrator photovoltaic module simulation by neuronal networks using spectrally corrected direct normal irradiance and cell temperature, Energy 84 (2015) 336–343.

COMUNICACIONES A CONGRESOS INTERNACIONALES

1. Fernandez, E.F., Almonacid, F, Nabin, S; Mallick, T., Sanchez, I., Cuadra, J.M., **Soria-Moya, A.** y Pérez-Higueras, P (2014). *Performance analysis of the lineal model for estimating the maximum power of a HCPV module in different climate conditions. 11th International Conference on Concentrator Photovoltaic Systems. AIP Conference Proceedings*, 1616, 187-190.
2. **Soria-Moya, A.**, Fernández, E. F., Almonacid, F. y Mallick, T. K. (2015). *Spectral losses of high concentrator photovoltaic modules depending on latitude. 12th International Conference on Concentrator Photovoltaic Systems. AIP Conference Proceedings*, 1679, 050013.
3. Fernández, E. F., Theristis, M., Almonacid, F.,**Soria-Moya, A.**, Pérez-Higueras, P. y Georghiou, G. (2016). *Analytical equations for the spectral correction of III-V concentrator photovoltaics. 13th International Conference on Concentrator Photovoltaic Systems. In press.*